VNIVERSITAT DE VALÈNCIA

DEPARTAMENT DE FISICA TEÒRICA

New results on black hole entropy in loop quantum gravity

TESIS DOCTORAL

Enrique Fernández Borja

DIRIGIDA POR

Prof. José Adolfo de Azcárraga Feliu

Dr. Alejandro Corichi Rodríguez Gil

Julio, 2009

Dr. José Adolfo de Azcárraga, catedrático del departamento de Física Teórica de la Universidad de Valencia,

CERTIFICA:

Que la presente memoria, **New results on black hole entropy in Loop Quantum Gravity** ha sido realizada bajo su codirección en el Departamento de Física Teórica de la Universidad de Valencia por D. Enrique Fernández Borja y constituye su Tesis Doctoral, que presenta para optar al grado de Doctor en Física.

Y para que así conste, en cumplimiento de la legislación vigente, firma el presente Certificado en Valencia a 30 de junio de 2009.

Fdo.: José Adolfo de Azcárraga Feliu

Dr. Alejandro Corichi Rodríguez Gil, investigador titular B del Instituto de Matemáticas Unidad Morelia de la Universidad Nacional Autónoma de México,

CERTIFICA:

Que la presente memoria, **New results on black hole entropy in Loop Quantum Gravity**, ha sido realizada bajo su codirección en el Departamento de Física Teórica de la Universidad de Valencia por D. Enrique Fernández Borja y constituye su Tesis Doctoral, que presenta para optar al grado de Doctor en Física.

Y para que así conste, en cumplimiento de la legislación vigente, firma el presente Certificado en Morelia a 30 de junio de 2009.

Fdo.: Alejandro Corichi Rodríguez Gil

A mi madre.

AGRADECIMIENTOS

La memoria de esta tesis que ahora tienes en tus manos es la culminación de un periodo fantástico de mi vida tanto académica como personal. Sin lugar a dudas, el que esta tesis haya sido posible está relacionado con un gran número de personas a las que no puedo más que ofrecerles mi más sincero agradecimiento.

He de agradecer profundamente a Joaquín Olivert la confianza depositada en mi y la total libertad que me ofreció a la hora de elegir el campo de investigación para la realización de mi tesis doctoral. Joaquín me ha enseñado que esta vida investigadora, algunos lo llaman trabajo, únicamente se puede llevar a buen término teniendo ilusión, interés y perseverancia. Sus consejos y su constante apoyo han sido esenciales para mi formación, y su profundo conocimiento de la matemática han influido en mi manera de entender la física y la investigación.

Otra persona a la que no puedo más que mostrar mi agradecimiento es Alejandro Corichi. Alejandro apostó, totalmente a ciegas, por mí cuando me presenté ante él en Loops'05 y le pedí que codirigiera esta tesis. Su conocimiento y su supervisión científica no pueden ser debidamente ponderadas en estas líneas. Sin embargo, más allá de todo esto, han sido su confianza y su apoyo los que han hecho que hacer esta tesis e introducirme en la comunidad científica relacionada haya sido un proceso fácil y satisfactorio. Es todo un honor haber compartido este periodo con él.

No puedo dejar pasar esta oportunidad de dar una y otra vez las gracias a José Adolfo de Azcárraga. En un momento crítico de mi investigación, momento en el que creía que tendría que abandonarla, Adolfo me brindó todo su apoyo. Es justo decir que si hoy me encuentro escribiendo estas líneas en gran parte se lo debo a él. Nunca podré agradecer lo suficiente sus continuos consejos acerca de la vida científica, las conversaciones mantenidas y la total libertad que me ha brindado en mi investigación. Ahora, gracias a Adolfo, tener una mente abierta es algo que considero indispensable para dedicarse a la ciencia.

Respecto a esta vida he de decir que, dejando aparte todo lo que he aprendido de las personas que me han rodeado, que no ha sido poco, he tenido la suerte de compartir momentos, inquietudes, ilusiones y desilusiones con muchas personas. Especialemente me gustaría agradecer aquí a Guillermo Mena y Luis

Garay su amistad y su confianza; siempre es un placer escucharlos porque nunca dejan de sorprenderme y mostrarme nuevas perspectivas. A Carlos Barceló y José Luis Jaramillo por todo el aprecio que me han ofrecido y por su interés en mi trabajo. No puedo olvidar a Igor Bandos, José Navarro Salas y a Alessandro Fabbri; sus consejos y su apoyo han sido muy importantes para mi durante el tiempo de realización de esta tesis. Y por supuesto, a Víctor Aldaya con el que comparto su forma de entender la ciencia y la vida, así que supongo que sobran las gracias. De todas formas, gracias Víctor.

Un especial agradecimiento ha de ir dedicado a Fernando Barbero y Eduardo Villaseñor por la oportunidad de trabajar y colaborar con ellos, por enseñarme montones de cosas que yo a duras penas he conseguido aprender y por estar seguro de que siempre podré contar con ellos, simplemente gracias.

A nivel institucional no puedo olvidarme de agradecer al Departamento de Astronomía y Astrofísica de la Universidad de Valencia por su apoyo en los primeros años de esta tesis, así como al Laboratorio de Procesado de Imágenes de la Universidad de Valencia por su financiación durante esos años. Y mi más sincero agradecimiento a todo el Departamento de Física Teórica de la Universidad de Valencia; trabajar en él ha sido fácil y satisfactorio.

Hay dos personas a las que no hace falta agradecerles nada y se lo tengo que agradecer todo; son mis amigos y con eso sobra. Con Iván Agulló y Jacobo Díaz he trabajado, me he divertido, he caido y me he vuelto a levantar. Iván siempre ha estado ahí, mostrándome el contrapunto a todo lo que pensaba, lo cual ha hecho que aprenda a manejar distintas situaciones con distintos puntos de vista. Su forma de entender el trabajo y su amistad han sido, son, y seguirán siendo parte esencial de mi vida. Jacobo no ha dejado de sorprenderme desde el día que empezamos nuestra licenciatura, con él he compartido la totalidad de este periodo de tiempo, nos hemos arriesgado juntos en este trabajo, hemos compartido alegrías y penas dentro y fuera de él. Ha sido genial compartir con ellos, y seguir compartiendo, mi vida. Gracias Amigos.

Tengo la suerte de contar con buenos amigos que son fundamentales en mi vida. Su presencia ha sido una válvula de escape y un colchón. Me han aguantado en euforias y decepciones, me han mantenido con los pies en el suelo cuando estaba volando demasiado y me han hecho volar cuando tenía la cabeza metida en el suelo. Gracias Ana, Eduardo, Víctor, Jóse Antonio, Mary y Julia.

Esta tesis ha deparado en hacer nuevos amigos hacia los que profeso una gran admiración científica y un profundo cariño. Gracias Etera. Gracias Hanno. Gracias Tomek.

Y por supuesto, gracias Iñaki, gracias por tu amistad, por tu forma de entender la vida, por todo lo que hemos aprendido juntos y por todo lo que hemos desaprendido. Gracias por orlar las tejas azules de ribetes bermellón.

Finalmente, he de agradecer a toda mi familia por su apoyo incondi-

cional,por ser el punto fijo al que uno siempre puede volver; si soy algo en esta vida será por ellos. Gracias a todos por vuestro amor, por vuestra compañía y por ser mi familia. Y a ti Mamá, gracias, gracias, gracias... ¿Qué puedo decir? Gracias por ser la mejor madre que pude tener, no la cambiaría por nada del mundo. Sé que no ha sido fácil llegar hasta aquí, pero lo hemos conseguido. Gracias.

Y por último, gracias a la persona que se ha encargado de empujarme cuando me paraba, que me ilusionaba cuando todo estaba oscuro, que ha compartido todos y cada uno de los momentos junto a mi, que me hace ser como soy por ser ella como es. Gracias por esos ojos azules, por las sonrisas y por no cansarte de explicarme sin palabras una y otra vez qué es estar feliz. Gracias Sònia.

INTRODUCCIÓN GENERAL Y RESUMEN

Hoy día es un hecho bien aceptado que un agujero negro posee una entropía y que ésta viene dada por la fórmula de Bekenstein-Hawking [1]. Dicha entropía depende del área del horizonte de sucesos (A) a través de la famosa fórmula:

$$S_{BH} = \frac{A}{4\ell_{\rm P}^2}, \tag{0.1}$$

donde $\ell_{\rm P}^2$ es el área de Planck.

Hagamos un breve repaso de los conceptos que llevaron a la idea de asignar una entropía a un agujero negro. Inicialmente Hawking a principios de la década de los 70 demostró el conocido *teorema del área* [2]. Según este resultado el área de un agujero negro no puede disminuir mediante ningún proceso físico. Esto implica que el área de un agujero negro únicamente puede mantenerse constante o crecer, de forma análoga al comportamiento de la entropía de un sistema en equilibrio en la termodinámica usual. Esta idea fué propuesta inicialmente por Jacob Bekenstein [1], asignando al agujero negro una entropía proporcional a su área.

Este trabajo de Bekenstein fué controvertido dado que asignar una entropía a los agujeros negros implica que dichos sistemas poseen temperatura. Sin embargo, cualquier sistema con temperatura emite radiación lo que va en contra de las características clásicas de un agujero negro dado que, en principio, estos objetos no emiten nada. La cuestión dio un giro sorprendente tras el famoso trabajo de Stephen Hawking [1] donde mostraba que, al incorporar campos cuánticos en un espaciotiempo que contiene un agujero negro, éste emite radiación exactamente térmica. Este resultado mostraba que la temperatura de un agujero negro (sin carga ni rotación) es inversamente proporcional a su masa. Sorprendentemente, esta temperatura es compatible con una entropía dada por la fórmula (0.1).

En 1973 se describieron las leyes de la mecánica de los agujeros negros que son formalmente análogas a las leyes de la termodinámica. Estas leyes establecen:

- Ley Cero: En un agujero estacionario la gravedad superficial κ es constante en el horizonte.

- Primera Ley: Existe una relación entre las variaciones de la masa, el momento angular y el área del horizonte (para agujeros sin carga eléctrica), dada por (en unidades $G = c = \hbar = \kappa_B = 1$):

$$\delta M = \frac{1}{8\pi}\kappa\delta A + \Omega\delta J, \tag{0.2}$$

  donde A es el área del horizonte del agujero negro, Ω su velocidad angular y J su momento angular.

- Segunda ley: La entropía de un agujero negro viene dada por $S = \frac{1}{4}A$.

- Tercera ley: No es posible reducir la gravedad superficial de un agujero negro a cero en un número finito de pasos. Esta ley, que correspondería a la tercera ley de la termodinámica (que establece que la entropía de un sistema tiende a cero cuando hacemos tender a cero su temperatura), ha sido desbancada de su estatus ya que es bien conocido que existen violaciones a la misma en diversos sistemas. La existencia de agujeros negros extremales, con gravedad superficial nula pero con area de horizonte finita, es una muestra de ello.

Es curioso señalar que, utilizando argumentos dimensionales simples, resulta necesario incorporar la constante de Planck a dichas leyes para que la correspondencia sea consistente (ver [3] y las referencias allí citadas). La necesidad de incorporar la constante de Planck es una indicación de que para entender la termodinámica de los agujeros negros hemos de recurrir a una teoría de la gravedad a nivel cuántico.

No insistiremos en el hecho de que actualmente disponemos de dos magníficas teorías Físicas para describir la gravitación y el mundo microscópico, la Relatividad General y la Mecánica Cuántica. Dichas teorías han sido comprobadas experimentalmente durante los últimos 100 años y han demostrado tener una gran potencia predictiva. Sin embargo, dichas teorías no han podido ser unificadas en el sentido conceptual. La búsqueda de una teoría cuántica de la gravitación ha sido, y en la actualidad sigue siendo, un motor de nuevas ideas dentro de la Física. Aunque por el momento no podemos decir que tengamos un esquema coherente sobre dicha teoría, las propuestas puestas encima de la mesa son interesantes y en algunos casos prometedoras.

Como criterio general, cualquier propuesta de teoría de gravedad cuántica ha de ser capaz de explicar la entropía de un agujero negro identificando los microestados que dan lugar a (0.1) a través de la definición de Boltzmann $S = k_B \ln N$, donde N es el número de estados responsables de dicha entropía y k_B la constante de Boltzmann. Esta tesis doctoral versa sobre el cálculo de la entropía de agujeros negros dentro del esquema que proporciona la gravedad

cuántica de lazos (*l*oop quantum gravity, LQG) [3-10].

LQG es una propuesta de cuantización canónica de la Relatividad General (GR) que respeta la invariancia bajo difeomorfismos presente en la teoría clásica. En otras palabras, LQG es una propuesta de cuantización de la gravedad en la que no se fija fondo métrico alguno. Otra forma de expresar este hecho es diciendo que LQG es una teoría de la geometría cuántica. Introduciremos brevemente las bases de LQG en el siguiente capítulo. Desgraciadamente, a día de hoy no ha sido posible resolver la dinámica de la teoría. Esto hace que no dispongamos más que de un espacio de Hilbert cinemático matemáticamente bien definido, pero no conozcamos los verdaderos estados físicos. Este hecho nos obliga a tomar un camino "efectivo" para calcular la entropía de un agujero negro. En la práctica, esto significa que en el modelo que vamos a presentar en esta tesis partimos de un espaciotiempo clásico que contiene una frontera interna. Dicha frontera es considerada como el horizonte del agujero negro y se modeliza a través de un horizonte aislado [12, 13].

La elección de los horizontes aislados viene motivada fundamentalmente por su naturaleza *local*, lo que significa que, al contrario de lo que ocurre con los horizontes de sucesos (que son conceptos teleológicos cuya identificación requiere del conocimiento completo de la historia del espaciotiempo que contiene a un agujero negro), para identificarlos no es necesario conocer la historia completa del espaciotiempo. La definición de estos horizontes y su cuantización será descrita el el capítulo 3 de esta tesis. Es importante señalar que la presencia de un frontera interna induce la aparición de un término de frontera en la acción gravitatoria que se emplea en LQG que tiene la estructura de una acción de una teoría de Chern-Simons. Como veremos, la geometría cuántica induce defectos topológicos sobre la sección bidimensional del horizonte que hacen que esta teoría no sea trivial. Por lo tanto, a nivel cuántico encontramos que sobre el horizonte tendremos nuevos grados de libertad que serán los responsables de la entropía del agujero negro [14].

Originalmente, dentro de esta teoría, el cálculo de la entropía de agujeros negros se inició por los trabajos de Rovelli y Krasnov [15, 16]. Sin embargo, nada en estos trabajos hacía referencia a que el cálculo estuviera comprometido con un horizonte. Por este motivo en el trabajo seminal de Ashtekar, Baez, Corichi y Krasnov [14] se incorporó el concepto de horizonte aislado y se cuantizó un espaciotiempo con dicho horizonte como frontera interna. Es en este esquema en el que se basan los cálculos presentados en esta tesis.

Los puntos esenciales a destacar en esta tesis son los siguientes:

1. Dado que trabajaremos usando la descomposición $3+1$ de la relatividad general, en esta memoria llamaremos usualmente a horizonte a la superficie (esférica) bidimensional que es la intersección de la 3-superficie

de Cauchy con el horizonte aislado. Sobre este horizonte tendremos definida una teoría de Chern-Simons que, como veremos, tiene $U(1)$ como grupo gauge. Uno de los principales puntos de esta tesis es el intento de relacionar el cálculo de la entropía de horizontes aislados en LQG con una teoría de campos cuánticos invariantes conformes (CFT) siguiendo la analogía de Witten [17]. Expondremos este resultado en el capítulo 4.

2. Mostraremos cómo el esquema geométrico que lleva a la identificación de los estados responsables de la entropía del agujero negro se puede traducir a un problema combinatorio. Los estados quedan definidos por unas listas de etiquetas semienteras que han de verificar ciertas condiciones. Esto será explicado en el capítulo 5 de esta tesis.

3. En la literatura aparecen dos identificaciones distintas de los estados de superficie que varían en las etiquetas asignadas, las propuestas de Domagala, Lewandowski y Meissner (DLM) [18] y la de Ghosh y Mitra (GM) [19]. En esta tesis mostraremos los resultados para los dos casos sin entrar en el problema de juzgar cuál de las dos definiciones es correcta. Sin embargo, sí que expondremos las diferencias y similitudes entre ambos recuentos.

4. Explicaremos brevemente ambos conteos y mostraremos las hipótesis y los resultados que dan sobre la entropía del agujero negro. Ambos reproducen una entropía proporcional al área y una corrección logarítmica de coeficiente $(-1/2)$. Ahora bien, en la definición de los operadores geométricos en LQG depende de un parámetro indeterminado, conocido como parámetro γ de Barbero-Immirzi (BI) [28]. Para recuperar el resultado $A/4$ (en las unidades correspondientes) se ha de fijar el valor de dicho parámetro. El problema es que los conteos expuestos dan un valor distinto para γ.

5. Originalmente estos conteos se efectuaron en el límite asintótico de grandes áreas. En esta tesis mostraremos un conteo detallado de los estados mediante un algoritmo computacional de conteo explícito de estados. Este algoritmo, que sólo alcanza agujeros negros de varios cientos de areas de Planck debido al crecimiento exponencial del número de estados a contar, sirve para verificar los resultados previos para ambos conteos.

6. Adicionalmente encontraremos una oscilación en la entropía que, en cada conteo, tiene un periodo constante. Como sabemos, para calcular la entropía en un colectivo microcanónico fijamos la variable macroscópica de interés, en este caso el área del agujero negro A_0 y contamos los estados que caen dentro del intervalo $[A_0 - \delta, A_0 + \delta]$. Mostraremos que para un

valor concreto de δ se obtiene una entropía discretizada, es decir que aumenta con el área como una función de tipo escalera. Estudiaremos cuidadosamente esta estructura en la tesis.

7. El estudio del origen de esta escalera nos llevará a identificar una curiosa estructura en bandas en la degeneración de estados de superficie. La distancia entre los picos de estas bandas es justamente el valor del periodo de las oscilaciones encontradas en el algoritmo de conteo o en la anchura de los escalones de la entropía. De hecho, la distancia entre picos es numéricamente similar a $\Delta A = 8 \ln 3\gamma$, donde γ será el valor del parámetro de Barbero-Immirzi en cada conteo expuesto. Una de las cuestiones abiertas es si ciertamente este ΔA es proporcional a $8 \ln 3$. (Ver [20] para una perspectiva diferente).

8. Posteriormente se describirá por qué en los conteos DLM y GM no hay señales de este comportamiento escalonado de la entropía con el área y se mostrará que efectivamente se puede argumentar que dichos conteos contienen dicha información. De hecho, encontramos cotas a la desviación de ΔA con respecto al valor $8\gamma \ln 3$. Desgraciadamente aún estamos lejos de encontrar este valor de forma analítica.

9. Para finalizar, mostraremos cómo podemos modificar el conteo para incorporar técnicas procedentes de teoría de números. La principal motivación en ese punto está relacionada con el deseo de resolver el problema combinatorio de una forma analítica. En concreto nuestro objetivo es llegar a una expresión manejable que nos permita obtener un desarrollo asintótico para determinar si efectivamente esta estructura en escalera de la entropía se mantiene para agujeros negros de grandes áreas. Este tratamiento es interesante por varios motivos, el primero es que permite una reexpresión del espectro del operador área, que como mostraremos es muy conveniente y efectiva. Por otro lado, permite dar una solución completa al problema combinatorio, siendo capaces de aislar todas las fuentes de degeneración tal y como explicaremos en la sección 4.6. Es importante comentar que la solución del problema combinatorio, escrita en estos términos, conduce a expresiones que habrán sido mostradas en el tratamiento del problema con técnicas de CFTs, lo cual parece indicar la robustez de ambos métodos. Además estas técnicas permiten reexpresar el problema en términos de funciones generatrices [21] que hacen que la implementación computacional del problema y su estudio asintótico sean más manejables. Finalmente, aunque aún no hay resultados definitivos, estamos trabajando para confirmar o descartar la persistencia del fenómeno de la discretización de la entropía a escalas macroscópicas.

Nos gustaría insistir en que los resultados expuestos en esta tesis tienen validez única y exclusivamente dentro del contexto de la cuantización de horizontes aislados dentro del esquema propuesto por ABCK en LQG. Durante la tesis indicaremos cuáles son los posibles problemas de este esquema. Por supuesto, lo deseable sería poder identificar procesos de colapso y formación de agujeros negros dentro de la teoría completa y no tener que recurrir a una cuantización de un espaciotiempo clásico con una frontera desde el inicio. Sin embargo, el formalismo ABCK es un magnífico punto de partida para estudios más ambiciosos y ha mostrado con creces su potencia y versatilidad. Dados los últimos avances, de los cuales esta tesis forma una pequeña parte, se abren ante nosotros nuevas posibilidades que nos permitiran y mejorando este modelo. En concreto, las nuevas líneas de investigación que esperamos afrontar en un futuro próximo dentro de este tema serán:

- Aclarar el papel jugado por la teoría de Chern-Simons y su conexión con teoría de campos con invariancia conforme. Esta cuestión se enfocará en dos vertientes. Por un lado es necesario reformular este problema empelando una teoría de Chern-Simons $SU(2)$ y estudiar de qué forma se induce la restricción al $U(1)$ que aparece en el contexto de los horizontes aislados como frontera interna. Además, es de sumo interés identificar que CFT es la análoga a esta Chern-Simons $U(1)$. Esta línea es de gran relevancia principalmente por dos motivos: el primero es que mejoraría nuestro entendimiento del problema y podría dilucidar cuales son las etiquetas correctas de los estados de superficie, diferenciando entonces entre el conteo DLM y el GM. En segundo lugar, esta perspectiva es muy cercana al espíritu del cálculo de la entropía en teoría de cuerdas pudiendose encontrar puntos en común entre ambas formulaciones.

- Son muy sugerentes las similitudes formales que aparecen entre este esquema y los modelos teóricos del efecto Hall cuántico. El efecto Hall cuántico se basa en física bidimensional donde los electrones en una placa metálica sometida a un campo magnético se pueden considerar sometidos a una teoría de tipo Chern-Simons abeliana siendo los electrones considerados defectos topológicos de la superficie. Un estudio detallado de este punto podría abrir la puerta a poder reformular el problema empleando las técnicas usadas en teoría de materia condensada. Aunque parece que la similitud no es directa, creemos que es un punto abierto que es importante estudiar.

- Una comprensión más profunda de la degeneración de estados en un agujero negro podría abrir las puertas para un estudio sobre la espectroscopía de los agujeros negros en este contexto. Tenemos resultados preliminares [22] que necesitan de una mayor formalización.

Dentro de la cuantización canónica no perturbativa de la relatividad general hay otras propuestas para calcular la entropía de agujeros negros [23]. En esta tesis no tratamos sobre estos temas, sin embargo sería interesante ver cuales son los puntos comunes con el formalismo presentado aquí y si estos resultados ser extrapolados a otros esquemas.

Durante la redacción final de esta tesis han aparecido dos artículos [24, 25] que plantean situaciones interesantes en el tema de la entropía de agujeros negros en LQG, dentro del esquema de horizontes aislados, que se apartan en cierto modo del formalismo original dado por [14], en el cual se basa este trabajo. En [24] se da una explicación a un problema que expondremos en este trabajo relacionado con el nivel de la teoría de Chern-Simons. Como veremos, dicho nivel está relacionado en este contexto con el área del horizonte de un agujero negro, sin embargo esta cantidad ha de ser un número natural para poder acometer el proceso de cuantización. Indicaremos qué solución se dió en ABCK y en qué se contrapone con el artículo indicado.

Por otro lado, los resultados presentados en [25] parecen indicar que el formalismo puede acomodarse para incorporar una teoría de Chern-Simons con grupo gauge $SU(2)$ en el horizonte. Como expondremos, en ABCK los grados de libertad en el horizonte vienen dados por una teoría abeliana. En nuestra opinión esta característica es inherente al formalismo de horizonte aislados, por lo que un estudio de este artículo será muy interesante. Sin embargo, las técnicas de conteo que vamos a presentar en esta tesis pueden resolver el problema del cálculo de la entropía dentro del esquema presentado en [25] como ha sido puesto de manifiesto en [26].

PUBLICATIONS

The bulk of this Ph.D. is based on the following publications:
Esta tesis ha dado lugar a las siguientes publicaciones:

- Alejandro Corichi, Jacobo Díaz-Polo and Enrique Fernández-Borja
  Quantum geometry and microscopic black hole entropy
  Class. Quantum Grav **24**, 243-251 (2007).

- Alejandro Corichi, Jacobo Díaz-Polo and Enrique Fernández-Borja
  Black Hole Entropy Quantization
  Phys. Rev. Lett. **98**, 181301 (2007).

- Alejandro Corichi, Jacobo Díaz-Polo and Enrique Fernández-Borja
  Loop quantum gravity and Planck-size black hole entropy
  J. Phys. Conf. Ser. **68**, 012031 (2007).

- Jacobo Díaz-Polo and Enrique Fernández-Borja
  Black hole radiation spectrum in loop quantum gravity: isolated horizon framework
  Class. Quantum Grav. **25**, 105007 (2008).

- Iván Agulló, Jacobo Díaz-Polo and Enrique Fernández-Borja
  Black hole state degeneracy in loop quantum gravity
  Phys. Rev. D **77**, 104024 (2008).

- Iván Agulló, J. Fernando Barbero G., Jacobo Díaz-Polo, Enrique Fernández-Borja and Eduardo J. S. Villaseñor
Black Hole State Counting in Loop Quantum Gravity: A Number-Theoretical Approach
Phys. Rev. Lett. **100**, 211301 (2008).

- Iván Agulló, Enrique F. Borja and Jacobo Díaz-Polo
Computing Black Hole entropy in Loop Quantum Gravity from a Conformal Field Theory perspective
To appear in JCAP [`arXiv:0903.1667`] (2009).

- Iván Agulló, J. Fernando Barbero G.,Enrique F. Borja, Jacobo Díaz-Polo and Eduardo J. S. Villaseñor
The combinatorics of the $SU(2)$ black hole entropy in loop quantum gravity [`arXiv:0903.1667`] (2009).

CONTENTS

1. INTRODUCTION TO LQG

En este capítulo introduciremos brevemente la teoría de gravedad cuántica de lazos (loop quantum gravity, LQG). Identificaremos los estados descritos por redes de espín (spin networks) que conforman el espacio de Hilbert cinemático de la teoría y mostraremos la construcción del operador área que es el relevante en este trabajo.

Loop quantum gravity (LQG) is an attempt to make a consistent canonical quantization of general relativity (GR) [27]. This means that the main motivation for LQG is to enforce the diffeomorphism invariance of GR, for which one has to consider the geometry of the spacetime as a dynamical object at the same level as the other usual fields (matter fields). This kind of considerations leads to the neccesity of formulating the quantum theory of gravity in a background-free way. The aim of LQG is perhaps modest, its basic building blocks are GR and quantum mechanics (QM), but the principal task is the understanding of a background free quantum theory. As we will briefly sketch in this chapter the usual canonical quantization method requires important modifications in order to accomodate this point of view.

1.1 Preliminary ideas

LQG is constructed on the basis of the Ashtekar variables [6, 7, 11], that are gauge connections. The standard way of reaching LQG is to rewrite the Einstein-Hilbert action in term of these fields. In this setting, GR is recast, in some sense, as a Yang-Mills theory plus the proper constraints of the theory. In this section we present the basic steps to reach this formulation at the classical level.

The quantum theory is based on the Hamiltonian formalism, for which we consider that the four dimensional spacetime manifold $\mathcal{M}$ is topologicaly $\mathcal{M} = M \times \mathbb{R}$, where M is a 3-dimensional manifold and, through this chapter, we will take it to be a closed manifold (compact and whithout boundary). In terms of metric q_{ab} (the labels a, b stand for spatial indices) on M the phase space variables consist in the pairs $(q_{ab}, \tilde{\pi}^{ab})$, where the canonical momenta $\tilde{\pi}^{ab}$

are constructed from the extrinsic curvature K_{ab} of M and its trace K,

$$\tilde{\pi}^{ab} = \sqrt{q}\,(K^{ab} - \frac{1}{2} q^{ab}\,K). \tag{1.1}$$

The only nonvanishing Poisson bracket is:

$$\{\tilde{\pi}^{ab}(x), q_{cd}(y)\} = 2\kappa\,\delta^{a}_{(c}\,\delta^{b}_{d)}\,\delta^{3}(x,y), \tag{1.2}$$

where $x, y \in \mathcal{M}$ and $\kappa = \frac{8\pi\ell_{\mathrm{P}}^2}{\hbar}$.
The $(3+1)$ decomposition of the Einstein-Hilbert action [27] shows, after the appropriate canonical transformations, that the full Hamiltonian of the theory vanishes on shell. This indicates that GR is a fully constrained system, with constraints:

$$\mathcal{V}^b = D_a\,(\tilde{\pi}^{ab}) \approx 0 \qquad \text{and} \qquad \mathcal{S} = \sqrt{q}\,\left[R^{(3)} + q^{-1}(\tfrac{1}{2}\tilde{\pi}^2 - \tilde{\pi}^{ab}\tilde{\pi}_{ab})\right] \approx 0, \tag{1.3}$$

where $\approx$ means equality on shell. D_a is the covariant derivative compatible with the spatial metric q_{ab} and $R^{(3)}$ is the scalar curvature of the three dimensional manifold M.

$\mathcal{V}^b$ is called the vector constraint, which generates spatial diffeomorphisms on the 3-manifold, and $\mathcal{S}$ is the scalar constraint, which generates time evolution.

At this point it is important to translate this framework into the language of triads. This is a intermediate step in order to arrive at the connection formulation based on the Ashtekar variables. One can define the co-triads e^i_a through this relation:

$$q_{ab} = e^i_a\,e^j_b\,\delta_{ij}, \tag{1.4}$$

where δ_{ij} is the metric in the internal space of the frames and $i, j = 1, 2, 3$ labels that frames.

It is worth noting that we are enlarging the phase space because the co-triads e^i_a have 9 degrees of freedom in contrast with the metrics q_{ab} that just have 6. But, in this case, we have a new symmetry in the theory because (1.4)is clearly invariant under rotations. For this reason we have an additional constraint in the theory.

Now we are going to introduce an important object, the densitized triad:

$$\tilde{E}^a_i = \tfrac{1}{2}\,\epsilon_{ijk}\epsilon^{abc}\,e^j_b\,e^k_c, \tag{1.5}$$

where ϵ^{abc} is the naturally defined density one Levi-Civita, antisymmetric object. The interest of this densitized triad is that it containts all the information about the spatial metric and its determinant.

$$\tilde{E}^a_i \tilde{E}^b_j \delta^{ij} = q\, q^{ab}. \tag{1.6}$$

This property will be very useful in order to construct geometrical quantities like areas o volumes. Moreover, $\tilde{E}$ could be considered as the canonical conjugate momentum of the Ashtekar connection as we will be see in the following section.

1.2 Ashtekar variables

One can introduce the Ashtekar variables as follows:

$$^{\gamma}A^i_a := \Gamma^i_a + \gamma\, K^i_a, \tag{1.7}$$

where Γ^i_a is the *spin connection* compatible with the triad,

$$\partial_{[a} e^i_{b]} + \epsilon^i{}_{jk}\, \Gamma^j_a\, e^k_b = 0,$$

and K^i_a can be constructed from the densitized triad and the extrinsic curvature of the spatial manifold. It is important to note that since A^i_a is the combination of a connection with a vector, it is a connection itself.

It is important to note that $^{\gamma}E^a_i = E^a_i/\gamma$ is the conjugate variable associated with $^{\gamma}A^i_a$. The presence of the real parameter γ, the *Barbero-Immirzi* (BI) [28] parameter, labels a one-parameter family of classicaly (but not quantum mechanically) equivalent theories for each value of γ. In order to simplify the notation we will omit this label through the rest of the text. So, the canonical Poisson brackets in terms of this new conjugate pair are:

$$\{^{\gamma}A^i_a(x), ^{\gamma}\tilde{E}^b_j(y)\} = \kappa\, \delta^b_a\, \delta^i_j\, \delta^3(x,y)\,, \tag{1.8}$$

and,

$$\{^{\gamma}A^i_a(x), ^{\gamma}A^j_b(y)\} = \{^{\gamma}\tilde{E}^a_i(x), ^{\gamma}\tilde{E}^b_j(y)\} = 0. \tag{1.9}$$

A final comment. In the literature is usual to find that A^i_a is an $su(2)$ connection, the reason is that this algebra is isomorphic to $so(3)$ and $SO(3)$ is the original group introduce as the freedom inherent to the choosing the triads. However, we take $SU(2)$ instead of $SO(3)$ as the gauge group because $SU(2)$ is the preferred choice if one would incorporate fermions in the theory. So, we can say that the phase space of LQG is analogous to a $SU(2)$ Yang-Mills theory with the characteristic constraints of GR.

1.2.1 Constraints in terms of Ashtekar's variables

At this point we need rewriting the constraints in terms of the new variables (A, E) in which we want to describe GR. First of all the constraint associated with the invariance of the spatial metric through the $SU(2)$ transformations acting on the triads takes a very simple, and well known, form:

$$G_i = \mathcal{D}_a \tilde{E}^a_i \approx 0, \tag{1.10}$$

where $\mathcal{D}$ refers to the covariant derivative defined by the A^a_i, that is, $\mathcal{D}_a \tilde{E}^a_i = \partial_a \tilde{E}^a_i + \epsilon_{ij}{}^k A^j_a \tilde{E}^a_k$. It is easy to recognize the aparience of the Gauβ's law as is usual in Yang-Mills theor. This is the reason why $\tilde{E}^a_i$ is called *electric field*.

On the other hand, for the vector and scalar constraints we have,

$$\mathcal{V}_a = F^i_{ab} \tilde{E}^b_i - (1+\gamma^2) K^i_a G_i \approx 0 \tag{1.11}$$

where F^i_{ab} is the curvature of the connection. Finally, the scalar constraint takes the form

$$\mathcal{S} = \frac{\tilde{E}^a_i \tilde{E}^b_j}{\sqrt{\det(\tilde{E})}} \left[\epsilon^{ij}{}_k F^k_{ab} - 2(1+\gamma^2) K^i_{[a} K^j_{b]} \right] \approx 0. \tag{1.12}$$

1.3 Classical algebra of observables

In this section we will look for the phase space functionals that allow us to make a non-perturbative quantization consistent with the diffeomorphism invariance of GR. To this end we need constructing functionals which do not make reference to any fixed metric background. In order to accoplish this objective we have to study functionals of the connection and of the electric field.

We have to be consistent with the constraints of GR, so we will follow the Dirac point of view in the quantization procedure. This means that we will quantize the classical phase space obtaining as first step a kinematical Hilbert space, $\mathcal{H}_{\text{kin}}$, and them we will impose those constraints as operators on it. As will be manifest, this procedure is cumbersome because of the difficulty to define these operators. LQG provides us with a rigourous definition of $\mathcal{H}_{\text{kin}}$ and we can define some geometrical operators on it, such as areas and volumes.

The first attempts to choose the classical algebra of observables were based on the connection representation, but this leads to serious difficulties to define the theory. In order to respect the background independence that we are asking for the theory we can select the holonomy defined by the connection. An holonomy, $h_\alpha(A)$, is computed as the path ordered exponential of the integral of the connection around a loop α (a path in the manifold M), and we can

think in this holonomy as an element of the corresponding gauge group, $SU(2)$ in our case:

$$h_\alpha(A) = \mathcal{P} \exp\left(\oint_\alpha A_a \, \mathrm{d}s^a\right) \tag{1.13}$$

The advantage of this object is that it serves as a basis for the construction of gauge invariant functions and that the holonomy is background independent.

The simplest example of a gauge invariant function is the Wilson loop, which is computed as the trace of the holonomy. The consideration of Wilson loops along all the possible loops defined on M define the so called holonomy algebra $\mathcal{HA}$ [11].

Nowadays, the theory is constructed employing graphs Υ. These graphs are a set of n oriented edges e_I, $I = 1, \ldots, n$, and V vertices v_μ. Usually one works with closed graphs which are graphs where every edge ends and begins in a vertex. The graphs can be obtained as a combination of loops based on each vertex. In this case, the connection can be understood as a map from the graph to n-copies of the gauge group G, one for each edge. Moreover, the behavior of the holonomies under spatial diffeomorphism is quite simple,

$$\phi_* \cdot h(e_I) = h(\phi^{-1} \cdot e_I)\,, \tag{1.14}$$

where $\phi : M \to M$, is a spatial diffeomorphism and $h(e_I) = h_{e_I}(A)$ stands for the holonomy computed on an edge of a given graph. This means that the holonomy transforms convariantly under diffeomorphisms because the effect of transform is simply to move the edge in a natural way.

Following these ideas, we define the configuration space $\mathcal{A}_\Upsilon$ as the space constructed by assigning a holonomy to each edge to a graph. This space can be shown to be homeomorphic to $G^n = G \times \cdots \times G$. This construction is very symilar to the configuration space used in floating lattice gauge theory over the graph Υ.

The next step is to define the *cylindrical functions*:

$$C_\Upsilon := c(h(e_1), h(e_2), \ldots, h(e_N)) \tag{1.15}$$

that are functions of the connection through the holonomy along the edges of an embedded graph. The name of cylindrical functions comes from the fact that we are just exploring the connection along the direccions defined in the corresponding edges e_I.

Let us present at this point the functions based on the canonicaly conjugate of the connection. Following the previous scheme the natural option is looking for a smeared version of the $\tilde{E}^a_i$. In this case, we can go to a dual Lie-algebra valued two form from the $\tilde{E}^a_i$,

$$\Sigma_{ab\,i} := \tfrac{1}{2}\, \eta_{abc}\, \tilde{E}^c_i, \tag{1.16}$$

where η_{abc} is the naturally defined Levi-Civita symbol. This object should be smeared over a smooth bidimensional surface,

$$E[S,f] := \int_S \Sigma_{ab\,i}\, f^i \,\mathrm{d}S^{ab}\,. \tag{1.17}$$

where f^i is a $su(2)$ Lie-algebra valued smearing function on the 2-surface S. This object can be seen as the 'electric flux', which, as is evident from its construction, is a background independent object. The holonomies and fluxes define the *Holonomy-Flux* algebra $\mathcal{HF}$ [6, 7, 11]. Classically we have the following Poisson bracket bewteen the cylindrical functions and the electric flux:

$$\{C_\gamma,\, E[S,f]\} = \frac{\kappa}{2}\sum_p \sum_{I_p} \iota(I_p)\, f^i(p)\, X^i_{I_p}\cdot c, \tag{1.18}$$

where the sum is over the points p where the edges e_I of the given graph intersect the surface S, the I_p take into account the edges incoming or outgoing from p and $X^i_{I_p}\cdot c$ is the action of the i-th left/right invariant vector field on the I_p-th copy of the group if the I_p-th edge is pointing away /towards (resp.) the surface S. It is worth noting that the r.h.s. is non-vanishing only at those points where the graph Υ, the support for C_Υ, intersects the surface.

Finally, we have defined the classical observables which will be the basis for quantization, namely, the holonomies of the connection over edges of a given graph $h(e_I)$ and the smeared triad over a surface S, $E[S,f]$.

1.4 Quantization: The Hilbert space.

The purpose of this section is to provide a sketch of the quantization and the resulting kinematical Hilbert space of LQG. The details of this construction can be found in [11]. As usual, we have to define functions of the connection (analogous to choosing the configuration representation of wave functions in quantum mechanics) and a measure on this space to construct a well-defined inner product in the final Hilbert space.

Let us briefly describe now the essential ingredients of the construction of the kinematical Hilbert space of LQG.

1.4.1 Quantum configuration space and measure

We would like to define the kinematical Hilbert space as a L^2-space over the configuration space $\mathcal{H}_{\text{kin}} = L^2(\overline{\mathcal{A}}, \mathrm{d}\mu)$. So, we need indentifying the appropriate 'quantum' configuration space, the space $\overline{\mathcal{A}}$ consists of generalized connections [11]. In this case we do not require continuity of the connections. These

generalized connections act on the edges of a given graph and assing a group element to it. Moreover, the following composition rule holds for them:

$$h(e_1 \circ e_2) = h(e_1) \cdot h(e_2)\,;\ \forall\, e_I.$$

Another way to characterize the quantum configuration space is based on the projective limit procedure over graphs. To be concrete, for any given graph Υ with n edges we have a configuration space $\mathcal{A}_\Upsilon = SU(2)^n$. We can employ the natural invariant Haar measure (μ_H) on the $SU(2)$ group. In this case we can endow $\mathcal{A}_\Upsilon$ with a measure by simply taking the Haar measure on all copies of the group in the given graph. This allows us to consider square integrable funcitions in this setting. So, we can work out the following Hilbert space:

$$\mathcal{H}_\Upsilon = L^2(\mathcal{A}_\Upsilon, \mathrm{d}\mu_\Upsilon). \tag{1.19}$$

The key point for LQG is that we must to consider all the possible graphs on M and their associated configuration spaces $\{\mathcal{A}_\Upsilon\}_\Upsilon$. This leads to a family of Hilbert spaces $\{\mathcal{H}_\Upsilon\}_\Upsilon$, but these spaces must to be consistent with a partial ordering relation in the set of graphs. For a given pair of graphs, Υ and Υ', we say that Υ is larger than Υ' if the former contains the later, $\Upsilon \geq \Upsilon'$. We can introduce a projection $P_{\Upsilon\Upsilon'} : \Upsilon \to \Upsilon'$, which induces a projection operator in the configuration spaces and an inclusion operator for Hilbert spaces, namely: $P : \mathcal{A}_\Upsilon \to \mathcal{A}_{\Upsilon'}$, $\iota : \mathcal{H}_{\Upsilon'} \to \mathcal{H}_\Upsilon$. We need to be sure that a function defined on a graph is well defined on larger graphs, an important condition being that the inner product, between cylindrical functions, must be independent of the graph choosen to work on.

Following those arguments we can think of $\overline{\mathcal{A}}$ as the configuration space for the 'largest graph', so the $\mathcal{H}_{\mathrm{kin}}$ is the largest space containing all the $\{\mathcal{H}_\Upsilon\}$ in the projective set [7, 11]. In this picture we can define a measure μ_{AL}, known as the Ashtekar-Lewandowski measure, whose projection on an $\mathcal{A}_\Upsilon$ is the corresponding Haar measure μ_Υ. Eventualy, the $\mathcal{H}_{\mathrm{kin}} = L^2(\overline{\mathcal{A}}, d\mu_{AL})$ is the resulting Hilbert space, and it can be shown that the cylindrical functions introduced in the previous section belong to it.

1.4.2 Spin Networks: The Hilbert space basis

In the last subsection we have introduced the kinematical Hilbert space of LQG. We can understand it as the Hilbert space which contains the individual Hilbert spaces over all possible graphs Υ's in the spatial manifold, so we will denote it as:

$$\mathcal{H}_{\mathrm{kin}} = \otimes_\Upsilon \mathcal{H}_\Upsilon.$$

This Hilbert space is non-separable, but we can easily define a basis for each $\mathcal{H}_\Upsilon$. For this purpose, let us consider a single edge e_i of a given graph and decompose any function f on the group $SU(2)$, this decomposition reads:

$$f(g) = \sum_j \sqrt{j(j+1)}\, f_j^{mm'} \overset{j}{\Pi}_{mm'}\ (g), \tag{1.20}$$

where, we can employ the Peter-Weyl decomposition for $SU(2)$ and find the coefficients of this decomposition:

$$f_j^{mm'} = \sqrt{j(j+1)} \int_G \overset{j}{\Pi}_{mm'}\ (g^{-1})\, f(g) \mathrm{d}\mu_H(g), \tag{1.21}$$

in this case the functions $\overset{j}{\Pi}_{mm'}\ (g)$ are unitary representations of the group labeled by j (for the irreps), so they are the analogues of the Fourier basis in the decomposition.

Given a cylindrical function $\Psi_\Upsilon[A] = \psi(h(e_1), h(e_2), \ldots, h(e_N))$, we can then write an expansion for it as

$$\begin{aligned} \Psi_\Upsilon[A] &= \psi(h(e_1), h(e_2), \ldots, h(e_N)) \\ &= \sum_{j_1 \cdots j_N} f_{j_1 \cdots j_N}^{m_1 \cdots m_N, n_1 \cdots n_N}\ \phi^{j_1}_{m_1 n_1}(h(e_1)) \cdots \phi^{j_N}_{m_N n_N}(h(e_N)), \end{aligned} \tag{1.22}$$

where $\phi^j_{mn}(g) = \sqrt{j(j+1)}\ \overset{j}{\Pi}_{mn}\ (g)$ is the normalized function satisfying

$$\int_G \mathrm{d}\mu_\mathrm{H}(g)\, \overline{\phi^j_{mn}(g)}\ \phi^{j'}_{m'n'}(g) = \delta_{j,j'}\delta_{m,m'}\delta_{n,n'}\,.$$

The expansion coefficients can be obtained by projecting the state $|\Psi_\Upsilon\rangle$,

$$f_{j_1 \cdots j_N}^{m_1 \cdots m_N, n_1 \cdots n_N} = \langle\, \phi^{j_1}_{m_1 n_1} \cdots \phi^{j_N}_{m_N n_N} \mid \Psi_\Upsilon \rangle \tag{1.23}$$

which implies that we have a complete orthonormal basis for $\mathcal{H}_\mathrm{kin}$, so we can write

$$\mathcal{H}_\Upsilon = \otimes_j \mathcal{H}_{\Upsilon,j}; \tag{1.24}$$

where in the case of a single loop α we have $\mathcal{H}_{\alpha,j}$, a $(2j+1)$ dimensional Hilbert space [6, 7]. On the other hand, for a graph we have extra labels, the intertwiners, associated with the vertices, and the finite dimension of $\mathcal{H}_{\Upsilon,j}$ precisely acounts for this extra degrees of freedom. For this reason we can introduce an additional label for the graph, and obtain the resulting Hilbert space as

$$\mathcal{H}_\Upsilon = \otimes_j \mathcal{H}_{\Upsilon,j} = \otimes_{j,l} \mathcal{H}_{\Upsilon,j,l} \tag{1.25}$$

where each $\mathcal{H}_{\Upsilon,j,l}$ is one-dimensional, [6, 11].

An important issue is the gauge invariance of the states previously defined. In order to guarantee that invariance under finite gauge transformations of the connection we need to be consistent with a restriccion on the vertices of the defining graph of the cylindrical functions, namely

$$\sum_{v}\sum_{e_v} X^{i}_{e_v}\cdot\mathcal{N}\left[\Upsilon_{j,l},A\right]=0. \tag{1.26}$$

As this expresion indicates we have a sum over vertices v of the graph and a sum over the edges e_v for each vertex. The spin networks for which this condition holds are the 'gauge invariant spin networks'. This implies that the graph must be closed, in other words, without open edges. In the contex of spacetimes with inner boundaries we will see that there are some edges that 'end' at the boundary, so the gauge invariance restriccion takes the form of a boundary condition. This is a pivotal point in the geometrical framework which leads to the entropy counting.

1.5 Area Operator

Until this point we have introduced the basic elements for the construction of the kinematical Hilbert space. Now we are interested in the definition of the area operator acting on this space that plays a central role in the black hole entropy computation. Of course, there exist operators for volume and length, but in this thesis we are just concernied with the area. For an extensive treatment of the geometrical operators see [11, 29].

Classically the area associated to a surface S can be computed as

$$A[S]=\int_S d^2x\sqrt{h}.$$

The simplest operator that can be constructed representing the geometrical quantities of interest is the *area operator* associated to a surface S. The reason behind this is again the fact that the densitized triad is dual to a two form that can be naturally integrated along a surface. The difference between the classical expression for the area and the flux variable is the fact that the area is a gauge-invariant quantity. Let us first recall what the classical expression for the area function is, and then we will outline the regularization procedure to arrive at a well defined operator on the Hilbert space. The area $A[S]$ of a surface S is given by $A[S]=\int_S \mathrm{d}^2x\,\sqrt{h}$, where h is the determinant of the induced metric h_{ab} on S. When the surface S can be parametrized by setting, say, $x^3=0$, then the expression for the area in terms of the densitized triad

takes a simple form:

$$A[S] = \gamma \int_S \mathrm{d}^2x \, \sqrt{\tilde{E}^3_i \, \tilde{E}^3_j \, k^{ij}} \tag{1.27}$$

where $k^{ij} = \delta^{ij}$ is the Killing-Cartan metric on the Lie algebra, (recall that the canonical conjugate to ${}^\gamma A^i_a$ is ${}^\gamma \tilde{E}^a_i = \tilde{E}^a_i/\gamma$). Note that the functions are again smeared in two dimensions and that the quantity inside the square root is basically the square of the (local) flux. One expects, from the experience with the flux operator, that the resulting operator will be a sum over the intersection points p, so one should focus the attention on the vertex operator

$$\Delta_{S,\Upsilon,p} = -\left[(\hat{J}^p_{i(u)} - \hat{J}^p_{i(d)})(\hat{J}^p_{j(u)} - \hat{J}^p_{j(d)})\right] k^{ij}.$$

With this, the area operator takes the form,

$$\hat{A}[S] = \gamma \, \ell_{\mathrm{P}}^2 \sum_p \widehat{\sqrt{\Delta_{S,\Upsilon,p}}}. \tag{1.28}$$

We can now combine both the form of the vertex operator with Gauβ' law $(\hat{J}^p_{i(u)} + \hat{J}^p_{i(d)}) \cdot \Psi = 0$ to arrive at,

$$|(\hat{J}^p_{i(u)} - \hat{J}^p_{i(d)})|^2 = |2(\hat{J}^p_{i(u)})|^2, \tag{1.29}$$

where we are assuming that there are no tangential edges. The operator $\hat{J}^p_{i(u)}$ is an angular momentum operator, and therefore its square has eigenvalues equal to $j^u(j^u+1)$ where j^u is the label for the total 'up' angular momentum. We can then write the form of the operator

$$\hat{A}[S] \cdot \mathcal{N}(\Upsilon, \vec{j}) = \gamma \, \ell_{\mathrm{P}}^2 \sum_{v \in V} \sqrt{|\hat{J}^p_{i(u)}|^2} \cdot \mathcal{N}(\Upsilon, \vec{j}). \tag{1.30}$$

With these conventions, in the case of simple intersections between the graph Υ and the surface S, the area operator takes the well known form

$$\hat{A}[S] \cdot \mathcal{N}(\Upsilon, \vec{j}) = \gamma \, \ell_{\mathrm{P}}^2 \sum_{v \in V} \sqrt{j_v(j_v+1)} \cdot \mathcal{N}(\Upsilon, \vec{j}),$$

when acting on a *spin network* $\mathcal{N}(\gamma, \vec{j})$ defined over Υ and with labels $\vec{j}$ on the edges (we have not used an extra label for the intertwiners).

Let us now interpret these results in view of the new geometry that the loop quantization gives us. The one-dimensional excitations of the geometry carry a flux of area: whenever the graph pierces a surface it endows S with a quantum of area depending on the value of j. Furthermore, the eigenvalues of

the operator are discrete, giving a precise meaning to the statement that the geometry is quantized: there a minimum (non-zero) value for the area given by taking $j = 1/2$ in the previous formula. Thus the area gap $a_{\rm o}$ is given by

$$a_{\rm o} = \gamma\, \ell_{\rm P}^2 \frac{\sqrt{3}}{2}. \tag{1.31}$$

If the value of γ is of order of unity, then we see that the minimum area is of the order of the Planck area. In order to get a macroscopic value for the area we would need a very large number of intersections. The BI-parameter has to be fixed to select the physical sector of the theory. The current viewpoint is that the black hole entropy calculation can be used for that purpose.

There are operators corresponding to other geometrical objects such as volume, length, angles, etc. The main feature that area operator exhibits is that its spectrum is always discrete.

2. A BRIEF INTRODUCTION TO ISOLATED HORIZONS

En este capítulo introduciremos el concepto de horizonte aislado. Dichos horizontes tienen una definición geométrica cuasilocal, en contraposición con la definición global de los horizontes de sucesos. Describiremos la cuantización de un espaciotiempo que contiene a uno de dichos horizontes como frontera interna e identificaremos los estados responsables de la entropía del agujero negro.

The isolated horizon concept arises from the neccesity to generalize the event horizon definition. The event horizons are teleological in nature: to indentificate such an object one has to know the whole history of a given spacetime initial data. On the other hand, in many applications it is desirable a more local definition, and this is the main motivation for the introduction of isolated horizons. This kind of horizons have been fruitfully employed in different branches fo GR such as numerical relativity and mathematical physics [13].

The interest in isolated horizons is based in the following properties:

1. Their definition just implies local spacetime structures. Moreover, the horizon is stationary and the spacetime containing they are not required admit any Killing field.

2. The laws of the black hole mechanics are satisfied by these horizons. So, thermodynamical considerations make sense for them.

Let us recall the mathematical definition of isolated horizons:

A subset Δ of the boundary $\partial\mathcal{M}$ of a spacetime $(\mathcal{M}, g)$ is called an isolated horizon, provided that:

1. *$\Delta \equiv \mathbb{R} \times S^2$ is a null hypersurface and has zero shear and expansion and let l^a be its null normal.*

2. *The field equations and matter energy conditions hold at Δ.*

3. *The induced metric on Δ is Lie draged by the null generator l^a of Δ.*

Notice that all these geometrical conditions are imposed locally at Δ.

In this thesis we will interested in an undistorted, non-rotating isolated horizon [12, 13] that is an inner boundary placed in an asymptotically flat 4-dimensional spacetime. Moreover, these null surfaces are foliated by a family or marginally trapped 2-spheres such that the expansion of the inward pointing null normal to the foliation is constant and negative on each leaf. This foliation is unique and allows us to consider it as the definition of an isolated horizon.

To define the Hamiltonian framework we take a partial Cauchy surface M in this spacetime, so we find that the intersection of M with the horizon is a 2-sphere S. Due to the character of inner boundary of the isolated horizon one has to introduce boundary conditions in order to have a well-defined Hamilton framework in this context. The effects of the definition of isolated horizon and the boundary conditions are [14]:

1. The classical phase space defined for M is the usual one described in the previous chapter, (A, E).

2. Through the boundary conditions on the surface horizon the connection on the bulk is restricted to a $U(1)$ connection, W.

3. The gravitational action, and the symplectic structure, acquire a surface term in a natural way which describes a $U(1)$ Chern-Simons theory on the boundary S.

Let us remark that, as pointed out in [14], the $U(1)$ Chern-Simons theory appears in this framework in a natural way and that at the classical level the degrees of freedom at the horizon are determined by the bulk degrees of freedom by continuity. However, at the quantum level, once we introduce the generalized connections the surface states are independent of the bulk ones. On the other side, since the symplectic form splits in two parts, is natural to asume that the total quantum Hilbert space will be contained in the tensor product of a volume (or bulk) Hilbert space and a surface Hilbert space, $\mathcal{H}_V \otimes \mathcal{H}_S$.

Let us be more specific. The horizon boundary conditions can be understood as follows:

1. Only those 2-forms Σ for which the horizon area has the fixed value A_0 are admissible.

2. The pullback of A to the surface horizon is completely determined by a $U(1)$ connection W on the surface S and by the area A_0.

3. Finally, the pullback of Σ to S is completely determined by the curvature of W.

We can specify these conditions explicitly, let us fix a bijecction of the 2-sphere on itself, $r : S^2 \to S^2$. This r is fixed by a $U(1)$ subgroup of $SU(2)$. Then, the connection W can be defined as:

$$W_a := -\frac{1}{\sqrt{2}}\underline{\Gamma}^i_a r_i, \tag{2.1}$$

with curvature:

$$F_{ab} = -\frac{2\pi\gamma}{A_0}\underline{\Sigma}^i_{ab} r_i. \tag{2.2}$$

The quantities with the underbar indicate the pullbacks from the bulk to the horizon surface.

Taking all of this into account, we arrive at a phase space consisting pairs (A, Σ) of asymptotically flat, smooth fields on M satisfying the internal boundary conditions that define an isolated horizon. In this phase space we can find the following symplectic structure [14],

$$\begin{aligned}\Omega_{grav}((\delta A, \delta\Sigma), (\delta A', \delta\Sigma')) &= \frac{1}{8\pi G}\int_M Tr(\delta A \wedge \delta\Sigma' - \delta A' \wedge \delta\Sigma) \\ &+ \frac{A_0}{8\pi^2\gamma G}\oint_S \delta W \wedge \delta W',\end{aligned} \tag{2.3}$$

for arbitrary tangent vectors $(\delta A, \delta\Sigma)$ and $(\delta A', \delta\Sigma')$. It is worth noting that this symplectic structure has a surface term that corresponds to the one corresponding a Chern-Simons theory. We can say that the internal boundaries in spacetime gives rise to a Chern-Simons theory on them [11].

2.1 Quantization procedure

We have seen that on the surface we have an $U(1)$ Chern-Simons theory. Let us consider the action for this theory in its $2+1$ spliting

$$S_{CS} = \int_{\mathbb{R}} dt \int_S d^2x \epsilon^{\alpha\beta}(\dot{W}_\alpha W_\beta + 2W_t \partial_\alpha W_\beta). \tag{2.4}$$

We can see that this action leads to a trivial equation of motion, namely $F = 0$, where F is the curvature of the connection W. In the context of isolated horizon in LQG this equation will be modified.

We remark that we are not adding new degrees of freedom to the classical phase space, as reflected by the fact that we are not requiring that W to be closed. But, at the quantum level we promote these degrees of freedom to new dynamical ones, so we need to remove them imposing the boundary conditions

at this level. This means that we need implementing the constraint (2.2) as the kernel of an operator defined in $\mathcal{H}_V \otimes \mathcal{H}_S$, namely:

$$(1 \otimes \exp(i\hat{F}))\Psi = (\exp(-\frac{2\pi\gamma}{A_0}\hat{\underline{\Sigma}} \cdot r) \otimes 1)\Psi \tag{2.5}$$

where we make use of the exponentiated version of $\hat{F}$ to be consistent with the Chern-Simons theory [14]. This condition leads to the identification of a basis of the form $\psi_V \otimes \psi_S$ such that we can express:

$$\psi_V \otimes \exp(i\hat{F})\psi_S = \exp(-i\frac{2\pi\gamma}{A_0}\hat{\underline{\Sigma}} \cdot r)\psi_V \otimes \psi_S. \tag{2.6}$$

Fortunately, we know the eigenstates of $\hat{\underline{\Sigma}} \cdot r$ from LQG [29]

$$(\hat{\underline{\Sigma}} \cdot r)\psi_V = 8\pi\ell_{\mathrm{P}}^2 \sum_{i=1}^{n} m_i \delta^2(x, p_i)\eta\psi_V, \tag{2.7}$$

where we find that this operator takes values in a finite set of points on the surface S, called punctures, $\mathcal{P} = \{p_1, \ldots, p_n\}$, and m_i are half-integers known as spins. The $\delta^2(\cdot,\cdot)$ is the delta distribution on S and η is the Levi-Civita density on the horizon surface.

We can see here an interesting behavior because if the graph underlying the spin network (or linear combination of them) ψ_v does not intersect S, the right-hand side vanishes and so must the left-hand side. We can take an abritrarily small neighborhood D around a puncture, so that if $\mathcal{P} \cap D = \emptyset$ the same later argument holds. This means that the quantum curvature of W is flat except at the punctures, in this sense the flatness condition comming from the Chern-Simons theory does not follow from the analysis, and we must make the quantization of a Chern-Simons theory with punctures.

Surface Hilbert Space

Firstly we have to indetify the classical phase space related to the surface S. On one hand, we have a $U(1)$ connection W which is completely determined by the pullback of the connection A to the sphere S. This implies that the surface states will be funcitions of generalized $U(1)$ connections on S. So, by (2.7) we can work with generalized $U(1)$ connections that are flat everywhere except at $\mathcal{P}$, which are the points where the edges of the spin networks in the bulk pierce the surface S.

From the classical picture we can described the situation as follows. First, we have a $SU(2)$ principal bundle P on the bulk, and the restricction of this bundle to the sphere $P|_S$ has a $U(1)$ sub-bundle Q. Then, we can define a generalized connection on S as the map W which assign to each path η in S a holonomy $W(\eta)$ which can be considered as an element of $SU(2)$ taking

into account that we have a trivialization of $P|_S$ over each point of S. As it is shown in [14] the generalized connections defined in this way take values in the trivialization of the bundle Q, so we can understand this scheme as a symmetry breaking procedure (at least at the classical level). This will be very important later in the search of the relationship between this framework and the conformal field theory techniques. So, we are focussing in a sphere S with a finite set of points $\mathcal{P} = \{p_1, \ldots, p_n\}$, in this context we say that a generalized $U(1)$ connection W is flat except at the punctures when it assigns the same holonomies to paths as a connection W_0 on Q with the following properties:

1. W_0 is flat on $S - \mathcal{P}$.

2. For some neighborhood U_i of each puncture p_i, there exists some smooth trivialization of Q over U_i, and some analytic coordinate system (x, y) on U_i for which p_i has the coordinates (a, b), W_0 has the following form:

$$W_0 = W_1 + c\frac{(x-a)dy - (y-b)dx}{(x-a)^2 + (y-b)^2} \tag{2.8}$$

   on $U_i - \{p_i\}$, where $c \in \mathbb{R}$ and W_1 is a bounded smooth 1-form on $U_i - \{p_i\}$.

These conditions means that W is flat away from the punctures and at each puncture these is a singularity similar to the singularity produced by a magnetic flux line intersecting S transversely at a point in Maxwell theory. Moreover it is easy to show that W_0 assigns a well-defined holonomy to a path defined on S [14, 11]. For all these reasons we can work with the space of generalized $U(1)$ connections that are flat except at the punctures, a space that will be denoted $\mathcal{A}^{\mathcal{P}}$. We have the group of $U(1)$ gauge transformations (not necessarily continuous) of Q that equal the identity at the punctures, we denote this group by $\mathcal{G}^{\mathcal{P}}$ and the set $Diff^{\mathcal{P}}(S^2)$ of semianalytic diffeomorphisms which fix the points $\mathcal{P}$.

We take our phase space, denoted by $\mathcal{X}^{\mathcal{P}}$, as the quotient

$$\mathcal{X}^{\mathcal{P}} = \mathcal{A}^{\mathcal{P}}/(\mathcal{G}^{\mathcal{P}} \rtimes Diff^{\mathcal{P}}).$$

The reason for this is that the above semidirect product is a subgroup of the group of all automorphisms of the bundle Q and acts on $\mathcal{A}$ because of this space is defined in a gauge and diffeomorphism covariant way.

This phase space is *compact* and diffeomorphic to a $2(n-1)$-dimensional torus [14, 11]. This means that $\mathcal{X}^{\mathcal{P}}$ is topologically $U(1)^{n-1} \times U(1)^{n-1}$. In order to quantize it, we have to employ a geometric quantization procedure.

2.1.1 Coordinatizating $\mathcal{A}^{\mathcal{P}}$

We need to find suitable functions of the $U(1)$ connection W. The proper choice is to take the holonomies along arbitrary paths in S because these holonomies separate the points of the space of all connections, in the classical sector.

- We choose holonomies along closed loops in S and any open paths that connect the points of $\mathcal{P}$, these holonomies are invariant under $\mathcal{G}^{\mathcal{P}}$ transformations. We consider only holonomies along closed paths which enclose a puncture, otherwise the holonomy is trivial.

- It is worth noting that we are only interested in the homotopy type of paths with the same endpoints. The reason for this is that $Diff^{\mathcal{P}}$ does not change the homotopy type of a path because it preserves $\mathcal{P}$. So one cannot detach an open path from a puncture and one cannot drag a loop across any of them.

- For a set of n punctures we only need to fix $n-1$ mutually disjoint loops α_i and $(n-1)$ open paths β_i. The α_i encloses the puncture p_i and the β_i connect the puncture p_i with the puncture p_0. All the β_i arrive at p_0 in a C^∞ way.

- It is clear that a α_0 around the p_0 is the same that a path α encircling the $(n-1)$ punctures, because a path around all the punctures is contractible in S.

With this construction it is evident that the holonomies $W(\alpha_i)$ and $W(\beta_i)$ take values in $U(1)$, so, the phase space is topologically a $2(n-1)$ torus.

2.1.2 Induced symplectic structure

We are going to give now the induced symplectic structure in terms of the $W(\alpha_i)$ and $W(\beta_i)$ defined above.

- $\{W(\beta_i), W(\alpha_j)\} = \kappa\delta_{ij}W(\beta_i)W(\alpha_j)$ is the only non vanishing Poisson bracket.

- We can consider the phase space $\mathbb{R}^{2(n-1)}$ with canonical bracket $\{y_i, x_j\} = \delta_{ij}\kappa$. We recover the torus taking the quotient of $\mathbb{R}^{2(n-1)}$ by the discrete translation group $\Lambda_n = (2\pi\mathbb{Z})^{2(n-1)}$.

- This allows us to identify $W(\alpha_i)$ with $\exp(iy_i)$ and $W(\beta_i)$ with $\exp(ix_i)$.

- It is direct now to consider the symplectic structure which leads to these brackets: $\Omega = \frac{1}{\kappa'}\sum_{i=1}^{n-1} dy^i \wedge dx^i$

A very important point, in order to accomplish the geometric quantization procedure of this space is given by the prequantization step. This means that the Weil's integrality criterion must be satisfied [11]. If we take a closed two-surface on the torus, T^2_{ij} warping around the x_i, y_j directions and the non-trivial restriction from choosing $i = j$them:

$$\int_{T^2_{ii}} \frac{\Omega}{2\pi\hbar} = \frac{(2\pi)^2}{2\pi\hbar\kappa'} = 2\frac{A(S)}{8\pi\gamma\ell^2_{\mathrm{P}}} =: k, \tag{2.9}$$

where the integral above must be an integer number. This is the level of the Chern-Simons theory, the combination which appear in the surface part of the symplectic form, which at the light of the previous result must be integer.

2.1.3 States

Now we are going to give the states of the surface Hilbert space. Let us set $z = x + iy$ which defines the polarization on $\mathbb{R}^{2(n-1)}$, this is the positive Kahler polarisation, this makes that we can work within a complex $\mathcal{X}^{\mathcal{P}}$ which is a Kahler manifold. So, $\mathcal{H}^{\mathcal{P}}_S$ will be the space of holomorphic sections of a holomorphic complex bundle L over $\mathcal{X}^{\mathcal{P}}$ with a connection ∇ whose curvature is $i\Omega$. In this setting, the Hilbert space $\mathcal{H}^{\mathcal{P}}_S$ has a basis given by states ψ_a, which are *theta functions* [14, 11], as we let a range over vectors with congruents $a_i = \mathbb{Z}_k\backslash\{0\}$ for all i.

Of course, given theta functions $f(z)$ and $g(z)$ we have a inner product defined on this space:

$$\langle f, g\rangle = \int_{[0,2\pi]^{2(n-1)}} e^{-\frac{k}{2\pi}y\cdot y}\overline{f}(z)g(z)d^{n-1}xd^{n-1}y, \tag{2.10}$$

and the action of $\exp(-i\hat{F})$ on these states is given by:

$$\exp(-i\hat{F})\psi_{a_i} = e^{\frac{2\pi i a_i}{k}}\psi_{a_i}. \tag{2.11}$$

Sumarising, the Hilbert space $\mathcal{H}^{\mathcal{P}}$ has a basis given by the states ψ_a, where $a = (a_1, \ldots, a_n)$ with $a_i \in \mathbb{Z}_k\backslash\{0\}$ for all i. On the other hand, it is useful regard the a_i as elements of $\mathbb{Z}_k$, thus we need to require that:

$$a_1 + \cdots + a_n = 0 \in \mathbb{Z}_k; \tag{2.12}$$

we will explain the meaning of this expresion in the next section.

Finally, we can define the surface Hilbert space $\mathcal{H}_S$ as follows:

$$\mathcal{H}_S = \bigoplus_{\mathcal{P},a} \mathcal{H}^{\mathcal{P},a}_S$$

where the set of punctures is allowed to vary and the a ranges over the elements of $\mathbb{Z}_k^n$ compatible with 2.12. We need to add a restriction over the possible values of the a_i to be nonvanishing, because a state with $a_i = 0$ already is included in $\mathcal{H}_S^{\mathcal{P}-\{p_i\}}$.

2.1.4 The projection constraint

We have introduced the corresponding Hilbert spaces asociated to the bulk and the surface. Now we want to impose the constraint 2.5, called the projection constraint, on $\mathcal{H}_V \otimes \mathcal{H}_S$. The key point is that the eigenvalues of $\exp(-i\frac{2\pi\gamma}{A_0}\hat{\underline{\Sigma}}\cdot r)$ on ψ_V must be equal to the eigenvalue of $\exp(i\hat{F})$ on ψ_S. Actually, at the p_i puncture, the eigenvalues of $\exp(-i\frac{2\pi\gamma}{A_0}\hat{\underline{\Sigma}}\cdot r)$ are:

$$\exp(-i\frac{2\pi\gamma}{A_0}(8\pi\ell_{\mathrm{P}}^2 m_i)),$$

where m_i is an half-integer. On the other hand the holonomies given by $\exp(i\hat{F})$ are of the form:

$$\exp(i\frac{2\pi a_i}{k}),$$

where, as we have seen, the $a_i \in \mathbb{Z}_k$. This means that $a_i = -2m_i \bmod(k)$.

Moreover, a path encircling all the punctures is a contractible one over the sphere, this means that the holonomy (or curvature) of this path gives a trivial contribution to the curvature. This translates in the following condition:

$$a_1 + \cdots + a_n = 0. \tag{2.13}$$

We can rewritte this condition, which wil be called 'projection constraint', in terms of m-labels.

2.1.5 Surface diffeomorphism transformations

The diffeomorphisms can move the punctures over S but it is not possible to interchange p_i and p_j, because to do this one has to cross the paths defined to coordinatize the phase space. For this reason, we consider the punctures as distinguishable, so we cannot permute them. As we shall see in chapter 5, this point becames fundamental in the entropy counting problem.

3. THE CONFORMAL FIELD THEORY PERSPECTIVE

Dado que sobre la superficie del horizonte aparece definida de forma natural una teoría de Chern-Simons es razonable explotar la relación puesta de manifiesto en los trabajos clásicos de E. Witten entre esta teoría y las teorías cuánticas de campos con invariancia conforme. Este capítulo presenta los primeros pasos para conseguir entender esta relación y se expondrán, desde la perspectiva de la teoría cuántica de campos conformes, algunos resultados que serán recuperados, por otros medios, en los sucesivos capítulos de esta tesis.

3.1 Introduction

Nowdays, There are several approaches to the identification of the microscopic degrees of freedom responsible for the entropy of a black hole on the basis of the observation, which are mainly based on conformal field techniques at some stage. In particular, Carlip has suggested that conformal symmetry could play a fundamental role in this scenario (see [30] and references therein).

As we have explained before, in the isolated horizon framework, a black hole is introduced as an inner boundary of the spacetime manifold. Over this boundary, constraints implementing the isolated horizon properties are imposed. Naively, they reduce, already at the classical level, the $SU(2)$ gauge symmetry of the theory to a $U(1)$ gauge symmetry on the horizon. These $U(1)$ degrees of freedom, that at the quantum level fluctuate independently from the ones of the bulk, are described by a Chern-Simons (CS) theory and are responsible for the horizon entropy.

On the other hand, E. Witten proposed in [17] a correspondence between the Hilbert space of generally covariant theories and the space of conformal blocks of a conformally invariant theory. This idea was applied in [31] to the computation of the entropy for a horizon described by a $SU(2)$-CS theory, by putting its Hilbert space in correspondence with the space of conformal blocks of a $SU(2)$-Wess-Zumino-Witten (WZW) model.

The purpose of the present chapter is to use Witten's correspondence for the $U(1)$-CS theory describing the black hole horizon in LQG, looking for some

hints o the role of CFT techniques in this framework. Taking into account of that this $U(1)$ group arises as a result of the geometric symmetry breaking from the $SU(2)$ symmetry in the bulk, one can still make use of the well established correspondence between $SU(2)$ Chern-Simons and Wess-Zumino-Witten theories. However, in this case it will be necessary to impose restrictions on the $SU(2)$-WZW model in order to implement the symmetry reduction. Through this procedure we expect to eventually reproduce the counting of dimensions of the $U(1)$-CS Hilbert space.

3.2 Summarizing the black hole entropy counting

Let us summarize the main features and results of the LQG black hole entropy counting in the isolated horizon framework [14] (we will return to this topic in the next chapter). On a space-like slice M, the geometry of the bulk is described by a spin network. Some of the spin network edges end at the horizon surface S (the intersection of M and the isolated horizon), endowing it with an area given by

$$A = 8\pi\gamma\ell_{\mathrm{P}}^2 \sum_{I=1}^{N} \sqrt{j_I(j_I+1)}\ , \tag{3.1}$$

where $j_I \in \mathbb{N}/2$ label the $SU(2)$ irreducible representations corresponding to the N edges piercing the horizon. These edges carry an additional label $m_I \in \{-j_I, -j_I+1, ..., j_I\}$ (the corresponding spin projection) characterizing their intersection with the horizon (punctures).

On the other hand, the horizon geometry is described by a $U(1)$ Chern-Simons theory defined over a sphere with N distinguishable topological defects (corresponding with the punctures).The states of this theory are characterized by labels $a_I \in \mathbb{Z}_\kappa$ (κ being, in this chapter, the level of the CS theory, earlier denoted k) quantifying the deficit angles that give rise to the distributional curvature of the horizon concentrated at each puncture. The spherical topology of the horizon implies that these a_I labels must satisfy the so called projection constraint $\sum_I a_I = 0$. The matching of both (bulk and horizon) geometries through the boundary conditions gives rise to a relation between the a_I and m_I labels that reads

$$2m_I = -a_I \mod \kappa\ . \tag{3.2}$$

For a given value A of area, the entropy can be computed as

$$S(A) = k_B \ln \mathfrak{n}(A),$$

being k_B the Boltzman constant and $\mathfrak{n}(A)$ the number of independent Chern-Simons states compatible with the above constraints, taking into account the

distinguishable character of the punctures. This is to say, $\mathfrak{n}(A)$ is the number of different a_I-labeled horizon states (satisfying the projection constraint) such that, for each of them, there exists (at least) one (j_I, m_I)-labeled piercing from the bulk compatible with it and with the value A_0 of the horizon area. The relation between m_I and a_I labels allows us then to reformulate the entropy counting as a well defined combinatorial problem in terms only of the m_I labels as in [18]. Then, $\mathfrak{n}(A)$ can be rewritten as: $\mathfrak{n}(A) = 1 + \sum_{A' \leq A} d(A')$, where $d(A)$ is the number of all the finite, arbitrarily long, ordered sequences $\vec{m} = (m_1, ..., m_N)$ of non-zero half-integers, such that

$$\sum_{I=1}^{N} m_I = 0 \ , \quad \sum_{I=1}^{N} \sqrt{|m_I|(|m_I|+1)} = \frac{A}{8\pi\gamma\ell_{\mathrm{P}}^2} \ . \tag{3.3}$$

Explicit expressions for the solution of this combinatorial problem were obtained in [46, 21]. If we define $k_I = 2|m_I|$ and the occupancy numbers n_k as the number of punctures carrying a label value m such that $k = 2|m|$, then a set of numbers $\{n_k : k = 1, 2, ...\}$ characterizes a $\vec{m}$ sequence up to reorderings and sign assignments for $m_I = \pm\frac{1}{2}k_I$. Thus, $d(A)$ can be expressed in terms of the set C of all the $\{n_k\}$ sets compatible with a given area A by associating two sources of degeneracy to each of these sets $\{n_k\}$. The first is the number $R(\{n_k\})$ of different ways of reordering the k_I labels in order to obtain all the corresponding ordered sequences $\vec{k} = (k_1, ..., k_N)$. The second source of degeneracy is the number $P(\{n_k\})$ of different sign assignments for the associated m_I numbers, in such a way that the projection constraint is satisfied. With this

$$d(A) = \sum_{\{n_k\} \in C} R(\{n_k\}) \cdot P(\{n_k\}), \tag{3.4}$$

where the sum is extended over all the sets $\{n_k\}$ in C.
The set C of all $\{n_k\}$ configurations compatible with a given area eigenvalue can be computed analytically [46] using number-theory related techniques, through an exact characterization of the horizon area spectrum of LQG. The factor $R(\{n_k\})$ has its origin in the distinguishable character of punctures (acquired in the process of quantization of geometry) and can be obtained from basic combinatorics as $R(\{n_k\}) = (\sum_k n_k)!/\prod_k n_k!$, where the sum and product are extended to all values of k (note that, in practice, for a finite value A of area all the sums and products are always finite). Finally, the factor $P(\{n_k\})$ accounts for the dimensionality of the Hilbert space of the $U(1)$-CS theory once the boundary conditions have been fixed and was obtained in [46, 21] to be:

$$P(\{n_k\}) = \frac{1}{2\pi} \int_0^{2\pi} d\theta \prod_k n_k 2\cos(k\theta) \ . \tag{3.5}$$

3.3 Implementing the analogy

Let us begin by recalling the classical (non-quantum) scenario and how the symmetry reduction takes place at this level. The geometry of the bulk is described by a $SU(2)$ connection, whose restriction to the horizon S gives rise to a $SU(2)$ connection over this surface. As a consequence of imposing the isolated horizon boundary conditions this connection is reduced to a $U(1)$ connection. In [14] this reduction is carried out, at the classical level, just by fixing a unit vector r at each point of the horizon. By defining a smooth function $r : S \to su(2)$ we can choose a $U(1)$ sub-bundle from the $SU(2)$ bundle. This kind of reduction can be described in more general terms as follows (see, for instance, [32]). Let $P(SU(2), S)$ be a $SU(2)$ principal bundle over the horizon S, and ω the corresponding connection over it. A homomorphism λ between the closed subgroup $U(1) \subset SU(2)$ and $SU(2)$ induces a bundle reduction from $P(SU(2), S)$ to $Q(U(1), S)$, being Q the resulting $U(1)$ principal bundle with reduced $U(1)$ connection ω'. This ω' is obtained, in this case, from the restriction of ω to $U(1)$.
All the conjugacy classes of homomorphisms $\lambda : U(1) \to SU(2)$ are represented in the set $Hom(U(1), T(SU(2)))$, where $T(SU(2))$ is the maximal torus of $SU(2)$,

$$T(SU(2)) = \{diag(z, z^{-1}) | z = e^{i\theta} \in U(1)\}.$$

The inequivalent homomorphisms in the $Hom(U(1), T(SU(2)))$ can be labeled by an integer $p \in \mathbb{Z}$

$$\lambda_p : z \mapsto diag(z^p, z^{-p}) \ . \tag{3.6}$$

However the generator of the Weyl group of $SU(2)$ acts on $T(SU(2))$ by $diag(z, z^{-1}) \mapsto diag(z^{-1}, z)$. If we divide out by the action of the Weyl group we are just left with those maps λ_p with p a non-negative integer, $p \in \mathbb{N}_0$, as representatives of all conjugacy classes. These λ_p characterize then all the possible ways to carry out the symmetry breaking from the $SU(2)$ to the $U(1)$ connection that will be quantized later.

However, one can follow the alternative approach of first quantizing the $SU(2)$ connection on S and imposing the boundary conditions later on, at the quantum level. This would give rise to a $SU(2)$-CS theory on the horizon to which the boundary conditions have to be imposed. The correspondence with conformal field theories can be used at this point to compute the dimension of the Hilbert space of the $SU(2)$-CS as the number of conformal blocks of the $SU(2)$-WZW model, as it was done in [31]. It is necessary to require, then, additional restrictions to the $SU(2)$-WZW model that account for the symmetry breaking, and consider only the degrees of freedom corresponding to a $U(1)$ subgroup.

Let us briefly review the computation in the $SU(2)$ case, to introduce later the symmetry reduction. The number of conformal blocks of the $SU(2)$-WZW model[1], given a set of representations $\mathcal{P} = \{j_1, j_2, ..., j_N\}$, can be computed in terms of the so-called fusion numbers N_{il}^r [33] as

$$N^{\mathcal{P}} = \sum_{r_i} N_{j_1 j_2}^{r_1} N_{r_1 j_3}^{r_2} ... N_{r_{N-2} j_{N-1}}^{j_N} \ . \tag{3.7}$$

These N_{il}^r are the number of independent couplings between three primary fields, *i.e.* the multiplicity of the r-irreducible representation in the decomposition of the tensor product of the j_1 and j_2 representations $[j_1] \otimes [j_2] = \bigoplus_j N_{j_1 j_2}^j [j]$. This expression is known as a fusion rule.

In order to clarify, Fusion rule algebras are some kind of associtive algebras over the complex numbers which describe the possible couplings among three objects out of some given class. This construction emerges in several branches of mathematical physics, but for our porposes we can recall that $N^{\mathcal{P}}$ is the multiplicity of the $SU(2)$ gauge invariant representation ($j = 0$) in the decomposition of the tensor product $\bigotimes_{i=1}^N [j_i]$ of the representations in $\mathcal{P}$. The usual way of computing $N^{\mathcal{P}}$ is by using the Verlinde formula [33] to obtain the fusion numbers. But alternatively one can use the fact that the characters of the $SU(2)$ irreducible representations, $\chi_j = \sin[(2j+1)\theta]/\sin\theta$ where θ is the usual angle of the sphere on $SU(2)$, satisfy the fusion rules $\chi_i \chi_j = \sum_r N_{ij}^r \chi_r$. Taking into account that the characters form an orthonormal set with respect to the $SU(2)$ scalar product,

$$\langle \chi_i | \chi_j \rangle_{SU(2)} = \int_0^{2\pi} \frac{d\theta}{\pi} \sin^2\theta \chi_i(\theta) \chi_j(\theta) = \delta_{ij},$$

one can obtain the number of conformal blocks just by projecting the product of characters over the gauge invariant representation

$$N^{\mathcal{P}} = \langle \chi_{j_1} ... \chi_{j_N} | \chi_0 \rangle_{SU(2)} = \int_0^{2\pi} \frac{d\theta}{\pi} \sin^2\theta \prod_{I=1}^N \frac{\sin[(2j_I+1)\theta]}{\sin\theta} \ . \tag{3.8}$$

This expression is equivalent to the one obtained in [31] using the Verlinde formula; it gives rise to the same result for every set of punctures $\mathcal{P}$.

To implement, now, the symmetry breaking we have to restrict the representations in $\mathcal{P}$ to a set of $U(1)$ representations. This corresponds in the case of Chern-Simons theory to performing a symmetry reduction locally at each puncture. It is known that each $SU(2)$ irreducible representation j

[1] Notice that, though we are omitting the κ subindex (in this case it corresponds with the CS level), the group of the WZW theory is in fact the quantum group $SU(2)_\kappa$. The κ dependence is implicit in the allowed sets of representations $\mathcal{P}$.

contains the direct sum of $(2j+1)$ $U(1)$ representations $e^{ij\theta}\oplus e^{i(j-1)\theta}\oplus ...\oplus e^{-ij\theta}$. One can make an explicit symmetry reduction by just choosing one of the possible restrictions of $SU(2)$ to $U(1)$ which, as we saw above, are given by the homomorphisms λ_p. This corresponds here to pick out a $U(1)$ representation of the form $e^{ip\theta}\oplus e^{-ip\theta}$ with some $p\leq j$. The fact that we will be using these reducible representations, consisting of $SU(2)$ elements as $U(1)$ representatives, can be seen as a reminiscence from the fact that the $U(1)$ freedom has its origin in the reduction from $SU(2)$.

Having implemented the symmetry reduction, let us compute the number of independent couplings in this $U(1)$-reduced case. Of course, we are considering now $U(1)$ invariant couplings, so we have to compute the multiplicity of the $m=0$ irreducible $U(1)$ representation in the direct sum decomposition of the tensor product of the representations involved. As in the previous case, this can be done by using the characters of the representations and the fusion rules they satisfy. These characters can be expressed as $\tilde{\eta}_{p_I}=e^{ip_I\theta}+e^{-ip_I\theta}=2\cos p_I\theta$. Again, we can make use of the fact that the characters η_i of the $U(1)$ irreducible representations are orthonormal with respect to the standard scalar product in the circle. Then, the number we are looking for is given by

$$N^{\mathcal{P}}_{U(1)}=\langle\tilde{\eta}_{p_1}...\tilde{\eta}_{p_N}|\eta_0\rangle_{U(1)}=\frac{1}{2\pi}\int_0^{2\pi}d\theta\prod_I^N 2\cos p_I\theta\ , \tag{3.9}$$

where $\eta_0=1$ is the character of the $U(1)$ gauge invariant irreducible representation. Notice than (3.9) coincides with the value of $P(\{n_k\})$ given by (3.5).

3.4 Remarks and Conclusions

Let us put this result in context with the entropy counting. As we will explain in detail in the following chapters, there are several contributions involved in computing the entropy of a black hole within LQG. Some of them are related with the LQG framework, like the computation of the set C introduced in section 4.2 by characterizing the black hole area spectrum, or the number or reorderings of labels over the set $\mathcal{P}$ due to the distinguishability of the punctures originated in the quantization process. On the other hand, there are other objects, like $P(\{n_k\})$, that are related with the CS theory on the horizon. Once one has introduced all the conditions imposed by the LQG framework, what is left is the counting of states of a CS theory subject to some external inputs. If there is any connection between this CS theory and a Conformal Field Theory, one should expect this CFT to reproduce precisely this term $P(\{n_k\})$, subject to the same external inputs. This is exactly what we observe in the previous sections by identifying the p_I and k_I labels. We are, thus, proposing

a precise implementation of Witten's analogy through this symmetry reduced counting that yields the expected result.

From the physical point of view, the main change we are introducing, besides using the CS-CFT analogy, is to impose the isolated horizon boundary conditions at the quantum level, instead of doing it prior to the quantization process. Notice that this is a necesary preliminary step in the direction of introducing a quantum definition of isolated horizons.

4. THE COUNTING PROBLEM

En este capítulo exponemos los principales resultados, relacionados con el conteo de estados responsables de la entropía presentes en la literatura y los analizaremos a la luz de las nuevas técnicas presentadas en esta tesis.

This chapter has as purpose to present the actual status of the state counting which leads to the entropy within the Ashtekar-Baez-Corichi-Krasnov (ABCK) framework [14]. Following the geometrical setting explained in the previous chapters we can stablish the problem of computing the entropy as follows.

- We have to perform a counting of the horizon states, tracing out the bulk degrees of freedom (see [11] for details). At this point, we take a microcanonical point of view, we fix a value of the horizon area A_0 and we count the states within an interval $[A_0-\delta, A_0+\delta]$, where the *tolerance* δ is of the order of the Plank area.

- We have to translate this geometrical setting into a combinatorial problem. We must to count the $U(1)$-CS lists of labels a_i of the surface states that satisfy the projection constraint. These lists of labels will be related with lists of spin components m_i. Finally, the m-lists will be permissible if we can associate to it with a list of spins j_i whose area $8\pi\gamma\ell_{\rm P}^2\sum_i\sqrt{j_i(j_i+1)}$ belongs to the interval $[A_0-\delta, A_0+\delta]$ around A_0.

- Finally, we need to count all the combination of labels over a ordered set of punctures. This becomes a very complicated combinatorial problem.

It is worth noting that in the literature we can find two different ways to define the suitable labels for the surface states [18, 19]. We will describe these two countings in the following sections. Both proposals lead to a linear dependence of the entropy with the area of the horizon surface, at the leading order, and a logarithmic correction with a $-1/2$ precoefficient. The difference relies in the different value of the BI parameter which accounts for the $1/4$ factor of the Hawking-Bekenstein entropy,

$$S(A) = \frac{\gamma_c}{\gamma}\frac{A}{4\ell_{\rm P}^2} - \frac{1}{2}\ln\frac{A}{\ell_{\rm P}^2} + O(1), \tag{4.1}$$

where γ_c is a number which appears in the counting procedure as we will see in the following.

4.0.1 The Chern-Simons level problem

In this framework appear a problem related with the level k of the Chern-Simons theory defined over the surface S. It is clear that this level must be a positive integer. This fact induces a prequantized area for the horizon surface,

$$A_0 = 4\pi\gamma\ell_{\mathrm{P}}^2 k, \tag{4.2}$$

where A_0 stands for the area which results from $k = \dfrac{A_0}{4\pi\gamma\ell_{\mathrm{P}}^2}$. This is precisely the level which apears in the action for the Chern-Simons theory defined on the horizon. The problem here is that these values does not belong to the spectrum of the usual LQG area operator employed in this framework due to the presence of the terms $\sqrt{j(j+1)}$.

The solution to this mismatch given in the ABCK framework is to define the entropy in terms of the number of states within a small area interval around A_0. This thesis deals related with the computation of states following this approach. Other solution could be given for example with the introduction of a new area operator which could be used in the isolated horizon framework properly. This is out of the scope of this work but, in particular, it is a very interesting topic to be studied, see [24].

4.1 Domagla-Lewandowski-Meissner counting

The DLM counting follows the ABCK framework and is based in the following points:

1. The classical area is quantized in the following way:

   $$A_0 = 4\pi\gamma\ell_{\mathrm{P}}^2 k,$$

   where k is a natural number (the Chern-Simons level).

2. DLM propousal counts states labelled by finite sequences $(a_1, \ldots, a_n)$ given by $a_i \in \mathbb{Z}_k$ which are consistent with the projection constraint for an arbitrary number of punctures. (In this sense this counting is analogous to the propoused by ABCK).

3. The area operator eigenvalues satisfies the following inequality:

   $$A = 8\pi\gamma\ell_{\mathrm{P}}^2 \sum_{i=1}^{n} \sqrt{j_i(j_i+1)} \leq A_0 \tag{4.3}$$

Taken into account these points, the counting problem was established in [18] as follows:

'The entropy S of a quantum horizon of the classical area A_0 according to quantum geometry and the ABCK framework is $S = \ln N(A_0)$, where the number $N(A_0)$ is 1 plus the number of all the finite sequences $(m_1, \ldots, m_n)$ of nonzero elements of $\frac{1}{2}\mathbb{Z}$, such that the following equality and inequality are satisfied:

$$\sum_{i=1}^{n} m_i \;=\; 0, \quad \sum_{i=1}^{n} \sqrt{|m_i|(|m_i|+1)} \;\leq \frac{A_0}{8\pi\gamma\ell_{\mathrm{P}}^2}, \tag{4.4}$$

where γ is the Barbero-Immirzi parameter of quantum geometry'.

This makes sense because there exist a sequence $(j_1, \ldots, j_n)$ of nonzero elements of $\frac{1}{2}\mathbb{N}$ consistent with 4.3 for which exists a sequence $(m_1, \ldots, m_n)$ such that $a_i = -2m_i \; mod \; k$ and $m_i \in \{-j_i, -j_i + 1, \ldots, j_i\}$. So, we can make the counting just looking for sequences of m labels.

4.1.1 Interval vs inequality

As we can see, in this context we use the inequality

$$\sum_{i=1}^{n} \sqrt{|m_i|(|m_i|+1)} \;\leq \frac{A_0}{8\pi\gamma\ell_{\mathrm{P}}^2},$$

instead of the interval $[A_0 - \delta, A_0 + \delta]$ originaly proposed in the ABCK framework. The reason for that is that we are interested in counting only surface states that do not containt information about the actual area of the horizon (we can relate only the m labels with the a labels coming from the Chern-Simons theory, through the projection constraint). The use of the inequality is well suited because for each m-sequence we always can find a j-sequence of spins whose asociated area is within a given interval[1]. The trivial choice is to take $j_i = |m_i|$ for each m_i.

Moreover, as the relation between a and m is $mod\ k$, and the a must satisfy the projection constraint $\sum_{i=1}^{n} a_i = 0$ we have that

$$\sum_{i=1}^{n} m_i = c\frac{k}{2}, \tag{4.5}$$

[1] The proper relation between the interval and the inequality holds for the interval $[A_0 - \delta, A_0]$, where δ is easyly computed and his minimum value is $4\pi\gamma\ell_{\mathrm{P}}^2(\sqrt{15} - \sqrt{3})$. With this choice the relation between m and a is one-to-one and we can use the inequality instead of the interval.

where c is an integer number.

This allows us to make the following chain of inequalities:

$$A_0 = 4\pi\gamma\ell_{\mathrm{P}}^2 k \geq 8\pi\gamma\ell_{\mathrm{P}}^2 \sum_{i=1}^{n} \sqrt{|m_i|(|m_i|+1)} > \tag{4.6}$$

$$> 8\pi\gamma\ell_{\mathrm{P}}^2 \sum_{i=1}^{n} |m_i| \geq 8\pi\gamma\ell_{\mathrm{P}}^2 |\sum_{i=1}^{n} m_i| = \tag{4.7}$$

$$= 4\pi\gamma\ell_{\mathrm{P}}^2 k|c|. \tag{4.8}$$

So, we can stablish $\sum_{i=1}^{n} m_i = 0$ exactly and $\sum_{i=1}^{n} |m_i| \leq \frac{k}{2}$. This implies that the relation between m and a is one-to-one, and we can make the counting just taking into account m-sequences spin components, as we said previosly.

4.1.2 Solution to the combinatorial problem

In a very nice paper Meissner solved the combinatorial problem established by Domagala and Lewandowski [18]. His solution, in the simplified case where the projection constraint $\sum_i m_i = 0$ is not imposed, relies in the following points:

1. First, he counts the number of arbitrary length m-sequences such that the area inequality holds. This number is given by:

$$\begin{aligned} N(a) = \theta(a-\sqrt{3}/2)\Big(&2N(a-\sqrt{3}/2) + 2N(a-\sqrt{2}) + \cdots \\ &+2N(a-\sqrt{|m_i|(|m_i|+1)}) + \cdots \\ &+2\left[\sqrt{4a^2+1}-1\right]\Big) \end{aligned} \tag{4.9}$$

   where the a is given by $a = \dfrac{A_0}{8\pi\gamma\ell_{\mathrm{P}}^2}$, and $[\cdots]$ denotes the integer part.

2. Then he performs a Laplace transform of this expresion obtaining:

$$P(s) = \frac{2\sum_{k=1}^{\infty} \exp(-s\sqrt{k(k+2)/4)})}{s(1-2\sum_{k=1}^{\infty} \exp(-s\sqrt{k(k+2)/4)})} \tag{4.10}$$

   where $P(s)$ is the Laplace transform of $N(a)$ and, in this section, k is symply $2m$ for each puncture, in order to work with integer numbers.

3. Then, by assuming that all the poles of the Laplace transform are distinct and of finite order, Meissner performs an analytical continuation to the complex half-plane $Re(s) > 0$. So, the growth of $N(a)$ is determined by:

$$N(a) = \sum_{s_i, Re(s_i)>0} e^{s_i a} res(P(s), s_i) + \text{subleading} \tag{4.11}$$

4. Finally, the leading term for large areas is determined by the pole $s_M = 2\pi\gamma_M$ with zero imaginary part: $N(a) = Ce^{2\pi\gamma_M a}$,

$$\gamma_M = 0.2375\ldots$$

The asymptotic value of the entropy given by Meissner is:

$$S(A_0) = \frac{\gamma_M}{\gamma}\frac{A_0}{4\ell_{\rm P}^2} + O(\ln A). \tag{4.12}$$

Taking $\gamma = \gamma_M$ we recover the Bekenstein-Hawking entropy.

If one imposes the projection constraint $\sum_i m_i = 0$ the asymptotic solution is quite similar and the final result shows that this constraint has only the effect of adding a logarithmic correction to the above formula wihtout changing the value of the BI-parameter:

$$S = \frac{\gamma_M}{\gamma}\frac{A_0}{4\ell_{\rm P}^2} - \frac{1}{2}\ln(\frac{A_0}{\ell_{\rm P}^2}) + O(1). \tag{4.13}$$

4.2 Ghosh-Mitra Counting

In this section we describe an alternative proposal for the identification of the surface quantum states. For Ghosh and Mitra (GM) [19], these states are labelled not only by m but also by j labels. This means that these states also contain information about the actual area of the horizon surface. This option, of course, does not follow the original ABCK framework. However, we will treat this option in this thesis because the tools presented here can be used to perform not only the computation of the black hole entropy for the DLM but also for the GM proposal. The discusion about the correctnes of this GM proposal is out of the scope of this work.

Let us present the basis for this option:

1. The states are labelled by pairs (j, m). We have to count configurations of punctures such that, the j labels give us an area $A = 2\sum_{i=1}^{n}\sqrt{j_i(j_i+1)}$ within the interval $[A_0-\delta, A_0+\delta]$. And the m labels satisfy the projection constraint (in this section we are going to use units where $4\pi\gamma\ell_{\rm P}^2 = 1$).

2. We have a number of punctures given by s. We call s_j to the number of punctures which have a given j. So, $s = \sum_j s_j$.

3. Ignoring the projection constraint, the number of states is given by

$$N = \frac{(\sum_j s_j)!}{\prod_j s_j!} \prod_j (2j+1)^{s_j}. \tag{4.14}$$

4. Then, this expresion is maximizing with respect to s_j (GM treat these variables as continuous ones). One can use Stirling's formula to obtain finally:

$$s_j = (2j+1)\exp[-\lambda\sqrt{j(j+1)}]\sum_k s_k \tag{4.15}$$

5. Summing over j, we obtain a normalization condition,

$$\sum_j (2j+1)\exp[-\lambda\sqrt{j(j+1)}] = 1, \tag{4.16}$$

where $\lambda = \gamma_{GM}/(2\pi)$. We can solve this equation, so, in this case,

$$\gamma_{GM} = 0.274\ldots$$

The entropy in this approach is given by $S = \ln N(A_0)$, and the result is,

$$S = \frac{\gamma_{GM}}{\gamma}\frac{A_0}{4\ell_{\rm P}^2}. \tag{4.17}$$

As before, in this context one can introduce the projection constraint and the treatment is similar to the previous one, and again the effect of the projection constraint is the introduction of a logarithmic correction with the same coefficient:

$$S = \frac{\gamma_{GM}}{\gamma}\frac{A_0}{4\ell_{\rm P}^2} - \frac{1}{2}\ln(\frac{A_0}{\ell_{\rm P}^2}) + O(1). \tag{4.18}$$

4.3 Explicit Counting

As we have explained there is an important issue regarding this formalism. Loop quantum gravity possesses a one parameter family of inequivalent representations of the classical theory labelled by γ, the BI-parameter (it is the analogue of the θ ambiguity in QCD [28]). It turns out that the BH entropy

calculation provides a linear relation between entropy and area for very large black holes (in Planck units) as,

$$S = \lambda\, A(\gamma),$$

where the parameter λ is independent of γ and depends only on the counting. We have put the γ dependence in the area, since the parameter appears explicitly in the area spectrum. The strategy that has been followed within the LQG community is to regard the Bekenstein-Hawking entropy $S = A/4$ as a requirement that large black holes should satisfy. This fixes uniquely the value of $\gamma = \gamma_0$ once and for all, by looking at the asymptotic behavior, provided that one has the 'correct counting' that provides the right value for γ_0. Whenever we have independent tests that call for a specific value of γ, one should rather find that the value γ_0 'works', or else LQG would be in trouble.

The parameter λ above depends on the calculation of the entropy, that is, on the counting of states compatible with whatever requirements we have imposed. The matter has not been free from some controversy. In the original calculations [14] (once isolated horizons were understood to be vital) , the number of states was underestimated; the entropy appeared to arise from a special set of states where the contribution to the area from each puncture was the same and corresponded to that of the minimum spin possible. Later on, it was realized that this calculation had failed to consider many states [18], and a corrected analytical estimation of entropy, and value of the Barbero-Immirzi parameter, was proposed in [18]. Furthermore, a still different calculation appeared soon afterward [19] which gave yet another value for γ. This situation suggests that a clear understanding of the black hole formalism and entropy counting within LQG is needed.

The simplest such test would be just to count states. The purpose of this section is to present precisely this. We count states, by means of a simple algorithm, of a quantum black hole within the existing formalism in LQG [14], compatible with the restrictions that this framework imposes. To be more precise, we restrict attention to spherical horizons (for which area is the only free parameter classically) of a fixed horizon area A_0 and compute the number of allowed quantum states, within an interval $[A_0 - \delta A, A_0 + \delta A]$ that satisfy the following: i) The quantum area expectation value satisfies: $\langle \hat{A} \rangle \in [A_0 - \delta A, A_0 + \delta A]$, and ii) for which a restriction on the quantum states of the horizon, $\sum_i m_i = 0$, is imposed. This last 'projection constraint' comes from the consistency conditions for having a quantum horizon that has, furthermore, the topology of a two-sphere (it is the quantum analogue of the Gauβ-Bonnet theorem). In the analytical treatments, it has been shown in detail that, for large black holes (in Planck units), the entropy behaves as:

$$S = \frac{A}{4} - \frac{1}{2} \ln A,$$

provided the BI-parameter γ is chosen to coincide with the value γ_{DLM}, that has to satisfy [18]:

$$1 = \sum_i 2 \exp\left(-2\pi\gamma_{DLM}\sqrt{j_i(j_i+1)}\right). \tag{4.19}$$

The solution to this transcendental equation is approximately $\gamma_{DLM} = 0.2375\ldots$ [18]. For the GM counting, the condition is [19]:

$$1 = \sum_i (2j+1) \exp\left(-2\pi\gamma_{GM}\sqrt{j_i(j_i+1)}\right). \tag{4.20}$$

whose solution is approximately $\gamma_{GM} = 0.273908\ldots$ [19].

Thus, there are two kind of tests one can make. The first one involves the linear relation between entropy and area that dominates in the large area regime. This provides a test for the value of the BI parameter. The second test has to do with the coefficient of the logarithmic correction $(-1/2)$, a subject that has had its own share of controversy. The analytical results show that this coefficient is independent of the linear coefficient and arises in the counting whenever the $\sum_i m_i = 0$ constraint is imposed.

In order to test the validity of the logarithmic correction and its relation to the constraint, we fix the value of the parameter $\gamma = \gamma_0$ and compute the number of states, both with and without the projection constraint. We subtract this functions and compare the difference with logarithmic functions. We look for the coefficient that provides the best fit. Once the logarithmic coefficient is found and the independence of the asymptotic linear coefficient is established, we perform a variety of countings for different values of γ, both with and without the projection constraint, and consider the slope c of the resulting relation $S = c\,A$, as a function of γ. For the function $c(\gamma)$ we look for the value $\tilde{\gamma}$ for which $c(\tilde{\gamma}) = 1/4$.

Another separate issue that one would like to consider is the applicability of the formalism for 'small' black holes. The isolated horizons boundary conditions are imposed classically in the variational principle, which means that the horizon is assumed to exist as a classical object. A natural question is whether the resulting picture can be trusted for small black holes, not far from the Planck regime where strong quantum gravity effects can be expected to appear. Another related question one might try to answer is the 'scale' at which the quantum horizon entropy approaches the expected form derived from semi-classical/large horizon area approximation. As we shall see, even when the limited computing power at our disposal, we shall be able to answer partially some of these questions.

The remainder of this section is as follows. In subsec. 4.3.1 we shall describe the algorithm that implements the counting of states. Subsec. 1.3 is devoted to describing the results found. We end this section with a discussion in subsec. 4.3.3.

4.3.1 The Counting

In this subsection we will focus only on the GM counting for simplicity; for a complete description for the DLM case see [39]. In the next section of this chapter we will compare both countings.

Counting configurations for large values of the area (or mass) is extremely difficult for the simple reason that the number of states scales exponentially. Thus, for the computing power at our disposal, we have been able to compute states up to a value of area of about $A = 550\ \ell_{\rm P}^2$ (recall that the minimum area gap for a spin 1/2 edge is about $a_0 \approx 6\,\ell_{\rm P}^2$, so the number of punctures on the horizon is below 100). At this point the number of states exceeds 2.8×10^{58}. In terms of Planck masses, the largest value we have calculated is $M = 3.3\,M_P$. When the projection constraint is introduced, the upper mass we can calculate is much smaller, given the computational complexity of implementing the condition. In this case, the maximum mass is about $1.7\,M_P$.

It is convenient to describe briefly what the program for counting does. What we are using is what it is known, within combinatorial problems, as a brute force algorithm. This is, we are simply asking the computer to perform all possible combinations of the labels we need to consider, attending to the distinguishability -indistinguishability criteria that are relevant [14], and to select (count) only those that satisfy the conditions needed to be considered as permissible combinations, i.e., the area condition and the spin projection constraint. An algorithm of this kind has an important disadvantage: it is obviously not the most optimized way of counting and the running time increases rapidly as we go to little higher areas. This is currently the main limitation of our algorithm. But, on the other hand, this algorithm presents an equally important advantage, and this is the reason why we are using it: its explicit counting guarantees us that, if the labels considered are correct, the result must be the right one, as no additional assumption or approximation is being made. It is also important to have a clear understanding that the algorithm does not rely on any particular analytical counting available. That is, the program counts states as specified in the original ABK formalism [14]. The computer program has three inputs: i) the classical mass M (or area $A_0 = 16\pi\, M^2$), ii) the value of γ, and iii) the size of the interval δA.

Once these values are given, the algorithm computes the level of the horizon Chern Simons theory $k = [A_0/4\pi\gamma]$ and the maximum number of punctures possible $n_{\rm max} = \left[A_0/4\pi\gamma\sqrt{3}\right]$ (where $[\cdot]$, indicates the principal integer value). At first sight we see that the two conditions we have to impose to permissible combinations act on different labels. The area condition acts over j's and the spin projection constraint over m's. This allows us to first perform combinations of j's and select those satisfying the area condition. After that, we can perform combinations of m's only for those combinations of j's with the correct area, avoiding some unnecessary work. We could also be allowed

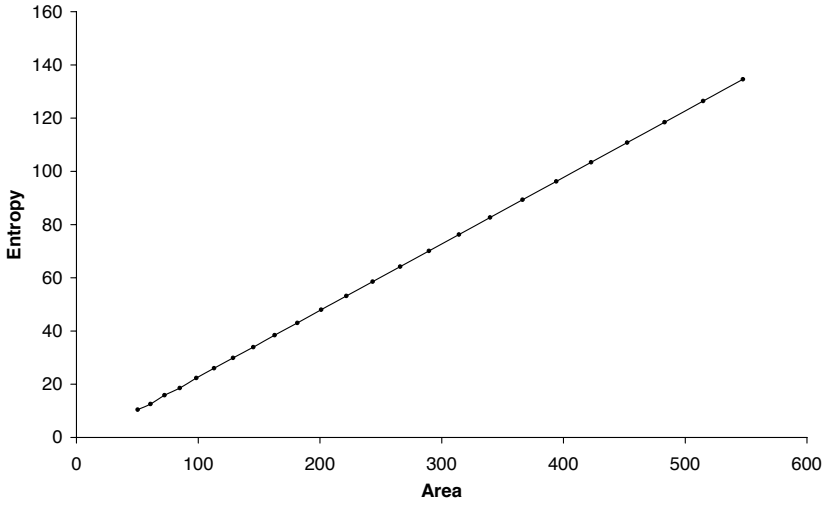

Fig. 4.1: The entropy as a function of area is shown, where the projection constraint has not been imposed. The BI is taken as $\gamma = 0.274$ and the area in Planck units.

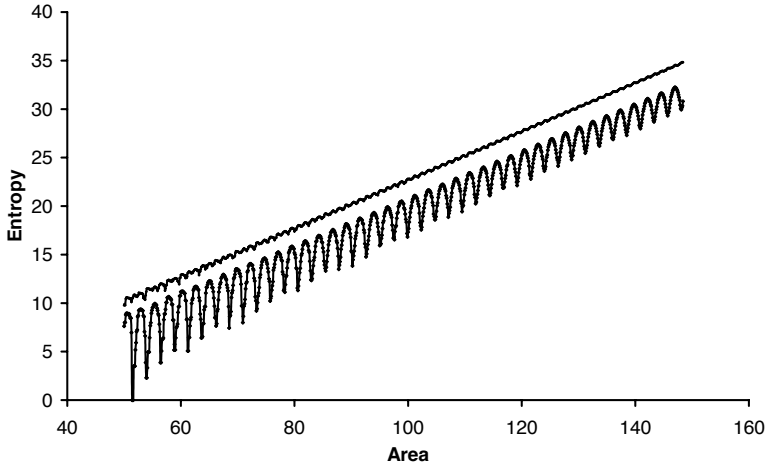

Fig. 4.2: Entropy *vs* Area (in Planck units) with and without the projection constraint. Whe have choosen $\delta A = 0.5$.

to perform the counting without imposing the spin projection constraint, by simply counting combinations of j's and including a multiplicity factor of $\prod_i (2j_i + 1)$ for each one, accounting for all the possible combinations of m's compatible with each combination of j's. This would reduce considerably the running time of the program, as no counting over m's has to be done, and will allow us to separate the effects of the spin projection constraint (that, as we will see, is the responsible of a logarithmic correction). It is very important to notice at this point that this separation of the counting is completely compatible with the distinguishability criteria.

The next step of the algorithm is to consider, in increasing order, all the possible number of punctures (from 1 to $n_{\max}$) and in each case it considers all possible values of j_i. Given a configuration $(j_1, j_2, \ldots, j_n)$ $(n \leq n_{\max})$, we ask whether the quantum area eigenvalue $A = \sum_i 8\pi\gamma\sqrt{j_i\,(j_i+1)}$ lies within $[A_0 - \delta A, A_0 + \delta A]$. If it is not, then we go to the next configuration. If the answer is positive, then the labels m's are considered as described before. That is, for each of them it is checked whether $\sum m_i = 0$ is satisfied.

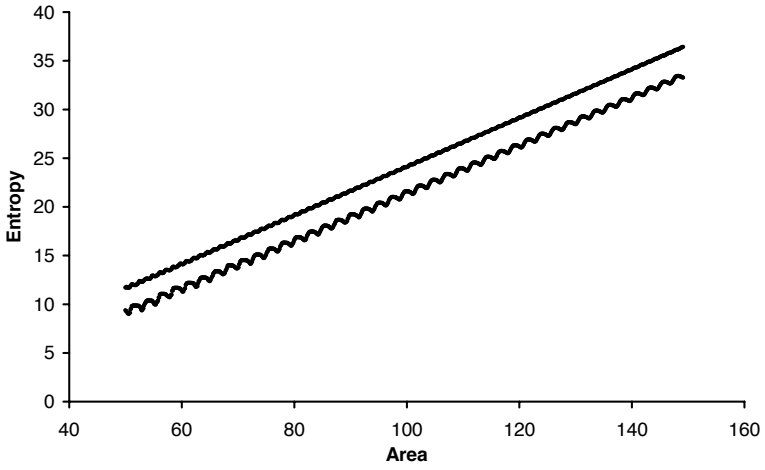

Fig. 4.3: Entropy *vs* Area with and without the projection constraint for an area interval $\delta A = 2$.

4.3.2 Results

Let us now present the results found. We shall separate this section in two parts. In the first one, we shall focus on the logarithmic correction, that is, in the results obtained when considering the spin projection constraint. In the second part, we shall report on the asymptotic linear relation that yields information about the BI-parameter.

Logarithmic Correction

In figure 4.1, we have plotted the entropy, as $S = \ln(\#\,\text{states})$ *vs* the area A_0, where we have counted all possible states without imposing the $\sum_i m_i = 0$ constraint, and have chosen a $\delta A = 0.5$. As it can be seen, the relation is amazingly linear, even for such small values of the area. When we fix the BI parameter to be $\gamma = \gamma_0 = 0.274$, and approximate the curve by a linear function, we find that the best fit is for a slope equal to 0.2502.

When we include the projection constraint, the computation becomes more involved and we are forced to consider a smaller range of values for the area

of the black holes. In Figure 4.2, we plot both the entropy without and with the projection constraint, keeping the same δA. The first thing to note is that for the computation with the constraint implemented, there are some large oscillations in the number of states. Fitting a straight line gives a slope of 0.237. In order to reduce the oscillations, we increased the size of δA to $\delta A = 2$. The result is plotted in Figure 4.3. As can be seen the oscillations are much smaller, and the result of implementing the constraint is to shift the curve down (the slope is now 0.241). In order to compare it with the expected behavior of $S = A/4 - (1/2)\ln A$, we subtracted both curves of Figure 4.3, in the range $A = [50, 160]$, and compared the difference with a logarithmic function. The coefficient that gave the best fit is equal to -0.4831 (See Figure 4.4). What can we conclude from this? While it is true that the rapidly oscillating function is far from the analytic curve, it is quite interesting that the oscillatory function follows a logarithmic curve with the "right" coefficient. It is still a challenge to understand the meaning of the oscillatory phase. Even when not conclusive by any means, we can say that the counting of states is consistent with a (n asymptotic) logarithmic correction with a coefficient equal to $(-1/2)$.

Barbero-Immirzi parameter

Let us now assume that the logarithmic correction is indeed there and that, as the analytical calculations suggest [18, 19], the projection constraint does not have any affect on the coefficient of the linear term, that is, on the BI-parameter. With this in mind, we have performed a variety of countings for different values of γ, without the projection constraint, and considered the slope c of the resulting relation $S = c\,A$, as a function of γ. For the resulting function $c(\lambda)$ we looked for the value $\tilde{\gamma}$ for which $c(\tilde{\gamma}) = 1/4$. This is shown in Figure 4.5.

In order to find this value, we have interpolated the curve and found the value $\tilde{\gamma} = 0.2743691$ for which the slope is equal to $1/4$. It is hard not to note that the value of $\tilde{\gamma}$ is amazingly close to the value γ_0 found analytically.

When we repeat this procedure including the $\sum_i m_i = 0$ constraint, just to have a rough idea, we have computed for a limited range of mass (in steps of 0.1) and for a variety of γ in $[0.18, 0.4]$, in steps of 0.01 and have plotted the results in Figure 4.6. The value γ' where the curve crosses $1/4$ is $\gamma' = 0.2552$, which is still far from the GM value (which one expects to get for larger BH), What is amazing is that, even when considering only these Plank size horizons, one can confidently say that there is an asymptotic linear relation between entropy and area and that the relevant coefficient is consistent *only* with the value of the BI parameter $\gamma_0 = 0.27398$, as found in [19].

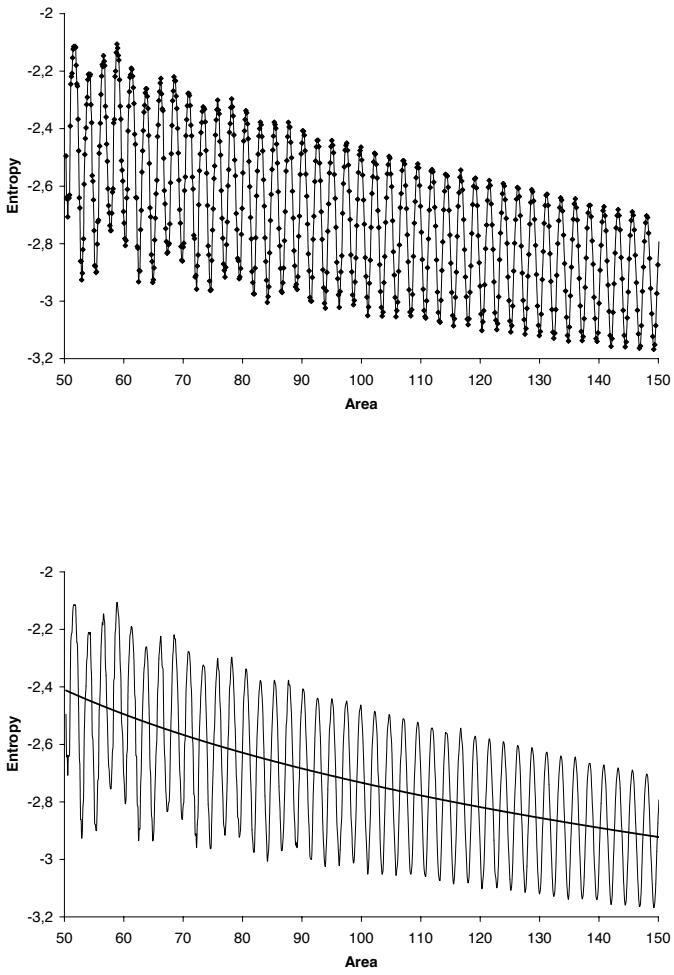

Fig. 4.4: The curves of Fig. 4.3 are subtracted and the difference, an oscillatory function, shown in the upper figure. The curve is approximated by a logarithm curve in the lower figure.

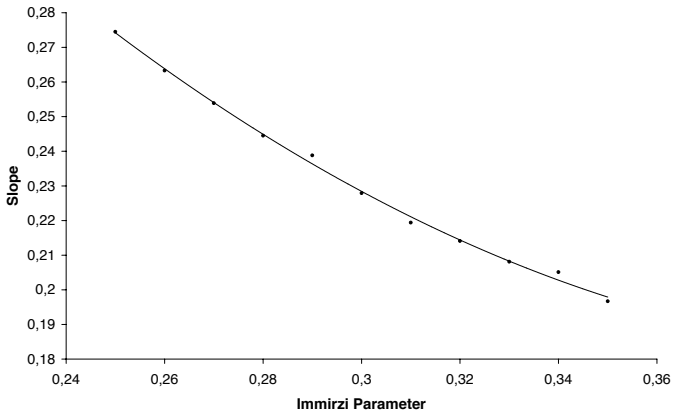

Fig. 4.5: The slope of the entropy area line is plotted as function of the BI-parameter without the projection constraint.

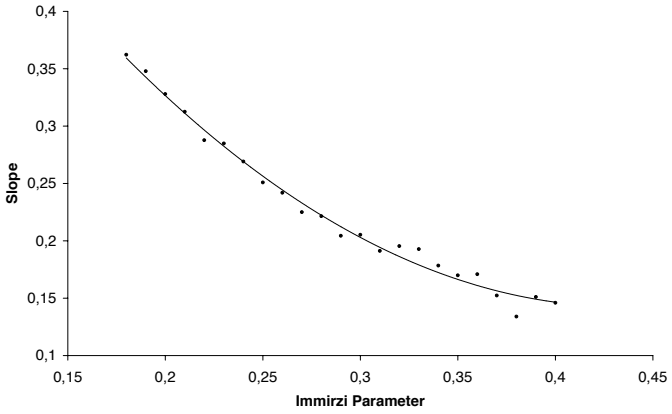

Fig. 4.6: The slope of the entropy area curve is plotted as function of the Barbero-Immirzi parameter with the projection constraint implemented.

4.3.3 Discussion and Outlook

Within loop quantum gravity, the issue of which states should be counted when computing the black hole entropy is a pressing one. The formalism for treating boundary conditions and the quantum horizon geometry established in [14] provides a clear and precise framework. This includes an unambiguous answer as to which states are to be distinguished and which are to be considered undistinguishable. In this section, we have followed a direct application of the formalism and have counted, using a simple algorithm, the states that satisfy the conditions and that yield an area close to a specified value A_0. What we have learned can be summarized as follows:

i) When we do not impose the projection constraint we find that, very rapidly, the entropy area relation becomes linear.
ii) The BI parameter that yields the desired agreement with $S = A/4$ is given by the value $\gamma_0 = 0.27398\ldots$, for the GM counting, and 0.2375... for the DLM.
iii) When the projection constraint is incorporated, which analytically gives the logarithmic correction, the curve gets shifted down and exhibits some oscillations, but follows on average the expected curve with the predicted coefficient $-1/2$ for both countings.
iv) For the rather small value of the BH area computed, and for $\gamma = \gamma_0$, the total entropy seems to approach a linear relation with a ratio S/A approaching $1/4$ from below, which is what one expects due to the logarithmic correction.

It is important to emphasize that the procedure followed here, in the algorithm implemented, is *not* assuming any of the analytical estimations available, but rather performing a direct counting by *brute force* of the microstates consistent with the macroscopic requirements and thus, responsible for the Black Hole entropy. Moreover, we can perform this procedure for the DLM setting and one find the correct value for the BI-parameter within this framework.

Even when the results presented here shed light on the relation between entropy and area, and the BI-parameter, one still needs more work to have completely conclusive results. In particular, more computing capacity to go further in the range of values analyzed is required.

Furthermore, the oscillations found in the entropy area relation will be explained in the next section. For instance, it is important to determine whether there there is some area scale set by the oscillations found in the entropy area relation. To this effect, we have found the frequency that best approximates the oscillations, and the frequency in areas gives an area scale of $\delta A_{\rm osc} = 2.407\ \ell_{\rm P}^2$. It remains a challenge to find an explanation for this scale.

It could also happen, for instance, that the thermodynamic quantities such as temperature (that is usually associated with $T = \partial M/\partial S$), and the specific heat get modified as one approaches the Planck scale. The usual, classical

relation between mass and entropy (using the relation $S = A/4$) implies that a Schwarzschild black hole has negative specific heat; as the energy of the Black Hole decreases, the temperature increases, making the system unstable. One could imagine, for instance, that the oscillations here found (that are seen to decrease for larger black holes), make the specific heat positive as one decreases the area for some (small) value and, thus, would 'stabilize' the black hole. Another intriguing possibility would be to learn something from this formalism (tailored for large equilibrium systems), about the evaporation process of small black holes and the issue of information loss.

4.4 Black hole entropy discretization

It has long been argued by Bekenstein that the proportionality between entropy and area, for large, classical black holes, can be justified from the adiabatic invariance properties of horizon area when subject to different scenarios (see [35] for a review). Further heuristic quantization arguments lead to the suggestion that area, when quantized, should have a discrete, equidistant spectrum *in the large horizon limit*,

$$A_n = \alpha\, \ell_{\rm P}^2\, n\,, \tag{4.21}$$

with α a parameter and n integer. The relation between area and entropy that one expects to encounter in the large horizon radius is then extrapolated to the full spectrum. This would imply that entropy too would have a discrete spectrum, a property that might also be expected if entropy is to be associated with (the logarithm of) the number of microstates compatible with a given macrostate. When this condition is imposed, then the area is expected to have an spectrum of the form,

$$A_n = 4\, \ell_{\rm P}^2\, \ln(k)\, n\,, \tag{4.22}$$

with k and n integers [35]. Even when appealing and physically well motivated, these arguments remain somewhat heuristic and have no detailed microscopic quantum gravity formalism to support them, (see however [24])

There is however an obvious inconsistency between loop quantum gravity and Bekenstein's considerations: the area spectrum in LQG is *not* evenly spaced. On the contrary, the LQG area spectrum is given by,

$$A = \sum_i 8\pi\gamma\, \ell_{\rm P}^2\, \sqrt{j_i\,(j_i+1)}\,, \tag{4.23}$$

where j_i are semi-integers and the sum is taken over all the punctures i at the horizon. The spectrum (4.23) is not only not equidistant, but it can be expected that the eigenvalues accumulate for values of A large in Planck units, given they do for the general area spectrum [29].

The inconsistency between loop quantum gravity and Bekenstein's heuristic arguments seemed to become less relevant when Dreyer noted [36] that LQG might also be consistent with the constraints imposed by asymptotically damped quasi-normal modes, as Hod had previously conjectured [37] within the Bekenstein's formalism. The idea is that the asymptotic frequency of these classical modes would correspond to the energy of horizon quanta through the standard relation $E = \hbar\omega$. This requirement would then imply that, in the Bekenstein approach, black holes have an equidistant spectrum given by

$$A = 4\,\ell_{\rm P}^2\,\ln(3)\,n\,,$$

whereas, in the LQG approach, a *minimum area gap*, associated to the quantum transition, would be given by $a_0 = 4\,\ell_{\rm P}^2\,\ln(3)$ (this requirement implies a particular choice of γ involving $\ln(3)$). Even when not fully consistent (area spectrum continues to be different), the appearance of a $\ln(3)$ factor seemed to be more than just a coincidence. This initial expectation was however lowered when it was shown that the entropy calculation in LQG gave a different proportionality factor between entropy and area that called for a different value of the BI-parameter that was no longer compatible with Hod's considerations [18, 19]. For a new an interesting propousal see [24]

The purpose of this section is to show that there is indeed a deep relation between entropy within the LQG formalism and Bekenstein's heuristic picture (supplemented by Hod's conjectures), even when the relation is much more subtle than it was originally conceived. To be precise, we shall show that a detailed analysis of the number of states compatible with the macroscopic conditions imposed on small, Planck size black holes within the LQG approach yields, when appropriately interpreted, a functional form of the entropy as function of horizon area that realizes in a precise manner Bekenstein's picture. The coincidence turns out to be not only qualitative, but it also incorporates two numbers that are important for both formalisms, namely $\ln(3)$ and the value γ_0 of the BI-parameter (that recovers the Bekenstein-Hawking relation $S = A/4$ for *large* black holes).

We have computed the number of states compatible with a horizon of area A_0 using the formalism developed in [14], that specifies which states have to be counted. We performed the counting using a simple algorithm described briefly in the previous section. In the entropy computation within the micro-canonical ensemble, one resorts to the usual prescription of counting states whose area eigenvalues $A = \langle\hat{A}\rangle$ lie in an interval $[A_0 - \delta A, A_0 + \delta A]$, and where a total projection constraint $\sum_i m_i = 0$ is imposed such that the horizon geometry is the quantum version of an isolated horizon [14]. The parameter δA that fixes the interval is normally assumed to be of the order of Planck area. As we have explained the entropy, as function of area A has some oscillatory behavior, whose amplitude depends on δA but with a constant periodicity

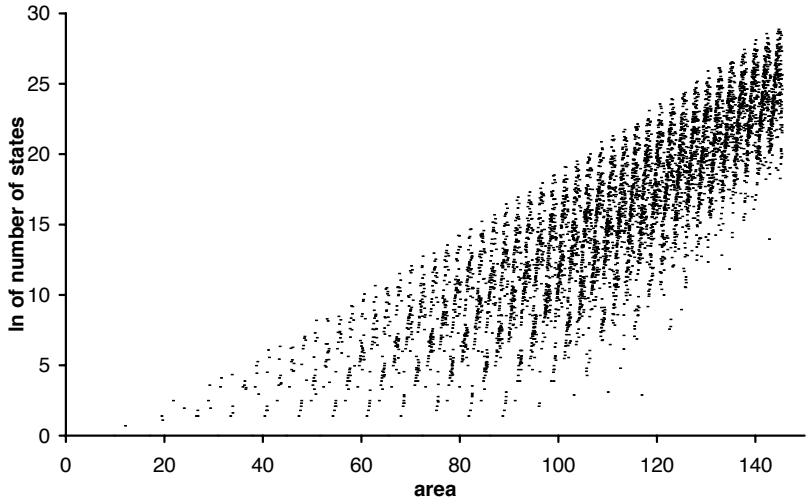

Fig. 4.7: The (ln of the) number of states as a function of area is shown. The Barbero-Immirzi parameter is taken as $\gamma = 0.274$ from [19] and [38]. The interval $[A_0 - \widetilde{\delta A}, A_0 + \widetilde{\delta A}]$ is taken to be rather small ($\widetilde{\delta A} = 0.005\,\ell_{\rm P}^2$) so that one is effectively counting the number of states as function of area. The area is shown in Planck units. Note that this does *not* represent the entropy, given that the interval is very small in Planck units.

that is independent of δA. Here we have taken further the analysis of this behavior in order to unravel the structure of these oscillations. As a first step we have taken a rather small interval $\widetilde{\delta A} = 0.005$ (in Planck units) with a point separation of 0.01, in order to isolate the 'spectrum' of the quantum black hole. Note that with this choice, one is covering the full set of values of area, without the intervals overlapping, and what one is doing is to separate the total number of black hole states in different ranges of area, as is done when drawing a histogram. The resulting number is not then employed to determine the entropy (for which a much langer δA is employed). The results are plotted in Fig. 4.7 and Fig. 4.8. The oscillatory behavior found in the entropy, as well as the patterns shown in these figures have a period of $\Delta A_0 = 2.41\,\ell_{\rm P}^2$ approximately.

The next step was to compute the entropy by counting the number of states within a given interval of area, with the choice that the size of the interval coincide with the periodicity of the oscillations, namely $2\,\delta A = \Delta A_0$. The resulting entropy is plotted in Figures 4.3 and 4.4 where more details can be appreciated.

Let us now discuss the results. From Figures 4.1 and 4.2 it is clear that the spectrum of the quantum black hole has some new and non-trivial features. Specially noteworthy is the periodic structure that arises when looking at this rather small scale (recall that each Planck area is covered by 100 intervals and thus corresponds to 100 points in the graph). The appearance of these 'mountain like' structures, that are also periodic with the same period as the oscillations could not have been inferred from the oscillations in the entropy function. Thus, the periodicity of the entropy area relation has to be associated with these new structures in the spectrum and not with other features such as the change in the number of punctures, a simple transition involving creation/annihilation of edges puncturing the horizon, or any other 'naive' explanation of that sort. It is certainly intriguing that this new length scale appears, that as we would like to emphasize, is not related to any other scale previously found in LQG.

Motivated by these considerations, it was natural to explore the entropy counting with an area interval δA given by this new scale $2\delta A = \Delta A_0$. The results, shown in Figures 4.3 and 4.4 are quite unexpected. The oscillations that are found for all other values of δA disappear and instead, one is left with a 'ladder' in the entropy *vs* area graph.

The first conclusion from this graph, is that if one interprets the (ln of the) number of states as physical entropy then there are regions where the area changes but the entropy remains constant. Any quantum transition between those states would then correspond, in a precise sense, to an adiabatic process. Furthermore, we see that entropy (and not area) has effectively only a discrete number of possible values it can take. This is precisely the conclusion that

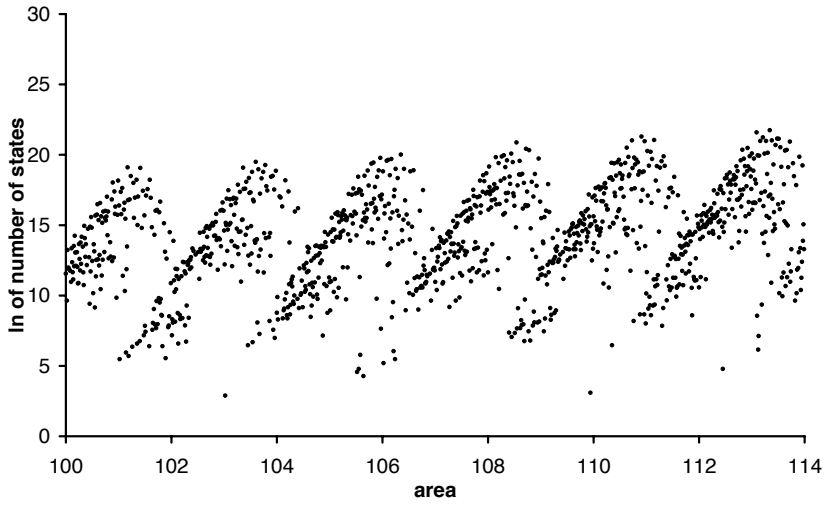

Fig. 4.8: The same as Fig. 4.1 but more detail is shown.

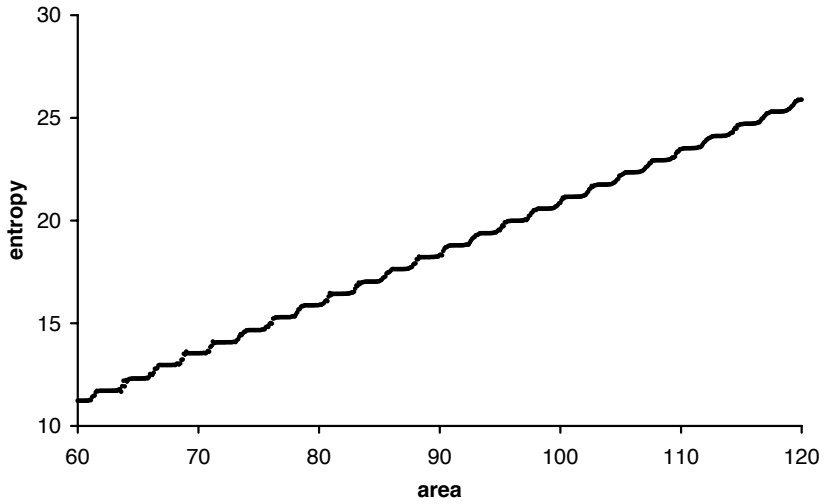

Fig. 4.9: The entropy as a function of area is shown, where the projection constraint has been imposed, the Barbero-Immirzi parameter is taken as $\gamma = 0.274$ and δA is taken to coincide with $1/2$ of the period of the oscillations in the number of states ΔA_0.

one can draw from Bekenstein's argument, namely that entropy should be equidistant for large black holes. Even when it can not be fully appreciated from the figures, what we observe is that the ladder is not completely regular for small black holes; the height of the ladder seems to increase, as the black holes grow, approaching a constant value for larger black holes. Thus, what we see that there is an emergent picture for small black holes within LQG that is consistent with Bekenstein's model. Furthermore, the manner in which the discrete equidistant values emerge is much more subtle than just assuming an equidistant area spectrum. From our perspective, it is a rather non-trivial result that loop quantum gravity does accommodate Bekenstein's picture for quantum black holes in such a subtle way.

In order to study the dependence of the period of both area and entropy on the value of γ, we performed a series of runs of the code with different values of the parameter γ. For the area, we found that the period is indeed linearly dependent with γ as has the following (conjectured) dependence:

$$\Delta A \approx 8\,\gamma \ell_{\mathrm{P}}^2\, \ln(3)\,. \tag{4.24}$$

The plot in Figures 4.3 and 4.4 were drawn for the value $\gamma_0 \approx 0.274\ldots$ of the parameter that reproduces the Bekenstein-Hawking relation $S = A/4$ in the large area limit (see [19] for details). The fact that the periodicity in area depends on the value of the Barbero-Immirzi parameter is not surprising since the operator and therefore its eigenvalues depend on it.

For the entropy, we have made the same estimations and the result is somewhat intriguing: the asymptotic size of the steps found in the entropy do not seem to depend on the value of the Barbero-Immirzi parameter γ. That is, if the conjectured numerical value of the area scale (4.24) is true, then what we find is an universal value in which the entropy is quantized, namely

$$\Delta S \approx 2\,\gamma_0\, \ln(3)\,. \tag{4.25}$$

It is certainly remarkable that, as black holes become large, entropy seems to be quantized in integer units of a quantity that contains both 'key' numbers: for the heuristic Bekenstein model, $\ln(3)$, and for loop quantum gravity, the value γ_0 of the BI parameter. The precise form of the entropy spectrum is slightly different from Eq. (4.22) (where $\Delta S = \ln(3)$), but one should also be aware that the relation (4.22) was arrived at by means of plausibility arguments rather than a hard core derivation. The conjectured entropy quantization condition derived from (4.25).

The main features we have found here about the quantum horizon system, namely the existence of a pattern in the black hole spectrum with a periodicity that permeates to the entropy area relation, and the appearance of a new scale associated with this period, could in principle be 'generic'. That is, one might imagine that these features are common to many quantum systems with a

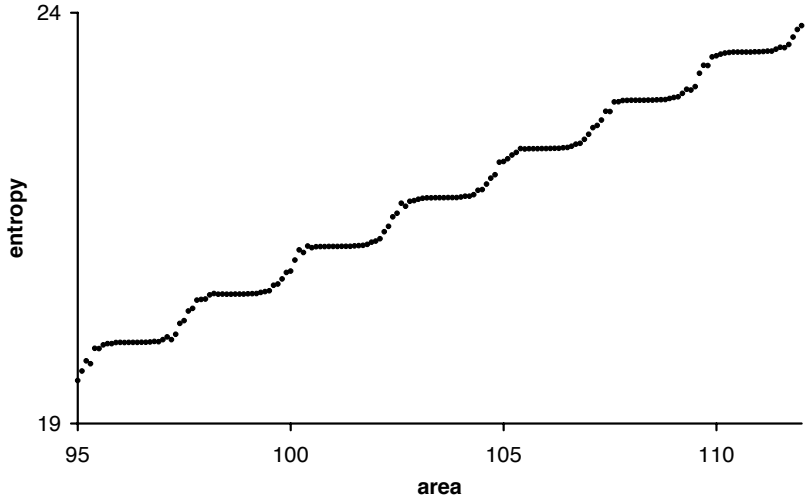

Fig. 4.10: Same as Fig. 4.3 but more detail is shown

finite number of degrees of freedom. In order to rule out this possibility we have repeated the analysis for a quantum horizon in which the area spectrum is equidistant and given by $A' = 8\pi\gamma\,\ell_{\rm P}^2 \sum_i j_i$ (an operator that has been suggested within LQG as well, see [16]). This would also correspond to the case (modulo a constant) of N decoupled harmonic oscillators in the micro-canonical ensemble. Perhaps not unexpectedly, we have seen that the black hole spectrum is in this case equidistant with an area separation of $\Delta A' = 8\pi\,\gamma\,\ell_{\rm P}^2$, which corresponds to the increase in area when one adds a couple of punctures (the projection constraint $\sum_i m_i = 0$ prevents one from having an odd number of punctures that have the minimum allowed spin, namely 1/2). There is no non-trivial periodic patterns in the spectrum and the entropy has discrete jumps that are directly associated to the fact that the area spectrum is equidistant.

Another possibility is that this behavior is a consequence of the particular counting procedure used, and that a different one [18] might not have the same properties. We have performed the counting using that procedure and have found the results to be robust: the entropy has discrete jumps and the relations 4.36 and 4.25 continue to be valid. Details will be discussed in the next section.

We will show there that the non-triviality of the loop quantum gravity area spectrum 4.23 is what brings the new and unexpected features to the entropy *vs* area relation that we have reported in this discussion, and is therefore responsible for black hole entropy quantization. Needless to say, these results can only be a hint of a deeper structure involving gravity, thermodynamics and the quantum that remains to be unravelled.

4.5 Toward understanding the band structure

As previously stated, two inequivalent proposals [18, 19] for characterizing the black hole degrees of freedom have received most of the attention. It is interesting that, within both of them, the problem of computing the black hole entropy can be reduced to a well defined *combinatorial* problem.

To exactly solve this combinatorial problem is, however, a rather non trivial task and, in order to obtain analytical solutions, some approximations have to be made. In particular the large area approximation permits to perform an analytic counting of the black hole microstates [18, 19]. Using this approximation the theory reproduces the semiclassical proportionality relation between entropy and area and gives an additional logarithmic term with a $-1/2$ coefficient,

$$S(A) = \frac{\gamma_c}{\gamma}\frac{A}{4\ell_{\rm P}^2} - \frac{1}{2}\ln\frac{A}{\ell_{\rm P}^2} + O(1)\ , \tag{4.26}$$

where γ_c is a numerical constant obtained from the counting. Fixing γ to be equal to γ_c ensures consistency with the Bekenstein-Hawking entropy law for

large areas. An important fact is that both definitions for the horizon states to be considered agree with (4.26), the only difference being the value of γ_c.

Alternatively, the complexity of the combinatorial problem can be overcome by telling a computer to make an *exact* counting by explicitly enumerating all states. Though the exponentially growing number of states limits the counting to modest black hole sizes (a few hundred Planck areas), the results in this regime agree with the analytical computations in the large area limit. Even more, this direct computation reveals a richer behavior shown by the spectrum when avoiding any approximation. The most degenerate quantum configurations accumulate around certain evenly spaced values of area, with a much lower degeneracy in the regions between those values, thus giving rise to an effective "quasidiscrete" equidistant area spectrum, despite the fact that the area spectrum in LQG is not equidistant. Furthermore, this phenomenon is independent on the particular choice for the characterization of the horizon degrees of freedom. This result provides a contact point between LQG and the Bekenstein's conjecture [35] and has important consequences for the physical properties of black holes, such as the entropy, which displays an effective discretization [43], or Hawking radiation, that could carry some quantum imprints coming from the horizon structure at the Planck scale [22].

This "band structure" arising in the black hole area spectrum of LQG calls for a more intuitive explanation, unraveling the origin of this phenomenon from the theory. This is the main goal of the present section. A recent work in this direction has been done by Sahlmann in [20], where he gives some quantitative information about the black hole area spectrum. In this section we will follow a rather different approach. Despite the complexity of the combinatorial problem, which makes a meticulous analysis unfeasible, the states can be properly handled by attending to a few properties that allow us to obtain the most relevant qualitative and quantitative information about the area spectrum, shedding some light on its behavior. In particular, this approach will help us to understand qualitatively the origin of the "band structure" and will also allow us to compute analytically the value of area corresponding to each "peak" of degeneracy.

We have organized the rest of the section as follows. In sections 4.5.1 to 4.5.4 we review the previous works, paying special attention to the aspects related with our arguments, and establishing the notation we are going to use, while sections 4.5.5 and 4.5.8 contain the main body of the present work. Section 4.5.1 is devoted to set up the combinatorial problem. In section 4.5.2 some previous analytical results are presented. Section 4.5.4 contains a summary of the computational results that showed the behavior that we are going to analyze. We present our qualitative picture and our quantitative analytical computations in section 4.5.5. The main results are analyzed in section 4.5.8. We finally conclude with an outlook in section 4.5.9.

4.5.1 Counting and labeling choices

Let us sumarize the issue we are discussing. As we have stablished before in the isolated horizon (IH) framework in LQG black holes are treated in an effective way, since they are introduced from the outset as an inner boundary of the spacetime manifold before the quantization procedure is carried out (see [14, 11] for details). Isolated Horizon boundary conditions are then imposed, which translate into quantum boundary conditions after the quantization procedure. The horizon states are described by a $U(1)$ quantum Chern-Simons gauge theory, while gravitational degrees of freedom of the bulk are represented by spin networks, a set of edges with spin-like quantum numbers (j, m) $(j \in \mathbb{Z}/2, m \in \{-j, -j+1, ..., j\})$ that intersect to each other at vertices. When an edge of the spin network pierces the horizon creating a puncture, it endows it with a "quantum" of area given by

$$a(j) = 8\pi\gamma\ell_{\mathrm{P}}^2\sqrt{j(j+1)}\ , \tag{4.27}$$

where j is the corresponding label of the edge, and with a quantum of curvature given by the label m (since the Isolated Horizon boundary conditions relate this label with the $U(1)$ Chern-Simons states on the horizon surface). Then, the quantum states of a black hole with area A must satisfy that the sum of the contribution to the area from each puncture equals the total horizon area,

$$A = 8\pi\gamma\ell_{\mathrm{P}}^2\sum_{i=1}^{p}\sqrt{j_i(j_i+1)}\ , \tag{4.28}$$

where p is the number of punctures on the horizon. Also a condition coming from the fact that the horizon is spherical must be imposed. This is

$$\sum_i m_i = 0\ , \tag{4.29}$$

which is called "projection constraint". The problem of counting the black hole microstates that account for its entropy is now reduced to a mathematically well defined *combinatorial* problem which can be stated as:

How many different configurations of labels distributed over a set of distinguishable[2] *punctures are there, for all possible finite numbers of punctures, such that the constraints* (4.28) *and* (4.29) *are satisfied?*

There exists a certain ambiguity at this point, since there are two proposals concerning which labels have to be considered to account for all microscopic

[2] The fact that punctures are distinguishable has its origin in some subtleties related with the action of diffeomorphisms during the quantization procedure, and plays a key role in the combinatorial problem.

Tab. 4.1: Comparison between the DLM and GM countings

	DLM	GM
Labels	m_i	(j_i, m_i)
Area	$8\pi\gamma\ell_{\rm P}^2 \sum_i \sqrt{\lvert m_i\rvert(\lvert m_i\rvert+1)}$	$8\pi\gamma\ell_{\rm P}^2 \sum_i \sqrt{j_i(j_i+1)}$
Projection constraint	$\sum_i m_i = 0$	$\sum_i m_i = 0$
Entropy	$S(A) = \frac{\gamma_{\rm DLM}}{\gamma}\frac{A}{4} - \frac{1}{2}\ln A$	$S(A) = \frac{\gamma_{\rm GM}}{\gamma}\frac{A}{4} - \frac{1}{2}\ln A$
BI parameter	$\gamma = \gamma_{\rm DLM} = 0.23753$	$\gamma = \gamma_{\rm GM} = 0.27407$

configurations. The issue of which is the proper counting is, however, beyond the scope of this thesis, as the behavior that we want to analyze is obtained within both of them.

The first of the two proposals was done by Domagala and Lewandowski in [18] and was complemented by Meissner in [18]. There, it is claimed that the horizon states are given by punctures carrying only the m_i labels (as these are the labels related to the horizon states through the IH boundary conditions). The constraint (4.28) is then reinterpreted in terms of $|m_i|$.

The second proposal is due to Ghosh and Mitra [19], and it considers that both labels, j_i and m_i, characterize the horizon quantum states. In this case, both constraints (4.28) and (4.29) can be imposed as written above. The structure, results and main differences between both models can be seen in Table 4.1.

For the purpose of this section, we need to deal with the labels related to area, so we will call this labels generically s_i, in such a way that the s_i will correspond to $|m_i|$ in the first case and to j_i in the second one. Furthermore, for the sake of simplicity, we will deal only with integer numbers, so that we will take $s_i = 2|m_i|$ or $s_i = 2j_i$ in each case. Then, in the DLM case, there will be two possible values of m_i for each s_i, namely $\{-\frac{s_i}{2}, \frac{s_i}{2}\}$, while in the GM one the possible values of m_i will be $\{-\frac{s_i}{2}, -\frac{s_i}{2}+1, ..., \frac{s_i}{2}\}$, so there will be $s_i + 1$ values of m_i for each s_i. This will be the only difference that we will have to introduce in our arguments in order to account for both counting models.

4.5.2 Previous analytical results

In this section we review briefly the previous analytical results on the counting of black hole microstates [14, 18, 19] present in the literature. When addressing the combinatorial problem described in the previous section, a key point is to consider that punctures are distinguishable, as shown in [14]. With this in mind, one should consider all possible orderings of labels over punctures. But given a certain configuration of s_i labels, all possible reorderings give rise to states with exactly the same area. One can then characterize a configuration

just by fixing the number n_s of punctures that take each particular value of s and introducing all possible orderings as a certain degeneracy associated with this configuration. Thus, in the remainder of the section, a given set of numbers $\{n_s\}_{s=1}^{s_{max}}$ (where s_{max} is the maximum value of s) will be called *configuration*. A configuration will be permissible if it satisfies the constraint (4.28), which in terms of n_s reads

$$4\pi\gamma\ell_{\rm P}^2\sum_{s=1}^{k} n_s\sqrt{s(s+2)} = A\ . \tag{4.30}$$

Then, in order to consider all quantum states contained in a given configuration, one has to take into account the degeneracy coming from two sources:

- one due to all possible reorderings of the $\{s_i\}$ labels over punctures,
- and the other coming from all possible combinations of the m_i labels associated to each configuration satisfying the constraint (4.29).

The difference between the two possible countings is contained in this last term. For the only reason of being able to explicitly write down some expressions, we are going to consider for the moment the term corresponding to the GM counting. One can then write the degeneracy associated to a given configuration $\{n_s\}_{s=1}^{s_{max}}$ as:[3]

$$d(n_1,...,n_{s_{max}}) = \frac{(\sum_s n_s)!}{\prod_s n_s!}\prod_s (s+1)^{n_s}\ , \tag{4.31}$$

where sums and products run from $s=1$ to s_{max}. In the above expression the projection constraint is not being introduced, but this fact will not affect the results that we are going to obtain in the remainder of the section. This degeneracy was studied in [19], where the question of which are the values of n_s that give rise to the maximal value of degeneracy, for a fixed value of area, was addressed.

The degeneracy $d(n_1,...,n_{s_{max}})$ (or equivalently $\ln d(n_1,...,n_{s_{max}})$) is maximized by varying n_s subject to the constraint (4.30), which is introduced via a Lagrange multiplier. This maximizing process can be easily worked out in the *large area limit*, where the variables $n_s \gg 1$ can be considered as continuous. The variational problem is then easily solved by using Stirling's approximation, which gives the result[4]

$$\hat{n}_s = \frac{n_s}{\sum_s n_s} = (s+1)e^{-\lambda\sqrt{s(s+2)}}\ , \tag{4.32}$$

[3] The factor $(s+1)^{n_s}$ is the one accounting for all the possible values of m_i associated to each s_i, so in order to make the analysis for the counting of [18] it will be enough to change this term by 2^{n_s}

[4] Although the equivalent expression obtained in [18] was presented on the basis of different considerations, it can also be given the same interpretation of a degeneracy maximizing distribution.

where for consistency, λ must satisfy the "normalization condition"

$$\sum_{s=1}^{s_{max}} (s+1)e^{-\lambda\sqrt{s(s+2)}} = 1 \ . \tag{4.33}$$

Numerical solutions of this equation, in the large area limit ($s_{max} \gg 1$) gives $\lambda_{\rm GM} = 0.861006$ (or $\lambda_{\rm DLM} = 0.746232$ in the case of the other counting proposal).

We will call this $\hat{n}_s$ distribution the *Maximal Degeneracy Distribution*[5] (MDD), and it will play a pivotal role from now on. Besides, it was shown in [18, 19] that the introduction of the projection constraint does not modify this distribution, so despite one starts without imposing it, the results can be considered as including this constraint.

It is worth noting that, in the MDD, the proportions between the different n_s are maintained for different values of area (the values of n_s grow proportionally), and then the values of $\hat{n}_s$ are independent of area. When plotting $\hat{n}_s$ (Figure 4.11), an interesting behavior is observed. Although the largest contribution comes from the smallest value of s (which contributes with approximately one half of the punctures), the contribution of the next few values of s is also significant. Nevertheless, the MDD shows an exponential decrease as s grows, so for s larger than the smallest few values the contribution will become negligible.

Once the MDD has been obtained, the total number of quantum states for a given value of area can be computed. The result is [18, 19]

$$d = \frac{\alpha}{\sqrt{A/\ell_{\rm P}^2}} \exp\left(\frac{\lambda}{4\pi\gamma\ell_{\rm P}^2}A\right) \ , \tag{4.34}$$

where $\alpha \sim O(1)$. It is seen that the number of quantum states grows exponentially with area; the extra factor $A^{-1/2}$ appears due to the introduction of the projection constraint (4.29). From this the entropy can be computed, obtaining

$$S(A) = \frac{\lambda}{\pi\gamma}\frac{A}{4\ell_{\rm P}^2} - \frac{1}{2}\ln\frac{A}{\ell_{\rm P}^2} + O(1) \ . \tag{4.35}$$

This result verifies the semiclassical Bekenstein-Hawking entropy formula for large areas provided that $\gamma = \lambda/\pi$. Substituting the value of λ for each counting the corresponding values for the Barbero-Immirzi parameter are obtained

$$\gamma_{\rm GM} = 0.274066858 \ , \quad \gamma_{\rm DLM} = 0.237532958 \ .$$

[5] We will use the term *distribution* as opposed to *configuration*, in the sense that it gives the proportions between the different n_s instead of the absolute value of each n_s. We will use this terminology in the next sections.

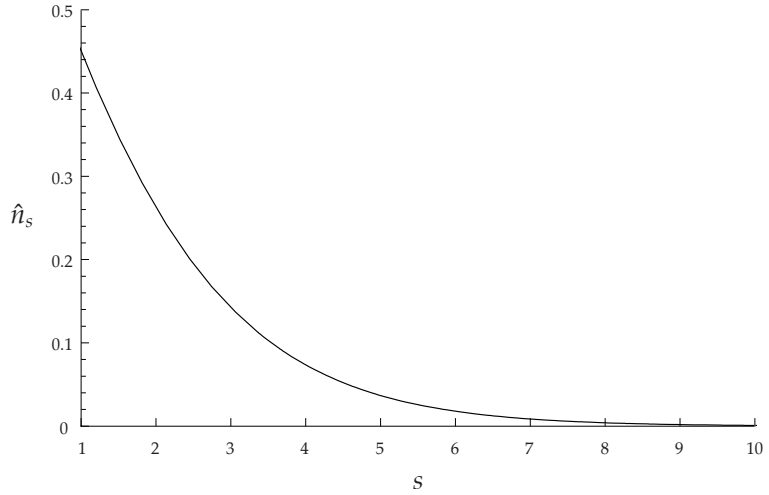

Fig. 4.11: The $\hat{n}_s$ given by the Maximal Degeneracy Distribution (MDD) is plotted as a function of s. The relevant contribution of the lower values of s and the exponential decrease as s grows are observed.

4.5.3 Large area limit

In the previous computations the large area approximation was involved. However, one can wonder about the meaning of "large area" in this context. If one looks at the normalization condition (4.33), it is easy to see that the value of λ obtained from it depends on the value of s_{max} to which we are summing up. Then, as the value of s_{max} depends on the area, we have a λ that is a function of area. Nevertheless, if one studies the function $\lambda = \lambda(A)$ (or equivalently $\lambda = \lambda(s_{max})$, as shown in Figure 4.12), one sees that the value of λ grows very quickly and saturates the asymptotic value for relatively small values of s_{max} (for s_{max} around 12 the value of λ only differs from the asymptotic value in a 0.006%). But this value of s_{max} corresponds to values of area around $45\ell_{\rm P}^2$. So for areas larger than that, we can say that we are already in the large area limit, as far as the distribution (4.32) is concerned.

4.5.4 Previous computational results

In the previous section, some approximations were employed in order to count the number of quantum microstates compatible with a macroscopic black hole. One can legitimately be worried about the fact that this approximations could be hiding part of the richness of the problem. Fortunately, in spite of its intrinsic complexity, an exact counting can be performed to see whether there

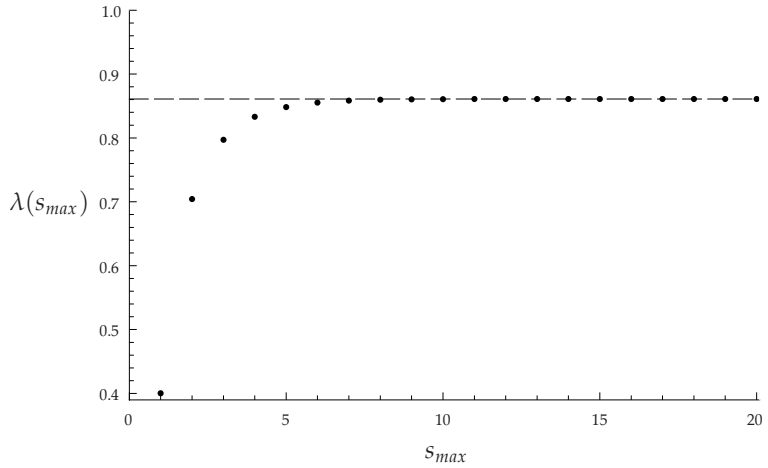

Fig. 4.12: The value of λ as a function of s_{max} is plotted, and compared with the asymptotic value.

is a richer structure in the spectrum or not. This can be done by means of an explicit enumeration computational algorithm. The strategy is to generate systematically all possible combinations of labels (for any possible number of punctures), and to check one by one whether it satisfies the required conditions. Then, by explicitly enumerating all states, one can make an exact counting of the black hole quantum configurations (for a given value of area) in this framework. This was done in [38, 43]; here we are going to review the main results obtained there and in subsequent work. Even when such an exact counting can be done, the price to pay for overcoming the complexity of the problem with an explicit enumeration is a severe restriction to the black hole sizes that can be analyzed due to the huge number of configurations to be counted. For that reason, the available computing power allowed to analyze black holes up to just a few hundred Planck area sizes. However, these computations were enough to confirm the results of the previous sections, namely the exponential growth of the number of states with area and, when imposing the projection constraint, the factor $A^{-1/2}$. The fact that this results are compatible with the analytical computations gives one some confidence in the interest of performing such a counting even though, due to computational limitations, one is restricted to work in a small horizon area regime, far below the large area limit in which the Isolated Horizon framework in LQG was originally formulated.

But besides confirming the previous analytical results, the exact counting showed a much richer behavior in the black hole area spectrum [43]. It

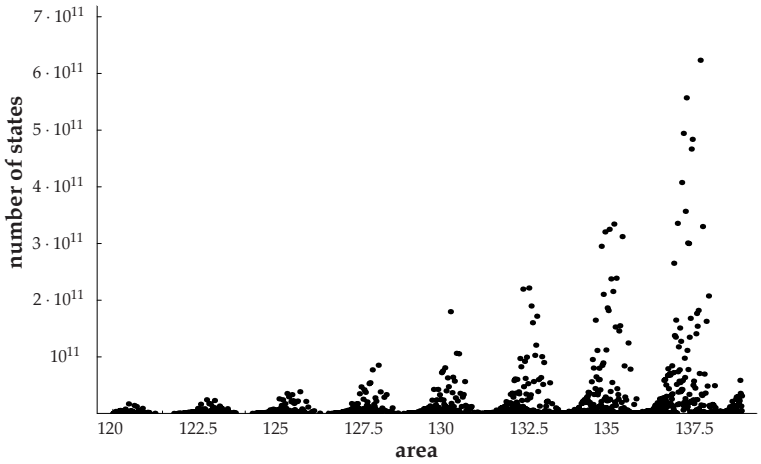

Fig. 4.13: Plot of the degeneracy (number of different horizon states in each area interval of $0.01 l_{\mathrm{P}}^2$). States accumulate around some equidistant values of area, exhibiting a band structure.

was found that the black hole quantum states are distributed according to a "band structure" in terms of the area. The most degenerate configurations cluster around evenly spaced values of area, giving rise to equidistant peaks of degeneracy, with some orders of magnitude less degeneracy in the regions between them (Figure 4.13). This fact gives rise to an *effective* equidistant quantization of the black hole area in LQG, even when the area spectrum in the theory (4.27) is not equidistantly quantized. The most relevant quantitative information about this phenomenon is the fundamental area gap between peaks, which is given by

$$\Delta A = \gamma \chi \ell_{\mathrm{P}}^2 \ , \tag{4.36}$$

where χ was estimated to be

$$\chi \approx 8.80 \ .$$

A remarkable fact is that this result was obtained for both choices of labels to be counted, and that all the difference resides just in the value of the Barbero-Immirzi parameter.

The obvious interest is now in the physical consequences of this structure. The first clear consequence is in the entropy-area relation. This periodic band structure in the area spectrum gives rise to a very distinctive signal in the black hole entropy, namely a stair-like behavior of entropy as a function of area,[6]

[6] For details on how to obtain the entropy shown in Fig.4.14 from the degeneracy of Fig.4.13 see [38, 43]

as shown in Figure 4.14. Furthermore, the particular structure of the area spectrum can also have some implications regarding the black hole radiation spectrum, as pointed out in [22].

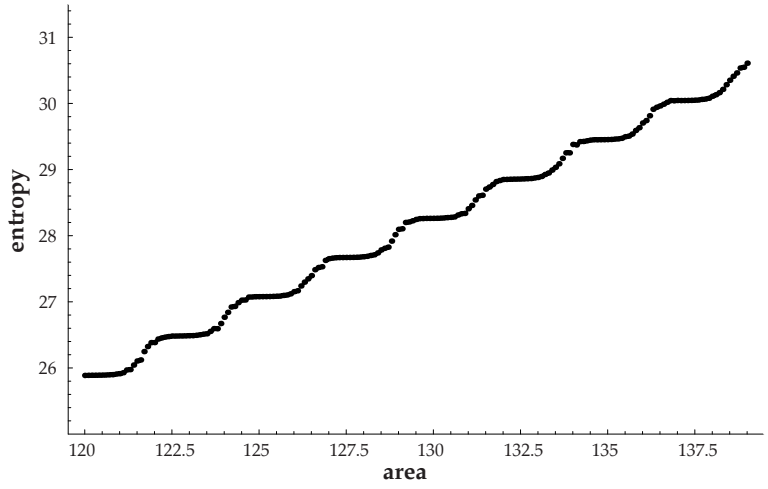

Fig. 4.14: Plot of the results for the entropy as a function of area (in Planck units) obtained with the computational counting. The stair-like behavior, with a step width corresponding to ΔA, is observed.

On the other hand this regular pattern in the black hole area spectrum provides a nice contact point with the heuristic ideas of Bekenstein and Mukhanov [35] about black hole area equidistant quantization. Even though the basic area spectrum in LQG is not equidistant, this phenomenon shows that in the case of black holes this equidistance in the spectrum appears in a rather subtle way, namely as a result of the non trivial degeneracy distribution. This point of contact becomes even more intriguing when one realizes that the value of χ is close to $8 \ln 3 \approx 8.788898$, as there is also a logarithmic constant arising from the heuristic considerations of Bekenstein and Mukhanov. It is evident that no reliable conclusion can be extracted from this numerical proximity but it is worth keeping it in mind to see if a more detailed work can confirm a deeper relation behind this coincidence.

4.5.5 The richness of discreteness

In this section we seek to understand where the equidistant structure in the black hole spectrum comes from. We are going to analyze what happens to the MDD when one takes into account the discrete nature of the problem.

Then, we are going to classify all configurations in sets characterized by two parameters, in such a way that the accumulation of states around the peaks of degeneracy becomes explicit and easy to study. Using these parameters, and some information extracted from the MDD, we will compute the value of area corresponding to each peak of degeneracy and then the area gap between peaks.

The first thing to consider is how is it possible to obtain information about the quasi-discrete structure of the spectrum using a distribution that was computed with approximations that seem to neglect all the information about this behavior. In this point the important thing to notice is that, in fact, the approximation that is hiding all the discrete information is to assume that one can find some configuration satisfying the MDD for any given value of area. When doing this, one is implicitly assuming that the n_s numbers can take any possible real value given by (4.32), that in general are not integer values. It is clear that a non integer value for n_s makes no sense. Then in order to find the actual maximally degenerate configuration, one should take the closest integer to each value of n_s given by the MDD. However, if one modifies the value of n_s, one is modifying also its contribution to the area. Then, there are two possible cases, depending on the value of area we start with:

- When one tries to find the closest integer configuration, the area changes of each n_s compensate each other in such a way that at the end the integer configuration that we find takes almost the same value of area. Then we will be able to find some highly degenerate integer configurations with the same value of area we started from. This case would correspond with a peak of degeneracy.

- When changing to the closest integer configuration, the deviations of each n_s add up giving rise to a global area change so that the resulting integer configuration lies, in fact, in a different region of the spectrum. If one tries to find some integer configuration with the same value of area than the continuous one, it will not suffice to just take the closest integer to each n_s. One would be forced to modify considerably the n_s distribution, in order to reach this value of area with integer n_s values. But then, the obtained configuration will follow a distribution no longer close to the maximal degeneracy one, and would then have a much lower degeneracy. Therefore, one will not be able to find a highly degenerate integer configuration for this value of area. Such values of area are the ones corresponding to the regions of low degeneracy between peaks.

Our task now is to find out which values of area correspond to the first case and which ones to the second. In order to do that, we will use a convenient classification of states.

4.5.6 Classifying states

The combinatorial problem we are trying to address is a very complicated one, given the large number of variables (degrees of freedom) that come into play. For this reason, it is very difficult to handle all the information in a straightforward way. In order to be able to understand the underlying structure, we are going to organize all these configurations according to two parameters that will allow us to have a reasonable number of variables while keeping enough information for our analysis and computations. The two parameters we are going to consider to classify configurations are:

- The number p of punctures of the configuration, $p = \sum_{s=1}^{s_{max}} n_s$, and
- the sum over all punctures of the s_i labels $S = \sum_{i=1}^{p} s_i = \sum_{s=1}^{s_{max}} s\ n_s$.

For each pair of values of these parameters, we will have a set of many possible configurations. But the interesting thing is that if one fixes a given pair (S, p), then the only freedom left to change the value of area associated to a configuration, is to distribute the S "units of s label" over the p punctures in different ways (or in other words, to change the n_s distribution). But the changes in area given by changing the distribution of n_s are very small compared with the change in area given by modifying the parameters S or p in one unit (the requirement that all n_s must be integer obviously implies that S and p can only take integer values). Then, by considering all possible n_s distributions, one is covering an almost continuous region of area in the spectrum, while modifying S or p results in a discrete jump to another area region. Of course, if one modifies radically the n_s distribution, from one extreme to the other, one can get changes in area larger than the one given by a change of one unit in S or p, so these different area regions could overlap at some points.

On the other hand, although changing S produces a jump in areas and so does a change in p, one could in principle modify both parameters in such a way that the final area change is small. In fact, as we are going to see, there is a way of changing S and p so that the area does not change. As pointed out in [22], there is a very precise relation in the area spectrum of LQG that will help us to obtain this interesting relation between S and p. One can check that the contribution to area given by one puncture with $s = 6$ is exactly the same as the contribution given by four punctures with $s = 1$. The interesting fact about this relation is that it is the only existing one for the low values of s that are relevant to the highly degenerate configurations[7] (as pointed out in section 4.5.2, the value of $\hat{n}_s$ decreases exponentially with s in the MDD).

[7] The next exact relation is found between one puncture with $s = 16$ and six punctures with $s = 2$, but the contribution of punctures with $s = 16$ to the highly degenerate configurations is completely negligible.

Then, given a configuration, one can obtain another one with exactly the same value of area by removing a puncture with $s = 6$ and adding four punctures with $s = 1$ (decreasing the value of n_6 in 1 unit and increasing n_1 in 4 units). But this change implies increasing the number of punctures p in three units and decreasing the sum of s over all punctures (S) in two. Therefore, different pairs of parameters (S, p) related by this transformation will be in the same area region.

We can write down this relation in a more concrete way. Given a value S_0 for S and a value[8] $p_0 = 1, 2, 3$ for p, all pairs (S_t, p_t) that satisfy the following relation:

$$(S_t, p_t) = (S_0 - 2t, p_0 + 3t) \ , \tag{4.37}$$

with $t \in \mathbb{Z}$ such that $S_t \geq p_t$, are in the same region of area. S_0 will be the maximum value of S and p_0 the minimum value of p among all pairs (S_t, p_t) satisfying this relation. Thus, if we consider the quantity $K = 3S_0 + 2p_0$, we can associate to the same value of area all pairs of parameters satisfying

$$3S + 2p = K \ . \tag{4.38}$$

Then, for each value of K we will obtain the configurations that appear in a certain region of area. In fact, it is important to notice that, if one takes into account the projection constraint, then the value of S can only be even (for an odd value of S would imply that $\sum_i m_i$ can only take half-integer values, and it could not be zero). With this in mind, K will only be allowed to take even values.

4.5.7 *Highly degenerate integer configurations*

Now, in order to account for the peaks of degeneracy, we have to consider the most degenerate integer configurations, which we will find with the help of the MDD. For a certain value of area, this distribution fixes a value for S and p, that we will call $S_{md}(A)$ and $p_{md}(A)$. Furthermore, as the values of $\hat{n}_s$ are constant with area, $S_{md}(A)$ and $p_{md}(A)$ will grow proportionally with area, giving rise to a constant quotient $\hat{s}_{md} = \frac{S_{md}}{p_{md}}$. Hence, not all the pairs (S, p) can contain maximally degenerate configurations; these configurations can only take values of S and p satisfying the quotient $\hat{s}_{md}$. However, it is important to notice that the values of $S_{md}(A)$ and $p_{md}(A)$ fixed by the MDD are not, in general, integer numbers. Then, if starting from a configuration satisfying the MDD one changes to the closest integer values for each n_s in order to find the actual maximally degenerate integer configuration, this would necessarily imply a change in S and in p to integer values. But as we have seen, to change S and p implies relatively large changes in area, unless such changes in S and p follow the

[8] Any value of p larger than 3 would be in correspondence with one of these tree values of p_0, i.e., a pair $(S, p = 4)$ will correspond to $(S_0 = S + 2, p_0 = 1)$, and so on.

"constant area" relation (4.38). Therefore, if those $(S_{md}(A), p_{md}(A))$ satisfy this relation for an even value of K, it will be possible to find, for the same value of area, some integer pair (S', p'), with even S', close to $(S_{md}(A), p_{md}(A))$, thus containing highly degenerate configurations. Otherwise, it will not be possible to find any highly degenerate configuration for that value of area, as explained at the begining of section 4.5.5.

In addition, among all configurations compatible with a given pair of values (S', p'), the most degenerate ones will be those having n_s distributions close to the MDD, and therefore they will all appear together in a region of area much smaller than the total area covered by the set of all configurations with these values of (S', p'). Then, although the regions of area corresponding to different pairs (S, p) can overlap (as pointed out above), the regions containing highly degenerate integer configurations will not. Thus, we expect to find the highly degenerate configurations clustered around some area values, each one corresponding to a different value of K.

We are going to compute in next section the values of area for which the MDD fixes a pair of values $(S_{md}(A), p_{md}(A))$ satisfying the constant area relation for each value of K, which will correspond to the values of area of the peaks of degeneracy.

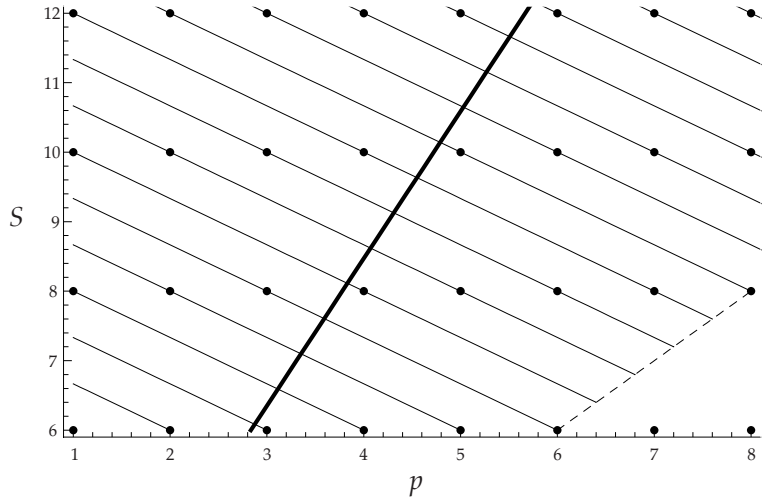

Fig. 4.15: Plot of the sum S of spin labels vs. the number p of punctures. All the discrete configurations are placed in the marked points. The thin lines represent "constant area surfaces" (K-lines) while the thick line cointains the values of (S, p) that satisfy the quotient $\hat{s}_{md}$ (MD-line).

We can understand the above discussion in a more graphical way looking

at Figure 4.15. The positive slope line represents the pairs (S, p) that satisfy the maximal degeneracy quotient $\hat{s}_{md}$ (MD-line). Each of the negative slope lines represent the values (S, p) related by (4.38) for each even value of K (K-lines). The marked points represent the allowed integer pairs (S, p). Only for those points at where the MD-line intersects some of the K-lines, a close integer pair (S', p') can be reached following the corresponding K-line (keeping area constant). In other words, the actual highest degeneracy configurations, that can only be found in the integer points close to the MD-line, correspond to the values of area associated to the point at which the corresponding K-line intersects this MD-line. The MDD provides the necesary information to compute the value of area associated to each point of the MD-line, as well as the slope of this MD-line. We can compute, therefore, the area of each intersection point and, thus, of the corresponding peak of degeneracy. Finally, computing the difference in area between two consecutive intersections (two consecutive even values of K) we will get the area gap between two peaks of degeneracy.

As a final remark in this section, we can analyze the effect of the projection constraint. In our model, this constraint is introduced by considering only even values of K (i.e. even values of S). Then, if the projection constraint was not introduced, there would be an additional line between each two consecutive K-lines in Figure 4.15. This would correspond to having an additional peak of degeneracy between each two. But looking at Figure 4.13 one can see that, given the proportions of the spacing between peaks and the width of those peaks, placing an additional one between each two would almost result in no low degeneracy regions between them, hiding then the "quasi-discrete" structure of the spectrum. Then, as pointed out in [20], the regular pattern we are studying is a general feature that affects to all states and not only those satisfying the projection constraint. But it is precisely the introduction of this constraint what makes the "discrete" structure to arise in a clear and relevant way.

4.5.8 Computation of ΔA

Let us then proceed whith the explicit computation of these quantities. The steps we are going to follow are:

- In the first place, using the MDD we will compute the quotient $\frac{S_{md}}{p_{md}}$ for maximally degenerate states ($\hat{s}_{md}$).
- From (4.38) we will obtain an explicit relation $S = S(p, K)$.
- We will use this explicit relation and the value of the quotient $\hat{s}_{md}$ to compute the number of punctures of the maximally degenerate state $p_{md}(K)$ for a given value of K (the value of p at which the MD-line intersects a K-line in Figure 4.15).

- Then, again using the MMD, we will compute the mean contribution to area $\hat{A}_{md}$ of a puncture in a configuration satisfying this distribution.
- Thus, the value of area associated to an intersection with a line characterized by K will be $A_{md}(K) = p_{md}(K)\hat{A}_{md}$.
- Finally, computing the difference between $A_{md}(K)$ for two consecutive even values of K ($A_{md}(K+2) - A_{md}(K)$), we will obtain the value of ΔA.

In order to compute $\hat{s}_{md}$ it is worth noticing that the quantity $\frac{S}{p}$ can be seen as the mean value of s of each puncture in a configuration. Then, to compute this value in the case of the MMD we can write

$$\hat{s}_{md} = \sum_s s\hat{n}_s. \tag{4.39}$$

Thus we can compute the value of $\hat{s}_{md}$ and we know that

$$\frac{S_{md}}{p_{md}} = \hat{s}_{md} \ . \tag{4.40}$$

Now, from the relation between S and p in a given band ($3S + 2p = K$), we can extract the following equation

$$S(p, K) = \frac{K}{3} - \frac{2}{3}p \ . \tag{4.41}$$

Plugging this into (4.40), we get

$$\frac{S_{md}(p, K)}{p_{md}(K)} = \frac{\frac{K}{3} - \frac{2}{3}p_{md}(K)}{p_{md}(K)} = \hat{s}_{md} \ ,$$

leading to

$$p_{md}(K) = \frac{K}{3\hat{s}_{md} + 2} \ . \tag{4.42}$$

We have then the number of punctures that correspond to a maximal degeneracy configuration for a given value of K (the intersection for a given K-line).

Now, to compute the mean contribution to the area from a puncture in a configuration satisfying the MDD, we proceed in the same way as we did to compute $\hat{s}_{md}$. We then write

$$\hat{A}_{md} = \sum_s a(s)\hat{n}_s = 4\pi\gamma\ell_{\mathrm{P}}^2 \sum_s \hat{n}_s\sqrt{s(s+2)} \ . \tag{4.43}$$

With this expression we can write the value of area associated to each of the intersections for each value of K,

$$A_{md}(K) = p_{md}(K)\hat{A}_{md} = \frac{K\hat{A}_{md}}{3\hat{s}_{md}+2} \ . \tag{4.44}$$

We have then arrived at the main goal of the section, i.e. obtaining the value of area associated to the corresponding peak of degeneracy for each value of K. With this expression we can compute numerically the value of area of each peak of degeneracy. We can also easily see that A_{md} has a linear dependence on K, so the peaks are evenly spaced. We can hence compute this spacing just by taking the difference between two consecutive values of K,

$$\Delta A = A_{md}(K+2) - A_{md}(K) = \hat{A}_{md}(p_{md}(K+2) - p_{md}(K)) = \frac{2\hat{A}_{md}}{3\hat{s}_{md}+2} \ . \tag{4.45}$$

Then, finally, writing explicitly all the terms in the above result, we can express the value of the area gap between peaks as

$$\Delta A_{\rm GM} = \chi_{\rm GM}\gamma_{\rm GM} = \frac{8\pi\gamma_{\rm GM} l_{\rm P}^2 \sum_s \sqrt{s(s+2)}(s+1)e^{-\lambda_{\rm GM}\sqrt{s(s+2)}}}{3(\sum_s s(s+1)e^{-\lambda_{\rm GM}\sqrt{s(s+2)}})+2} \ . \tag{4.46}$$

At this point, we can recall that the only difference in all this discussion between the label choice we are using and the other comes from the degeneracy associated to the combinations of m_i compatible with each configuration. Introducing this change, the result for the $\Delta A_{\rm DLM}$ in the case of the counting of [18] is

$$\Delta A_{\rm DLM} = \chi_{\rm DLM}\gamma_{\rm DLM} = \frac{8\pi\gamma_{\rm DLM} l_{\rm P}^2 \sum_s 2\sqrt{s(s+2)}e^{-\lambda_{\rm DLM}\sqrt{s(s+2)}}}{3(\sum_s 2se^{-\lambda_{\rm DLM}\sqrt{s(s+2)}})+2} \ , \tag{4.47}$$

with the corresponding $\lambda_{\rm DLM}$.

Analysis of the results

In this section we present the numerical values obtained for χ and analyze them. The resulting values of the expressions we have found can be easily computed using Mathematica$^{\rm TM}$ and we get

$$\chi_{\rm GM} = 8.789242 \ , \quad \chi_{\rm DLM} = 8.784286 \ . \tag{4.48}$$

The fact that the difference between these two values is in the fourth digit gives us a hint on the level of accuracy that is being reached. Besides, it was pointed

out in [43] that the value of χ is numerically close to $8\ln 3 = 8.788898$. One can see that the above results coincide, also up to the fourth digit, with this value, and furthermore, that $8\ln 3$ is contained between the two values of χ above. One can compute the deviations between the three values:

$$\frac{|\chi_{\rm GM} - 8\ln 3|}{8\ln 3} = 0.000039 = 0.004\% \ ,$$
$$\frac{|\chi_{\rm DLM} - 8\ln 3|}{8\ln 3} = 0.00052 = 0.05\% \ ,$$
$$\frac{|\chi_{\rm GM} - \chi_{\rm DLM}|}{\chi_{\rm GM}} = 0.00056 = 0.06\% \ .$$

Then, with a precision of 0.06%, the values of $\chi_{\rm GM}$, $\chi_{\rm DL}$ and $8\ln 3$ are the same. Of course, this is still not a rigorous proof that χ is equal to $8\ln 3$, but it is relevant to see how, when one improves the accuracy of the calculations, the numerical coincidence is still satisfied.

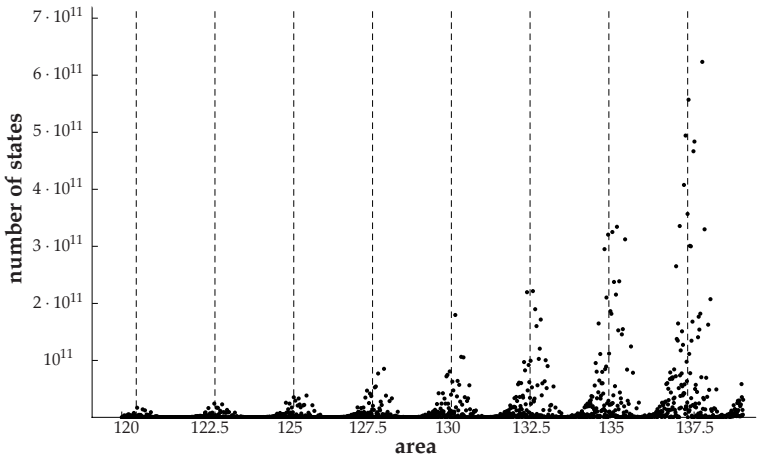

Fig. 4.16: Comparison between the analytical values for the area of the peaks (dashed vertical lines) and the actual peaks obtained from the computational data.

Let us end this section with two remarks.

- One can check whether the results obtained with the model presented here are in good agreement with the computational data obtained from the algorithm of [38]. It can be seen in figure (4.16) how the values for the area of the peaks that we obtained here fit the peaks observed in the spectrum obtained from the computer. We see how the analytical values

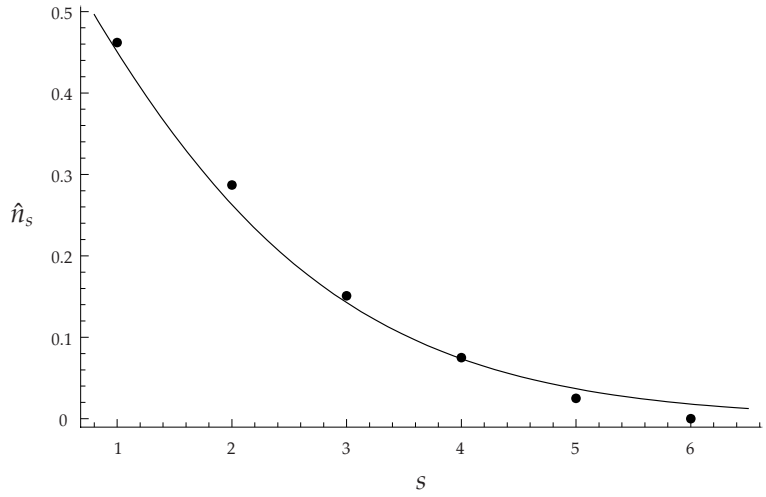

Fig. 4.17: The mean values of $\hat{n}_s$ obtained from the computational results (points) are compared with the exponential decrease expected from the MDD.

match in a nice way with the computational data. On the other hand, in figure (4.17) the mean values of the $\hat{n}_s$ obtained with the computer for the five most degenerate configurations of three consecutive peaks (with areas between 170 and $177\ell_{\mathrm{P}}^2$) are compared with those given by the MDD. One can check that, even for this extreme low value of area, the agreement is quite good, as expected from the analysis in section 4.5.3, so one can feel confident with the use of the MDD in the computations. Finally, using these computational data we have observed that, in fact, all configurations giving relevant contributions to the degeneracy at any given peak are characterized by pairs of values (S, p) that satisfy the relation (4.38) for the corresponding value of K, in complete agreement with the analysis presented in section 4.5.5. Thus, the computational data support the fact that the model presented here works reasonably well.

- At this point we can analyze the results previously obtained in [20]. There, the problem is addressed using a rather different approach, namely, reformulating it in terms of the so called random walks. It is very interesting to see how, within this alternative approach, the accumulation of states around certain values of area also becomes manifest. By treating the area spectrum of LQG as an effectively quasi-equidistant spectrum, a way to compute the area gap between peaks is then proposed. The

value for ΔA was obtained as 2/3 of the spacing in this effectively quasi-equidistant area spectrum. This 2/3 factor was introduced *ad hoc* in order to fit the computational data. A noteworthy fact is that this independent derivation gave rise to the same expresion (4.47). Nevertheless, from the point of view of the authors it is not easy to reconcile the introduction of this 2/3 coefficient with the qualitative picture of a quasi-equidistant spectrum being the origin of the observed regular pattern.

With the picture presented here, it is now rather easy indeed to understand where this coefficient comes from. The fundamental area gap in the quasi-equidistant spectrum of [20] corresponds to the mean area change given by increasing S in one unit in our formalism. But as we have seen, S only takes even values. Then the minimum increment in S must be two. Furthermore, if one comes back to the relation between S_0, p_0 and K ($K = 2S_0+3p_0$) then one can check that for each even value of S_0 there are three corresponding values of K (the ones corresponding to $p_0 = 1, 2, 3$) and then to three peaks of degeneracy. Hence, the mean area change given by increasing S in two units corresponds to three times the area gap between peaks. Thus, the fundamental gap of the quasi-equidistant spectrum in [20] is nothing but three halves of the area gap between peaks ΔA.

4.5.9 Conclusion and outlook

Let us summarize the results of the section. We have analyzed the combinatorial problem and we have qualitatively understood the reason why the highest degenerate configurations can only appear for some values of area and not for all of them. When the discrete nature of the problem is taken into account, there are regions of area for which the "discrete configurations" are not allowed to satisfy a distribution close to the one that gives the maximal degeneracy in the continuous case, thus giving rise to the observed pattern in the black hole area spectrum. We have also verified that the analysis is valid for both choices of labels, as the arguments presented here apply equally to both cases, so it seems now rather natural that the analyzed behavior of the spectrum appear with both counting procedures. Finally, our analytical computations allowed us to obtain the values of area for which the peaks of degeneracy should appear and showed that these values are evenly spaced. In addition, the results match in a nice way with the computational data obtained in [38], thus indicating the validity of the model. From this, we have also been able to compute the analytical value of the corresponding parameter χ for both label choices and we have found that the results coincide up to a precision of 0.06%. Furthermore, we have checked out that, up to this improved precision, the surprising numerical coincidence with $8 \ln 3$ keeps holding.

There are still some important open questions. On the one hand, one may ask which are the sources of this 0.06% deviation. Moreover, it would be very interesting to obtain an analytical proof for the conjectured value of $\chi = 8 \ln 3$. On the other hand, although the area gap between peaks obtained with our model has no dependence on the area, one may be interested in knowing what would happen to the width of the bands for large areas. Whether this width increases with area, thus hiding the quasi-discrete behavior, or not, is also an interesting issue to be investigated. A comprehensive analysis of the full combinatorial problem could shed light on some of these questions. But undoubtedly, the most important and interesting open question is to find a consistent physical interpretation to this intriguing behavior of quantum black holes.

4.6 Number theory techniques

In this section we are going to give a precise characterization of the area spectrum by relying on number-theoretic methods, and addressing the combinatorial problems related to the projection constraint. We do it for the original counting of states proposed in [14] and carried out in [18], and also for the one described in [19]. The method that we discuss in the following will allow us to have a full understanding of the different factors that come into play to reproduce the features previously observed in the black hole degeneracy spectrum. In addition, it can be efficiently used to perform *exact* entropy computations –extensible to large areas– that improve and confirm the results obtained by brute force methods presented previously.

4.6.1 Characterization of the area eigenvalues

We start by characterizing the area eigenvalues and their degeneracies. As we stablish in the former, the LQG the black hole area is given by an eigenvalue A of the area operator

$$A = 8\pi\gamma\ell_{\mathrm{P}}^2 \sum_{I=1}^{N} \sqrt{j_I(j_I+1)}\,, \tag{4.49}$$

. As before, the labels j_I are half-integers, $j_I \in \mathbb{N}/2$, associated to the edges of a given spin network state. They pierce the horizon at a finite set of N distinguishable points called punctures [14]. Horizon quantum states are further characterized by an additional label m_I. In the case where we have spherical symmetry a *projection constraint*

$$\sum_{I=1}^{N} m_I = 0 \tag{4.50}$$

must be satisfied by the m_I.

A first problem that we address is the characterization of the numbers belonging to the spectrum of the area operator restricted to the vector subspace spanned by spin network states having no vertices nor edges lying on the black hole horizon. In the following when we talk about the area spectrum we refer, in fact, to this restriction. The first question that we want to consider is: Given $A \in \mathbb{R}$, when does it belong to the spectrum of the area? In order to simplify the algebra and work with integer numbers we will write $j_I = k_I/2$ in the following, so that the area eigenvalues become

$$A = \sum_{I=1}^{N} \sqrt{(k_I+1)^2 - 1} = \sum_{k=1}^{k_{\max}} n_k \sqrt{(k+1)^2 - 1}.$$

Here we have chosen units such that $4\pi\gamma\ell_{\mathrm{P}}^2 = 1$, and the n_k (satisfying $n_1 + \cdots n_{k_{\max}} = N$) denote the number of punctures corresponding to edges carrying spin $k/2$. An elementary but useful comment is that we can always write $\sqrt{(k+1)^2-1}$ as the product of an integer and the square root of a square-free positive integer number (SRSFN) by using its prime factor decomposition. Hence, with our choice of units, only integer linear combinations of SRSFN's can appear in the area spectrum. The questions now are: First, given such a linear combination, when does it correspond to an eigenvalue of the area operator? If the answer is in the affirmative, what are the permissible choices of k and n_k compatible with this value for the area?

In the following we will take advantage of the fact that SRSFN's are linearly independent over the rational numbers (and, hence, over the integers) i.e. $q_1\sqrt{p_1} + \cdots + q_r\sqrt{p_r} = 0$, with $q_i \in \mathbb{Q}$ and p_i different square-free integers, implies that $q_i = 0$ for every $i = 1, \ldots, r$. This can be easily checked for concrete choices of the p_i and can be proved in general (see for instance [40]). We can answer the two questions posed above in the following way. Given an *integer* linear combination of SRSFN's $\sum_{i=1}^{r} q_i\sqrt{p_i}$, where $q_i \in \mathbb{N}$, we need to determine the values of the k and n_k, if any, that solve the equation

$$\sum_{k=1}^{k_{\max}} n_k \sqrt{(k+1)^2 - 1} = \sum_{i=1}^{r} q_i \sqrt{p_i}\,. \tag{4.51}$$

Each $\sqrt{(k+1)^2-1}$ can be written as an integer times a SRSFN so the left hand side of (4.51) will also be a linear combination of SRSFN with coefficients given by integer linear combinations of the unknowns n_k. As a preliminary step, let us find out –for a given square-free positive integer p_i– the values of k satisfying

$$\sqrt{(k+1)^2 - 1} = y\sqrt{p_i}\,, \tag{4.52}$$

for some positive integer y. This is equivalent to solving the Pell equation $x^2 - p_i y^2 = 1$ where the unknowns are $x := k+1$ and y. Equation (4.52) admits

an infinite number of solutions (k_m^i, y_m^i), where $m \in \mathbb{N}$ (see, for instance, [41]). These can be obtained from the fundamental one (k_1^i, y_1^i) corresponding to the minimum, non-trivial, value of both k_m^i and y_m^i. They are given by the formula

$$k_m^i + 1 + y_m^i \sqrt{p_i} = (k_1^i + 1 + y_1^i \sqrt{p_i})^m.$$

The fundamental solution can be obtained by using continued fractions [41]. Tables of the fundamental solution for the smallest p_i can be found in standard references on number theory. As we can see both k_m^i and y_m^i grow exponentially in m. By solving the Pell equation for all the different p_i we can rewrite (4.51) as

$$\sum_{i=1}^{r} \sum_{m=1}^{\infty} n_{k_m^i} y_m^i \sqrt{p_i} = \sum_{i=1}^{r} q_i \sqrt{p_i}.$$

Using the linear independence of the $\sqrt{p_i}$, the previous equation can be split into r different equations of the type

$$\sum_{m=1}^{\infty} y_m^i n_{k_m^i} = q_i, \quad i = 1, \ldots, r. \tag{4.53}$$

Several comments are in order now. First, these are diophantine linear equations in the unknowns $n_{k_m^i}$ with the solutions restricted to take non-negative values. They can be solved by standard algorithms (for example the Fröbenius method or techniques based on the use of Smith canonical forms). These are implemented in commercial symbolic computing packages. Second, although we have extended the sum in (4.53) to infinity it is actually finite because the y_m^i grow with m without bound. Third, for different values of i the equations (4.53) are written in terms of disjoint sets of unknowns. This means that they can be solved independently of each other –a very convenient fact when performing actual computations. Indeed, if $(k_{m_1}^{i_1}, y_{m_1}^{i_1})$ and $(k_{m_2}^{i_2}, y_{m_2}^{i_2})$ are solutions to the Pell equations associated to different square-free integers p_{i_1} and p_{i_2}, then $k_{m_1}^{i_1}$ and $k_{m_2}^{i_2}$ must be different. This can be easily proved by *reductio ad absurdum*.

It may happen that some of the equations in (4.53) admit no solutions. In this case $\sum_{i=1}^{r} q_i \sqrt{p_i}$ does not belong to the relevant part of the area spectrum. On the other hand, if these equations do admit solutions, the $\sum_{i=1}^{r} q_i \sqrt{p_i}$ belong to the spectrum of the area operator, the numbers k_m^i tell us the spins involved, and the $n_{k_m^i}$ count the number of times that the edges labeled by the spin $k_m^i/2$ pierce the horizon. A set of pairs $\{(k_m^i, n_{k_m^i})\}$ obtained from the solutions to equations (4.51), (4.52), and (4.53) will define what we call a *spin configuration*. The number of different quantum states associated to each of these is given by two degeneracy factors, namely, the one coming from reorderings of the k_I-labels over the distinguishable punctures (r-degeneracy) and the other originating in all the different choices of m_I-labels satisfying (2),

(m-degeneracy). The combinatorial factors associated to the r-degeneracy are straightforward to obtain and appear in the relevant literature.

4.6.2 The solution to the projection constraint

The problem that we have to solve is: Given a set of (possibly equal) spin labels j_I, $I = 1, \ldots, N$, what are the different choices for the allowed m_I such that (4.50) is satisfied? Notice that an obvious necessary condition for the existence of solutions is that $\sum_{I=1}^{N} j_I \in \mathbb{N}$.

In the standard DLM approach the number of different solutions for the projection constraint can be found by solving the following combinatorial problem (closely related to the so called *partition problem*): Given a set $\mathcal{K} = \{k_1, \ldots, k_N\}$ of N –possibly equal– natural numbers, how many different partitions of $\mathcal{K}$ into two disjoint sets $\mathcal{K}_1$ and $\mathcal{K}_2$ such that $\sum_{k\in\mathcal{K}_1} k = \sum_{k\in\mathcal{K}_2} k$ do exist? The answer to this question can be found in the literature (see, for example, [42] and references therein) and is the following

$$\frac{2^N}{M} \sum_{s=0}^{M-1} \prod_{I=1}^{N} \cos(2\pi s k_I/M) \ , \tag{4.54}$$

where $M = 1 + \sum_{I=1}^{N} k_I$. This expression can be seen to be zero if there are no solutions to the projection constraint.

Let us consider now the GM proposal. The problem is equivalent in this case to counting the number of irreducible representations, taking into account multiplicities, that appear in the tensor product $\bigotimes_{I=1}^{N}[j_I]$, where $[j_I] = [k_I/2]$ denotes the irreducible representation of $SU(2)$ corresponding to spin j_I. In order to solve this problem we rely on techniques developed in the context of conformal field theories [33] and in the spectral theory of Toeplitz matrices [34]. The starting point is to write the tensor product of two $SU(2)$ representations in the form

$$\left[\frac{k_1}{2}\right] \otimes \left[\frac{k_2}{2}\right] = \bigoplus_{k_3=0}^{\infty} \mathcal{N}_{k_1 k_2}^{k_3} \left[\frac{k_3}{2}\right] \ ,$$

where the integers $\mathcal{N}_{k_1 k_2}^{k_3}$, called *fusion numbers* (see *e.g.* [33]), tell us the number of times that the representation labeled by $k_3/2$ appears in the tensor product of $[k_1/2]$ and $[k_2/2]$. For each $k \in \mathbb{N} \cup \{0\}$, we introduce now the infinity *fusion matrices* $(C_k)_{k_1 k_2} := \mathcal{N}_{k_1 k}^{k_2}$, where k_1, $k_2 \in \mathbb{N} \cup \{0\}$. These can be shown to satisfy the following recursion relation

$$C_{k+2} = X C_{k+1} - C_k, \quad k = 0, 1, \ldots \tag{4.55}$$

where we have introduced the notation $X := C_1$. Explicitly $X_{k_1 k_2} = \delta_{k_1, k_2 - 1} + \delta_{k_1, k_2 + 1}$, which shows that X is a Toeplitz matrix (see [34]). The solution to

(4.55), with initial conditions $C_0 = I$ and $C_1 = X$, can be written as

$$C_k = U_k(X/2), \quad k = 0, 1, \ldots$$

in terms of the Chebyshev polynomials of the second kind U_k. The tensor product of an arbitrary number of representations can be decomposed as a direct sum of irreducible representations by multiplying the fusion matrices introduced above. By proceeding in this way we get

$$\left[\frac{k_1}{2}\right] \otimes \left[\frac{k_2}{2}\right] \otimes \cdots \otimes \left[\frac{k_N}{2}\right] = \bigoplus_{k=0}^{\infty} (C_{k_2} C_{k_3} \cdots C_{k_N})_{k_1 k} \left[\frac{k}{2}\right].$$

Notice that the product of matrices appearing in the previous formula is, in fact, a polynomial in X. The total number of representations, that gives the solution to the combinatorial problem at hand, is simply given by

$$\sum_{k=0}^{\infty} (C_{k_2} C_{k_3} \cdots C_{k_N})_{k_1 k}. \tag{4.56}$$

This is just the sum of the (finite number of non zero) elements in the k_1 row of the matrix $C_{k_2} C_{k_3} \cdots C_{k_N}$. A useful integral representation for this sum can be obtained by introducing a resolution of the identity for X as in [34] and the well-known identity $U_n(\cos\theta) = \sin[(n+1)\theta]/\sin\theta$. In fact, the number defined in (4.56) can be equivalently written as

$$\frac{2}{\pi} \int_0^{\pi} \mathrm{d}\theta \cos\frac{\theta}{2} \left[\cos\frac{\theta}{2} - \cos\left(K + \frac{3}{2}\right)\theta\right] \prod_{I=1}^{N} \frac{\sin(k_I + 1)\theta}{\sin\theta}, \tag{4.57}$$

where $K = k_1 + \cdots + k_N$. This is related to the well known Verlinde formula for $SU(2)$ (see [33]).

The procedure to calculate the black hole spectrum described above can be efficiently implemented in a computer, for instance using *Mathematica*. This allows us to analyze in detail the different factors that shape the degeneracy spectrum. First of all, the fact that the diophantine equations are decoupled allows us to obtain the configurations compatible with a given value of area $A = \sum_{i=1}^{r} q_i \sqrt{p_i}$ as the cartesian product of the sets of solutions to the diophantine equations for each p_i. Let us then begin by analyzing the results for area values of the form $A = q\sqrt{p}$, with $q \in \mathbb{N}$ and $\sqrt{p}$ a fixed SRSFN. What we see in this case is that the r-degeneracy –coming from the reordering of puncture labels– will be maximized by those configurations having both a large number of different values of k and a large number of punctures. For a fixed area value these two factors compete with each other because higher values of k imply a lower number of punctures. On the other hand the m-degeneracy shows an

exponential growth with area (both in the DLM and GM countings). When the two sources of degeneracy are taken into account –in the present case involving a single SRSFN– the total degeneracy can be seen to be dominated by the m-degeneracy. The reason for this dominance of the m-degeneracy is that the number of different (small) values of k available within the set of solutions to the Pell equation for a given p is limited, and hence only a few possibilities of reordering exist.

This situation is expected to change drastically when we consider areas $A = \sum_{i=1}^{r} q_i \sqrt{p_i}$, with $r > 1$, built as linear combinations of different SRSFN's. In this case it is possible to obtain configurations with a large number of different small values of k (associated to different SRSFN's). The effect of considering linear combinations involving several SRSFN's produces a very distinctive feature when the r-degeneracy is plotted as a function of area, namely, it creates a "band structure" where high values of degeneracy alternate with much lower ones. Furthermore, maxima and minima are evenly spaced. When this behavior is considered together with the m-degeneracy we obtain the regular pattern shown in Figure 4.13.

Several remarks are now in order. First, we want to point out that the result obtained from the explicit computational analysis carried out in [38] (by using the GM counting) is exactly recovered with the new approach. The fact that the same result is obtained from two completely independent procedures (a brute force approach and the algorithm proposed here) provides strong evidence for the reliability of both computations. Second, the structure of the degeneracy spectrum obtained by using the DLM and GM countings is basically equal. They differ only in the absolute values of the degeneracy whereas the band structure (including the position and spacing of the bands) is the same. This can be understood in our framework because the terms accounting for the r-degeneracy, responsible for this effect, coincide for both counting procedures. This justifies the appearance of the

1.

constant χ obtained in [38, 43, 44]. Third, once we understand how the r-degeneracy works, we see that the area values for which the degeneracy is large are those that can be written as linear combinations of the SRSFN's originating from small solutions k to the corresponding Pell equation. Thus, considering these linear combinations will suffice to account for the band structure. The remaining area values give rise only to very low degeneracies.

Summarizing, we have been able to find a number-theoretic/combinatorial way to tackle the problem of calculating the degeneracy spectrum of spherical black holes in LQG. Our procedure has several advantages over previous approaches. First, we have been able to characterize the area spectrum in a proper way, giving an algorithm to explicitly find every single spin configuration

contributing to each value of the area spectrum. In particular, the degeneracies of the area eigenvalues can be obtained. This has allowed us to reproduce and understand the band structure already observed in [38, 43, 44] for the black hole degeneracy spectrum in a much more efficient way. We not only recover previous results obtained by using a *brute force* algorithm, but easily extend them to area values significantly larger than those reached in [38]. Moreover, with our methods it is possible to compute the configurations and degeneracy even for much larger values of area. As a token we give the degeneracy for an area of $8320\sqrt{2}+14400\sqrt{3}+2240\sqrt{6}+4640\sqrt{15}+1120\sqrt{35}$, which is $3.46437296507975\cdots\times 10^{24420}$. Finally, the concrete procedures and explicit formulas given in this aproach offer a good starting point to study the asymptotic behavior of the entropy as a function of the area of a black hole. This could help us investigate whether the effective entropy quantization discussed here is present in macroscopic black holes.

5. CONCLUSIONS

Let us review the results presented in this thesis. We have performed an extensive study of the counting of states leading to the black hole entropy within the framework of isolated horizon in LQG (following the ABCK approach [14]). The following points are our results:

1. The surface states are described by a $U(1)$ Chern-Simons theory. But the origin of this $U(1)$ could be understood, at the classical level, as a breaking of the $SU(2)$ group of the LQG setting in the bulk. We have employed the correspondence between this theory and conformal field theory, following the ideas of Witten [17]. This allows us to emmploy the well-known Verlinde's formula and induce this breaking at the quantum level. The final result is given by (3.9), a formula whichi is also re-obtained by the method presented in the last section employing the number-theoretical techniques.

2. We have presented an explicit computational counting, namely a *brute force* method, to count all the states of an isolated horizon compatible with the condition of area and the projection constraint. This method, aviable for the DLM and GM approaches, shows that we can recover the leading linear behavior of entropy with area and moreover a logarithmic correction with a $(-1/2)$ coefficient. This is consistent with the appropriate value of the BI-parameter γ presented in the literature for both countings.

   Nevertherless, with this explicit counting we can no reach more than a few hundres Planck areas. This is due to the complexity of the combinatorial problem that appear in the counting of the states. In particular, the number of such states grows exponentially. Hence, we need to improve the computacional algorithm to try reach more realistic black holes.

3. This explicit counting exhibits an interesting behavior namely, the entropy is a stair-like function with area. Each step has a width with value $\Delta A = \chi\gamma\ell_{\mathrm{P}}^2$, where γ is the proper value for each counting presented here. On the other hand, χ has a value very close to $8\ln 3$.

4. It is clear that the DLM and GM countings are valid at the large area limit, but the aproximations performed in that computations hide the discrete structure of entropy with area. In anycase, we present here the a method in order to extract this effect from the previous results. As consequence of this work we can constraint the value of χ given by (4.48).

5. Finally, we have presented a new point of view for the black hole combinatorial problem. We rewrite the area spectrum making use of the square root of square free numbers (SRSFn). This allows us to make use of several diophantine equations on. We conclude that the area spectrum can be expresed as a finite linear combination of SRSFn with integer coefficients. We also address the combinatorial calculation of the states compatible with the projection constraint for both the DLM or the GM counting. It is worth mentioning that the solution to this problem leads to the same expresion obtained in the third chapter of this thesis which relies on CFT's thecniques.

Let us finish with some open question which will be addressed in future research.

i) It should be interesting to study further the role played by CFT in this problem. On the other hand, this problem could be related with the possibility to define properly the isolated horizon conditions at the quantum level.

ii) In the literature we find some controversy about the actual definition of the surface states. One possible method to select the correct ones would be through a better undertanding of the Chern-Simons theory present at the horizon. Specifically, we would study the posibility to carry out the ABCK framework employing an $SU(2)$ Chern-Simons theory, studying the consistency of the framework (the isolated horizon definition) with this theory. We expect that within this framework we could see in a natural way the reason of the restriction to a $U(1)$ gauge group.

iii) It will be interesting to explore the analogy between this problem and the quantum Hall effect.

iv) Finally, we are interested in the proper definition of the counting. As it has been point out before, it exists a problem with the prequantized value of the black hole area defined in terms of level of the Chern-Simons theory. This level k must be integer in order to have a well-define quantization procedure, but this means that the area A_0 induced on the horizon surface must be $A_0 = 4\pi\gamma\ell_{\mathrm{P}}^2 k$. Unfortunately, this value does not belong to the spectrum of the standard area operator used in LQG. We would like to explore this problem in the future in

order to give a consistent solution.

BIBLIOGRAPHY

[1] Bekenstein, J. D. 1973, *Black holes and entropy*, Phys. Rev. **D7** 2333-46 Hawking, S. W. 1975, *Particle creation by black holes*, Commun. Math. Phys. **43** 199

[2] Hawking, S. W. 1972, *Black holes in general relativity*, Commun. Math. Phys. **25** 152

[3] Wald, R. M. 2001, *The thermodynamics of black holes*, Living Rev. Relativity **4** url: http://www.livingreviews.org/lrr-2001-6

[4] Rovelli, C. and Upadhya, P. 1998, *Loop quantum gravity and quanta of space: A primer*, (gr-qc/9806079)

[5] Smolin, L. 2004, *An invitation to loop quantum gravity*, (hep-th/0408048)

[6] Corichi, A. 2005, *Loop Quantum Geometry: A primer*, J. Phys.: Conf. Ser. **24** 1-22 (gr-qc/0507038)

[7] Ashtekar, A. and Lewandowski, J. 2004, *Background independent quantum gravity: A status report*, Class. Quant. Grav. **21** R53 (gr-qc/0404018)

[8] Pérez, A. 2004, *Introduction to loop quantum gravity and spin foams*, (gr-qc/0409061)

[9] , Nicolai. H, Peeters, K. and Zamaklar, M. 2005 *Loop quantum gravity: An outside view*, (hep-th/0501114)

[10] Rovelli, C. 2004, *Quantum gravity*, Cambridge University Press

[11] Thiemann, T. 2007, *Introduction to modern canonical quantum general relativity*, Cambridge University Press

[12] Booth, I. 2005, *Black hole boundaries*, Can. J. Phys.**83** 1073-1099

[13] Ashtekar, A, Krishnan, B. 2004, *Isolated and Dynamical Horizons and Their Applications*, Living Rev. Relativity **7**
url: http://www.livingreviews.org/lrr-2004-10

[14] Ashtekar, A. Baez, J. Corichi, A. Krasnov, K. 1998, *Quantum geometry and black hole entropy* , Phys. Rev. Lett. **80**, 904; Ashtekar, A. Baez, J. Krasnov, K. 2000, Quantum Geometry of isolated horizons and black hole entropy, *Adv. Theor. Math. Phys.* **4**, 1; Ashtekar A, Corichi A, Krasnov K. 2000, *Isolated Horizons: The classical phase space*, Adv. Theor. Math. Phys. **3**, 419.

[15] Rovelli, C. 1996, *Black hole entropy from loop quantum gravity*, Phys. Rev. Lett. **77** 3288

[16] Krasnov, K. 1998, *On Quantum statistical mechanics of Schwarzschild black hole*, Gen.Rel.Grav. **30**:53-68

[17] Witten, E. 1989, *Quantum field theory and the Jones polynomial*, Comm. Math. Phys. **121**:351-399

[18] Domagala, M., Lewandowski, J. 2004, *Black hole entropy from quantum geometry*, Class. Quantum Grav. **21** 5233; Meissner, K. A. 2004, *Black hole entropy in loop quantum gravity*, Class. Quantum Grav. **21** 5245

[19] Ghosh, A., Mitra, P. 2005, *An improved stimate of black hole entropy in the quantum geometry approach*, Phys. Lett. B **616**, 114; 2006, *Counting black hole microscopic states in loop quantum gravity*, Phys. Rev. **D74**, 064026

[20] Sahlmann, H. 2007, *Toward explaining black hole entropy quantization in loop quantum gravity* , Phys. Rev. **D76**, 104050

[21] Babero G., J. F., Villaseñor, E. 2008, *Generating functions for black hole entropy in Loop Quantum Gravity*, Phys. Rev. **D77**, 121502

[22] Díaz-Polo, J., Fernández-Borja, E. 2008, *Black hole radiation spectrum in loop quantum gravity: isolated horizon framework*, Class. Quantum Grav. **25** 105007

[23] Livine, E. R., Terno, D. R. 2006, *Quantum Black Holes: Entropy and entanglement on the horizon* , Nuc. Phys. **B 741** 131; Ansari, M. H. 2007, *Spectroscopy of a canonical quantized horizon*, Nuc. Phys. **B 783** 179; Donnelly, W. 2008, *Entanglement entropy in loop quantum gravity*, Phys. Rev. **D77** 104006

[24] Barbero J. F., Lewandowski, J., Villaseñor, E. 2009, *Flux-area operator and black hole entropy*, [arXiv: 0905.3465v1]

[25] Engle, J., Pérez, A., Noui, K. 2009, *Black hole entropy and $SU(2)$ Chern-Simons Theory*, [arXiv: 0905.3168v1]

[26] Agulló I, Barbero J. F., Díaz-Polo J, Fernández-Borja E, Villaseñor E. J. S, 2008, *The combinatorics of the $SU(2)$ black hole entropy in loop quantum gravity*, [arXiv:0906.4529]

[27] Wald, R. M. 1984, *General Relativity*, Chicago University Press

[28] Barbero, J. F. 1996, *Real Ashtekar variables for Lorentzian signature space-times*, Phys. Rev. **D51**, 5507; Immirzi, G. 1997, *Quantum Gravity and Regge Calculus*, Nucl. Phys. Proc. Suppl. **57**, 65

[29] Ashtekar, A., Lewandowski, J. 1997, *Quantum theory of geometry. 1: Area operators.*, Class. Quantum Grav. **14** A55

[30] Carlip, S. 1999, *Black hole entropy from conformal field theory in any dimension*, Phys. Rev. Lett. **82**, 2828; 2007, *Black hole thermodynamics from Euclidean horizon constraints*, Phys. Rev. Lett. **99**, 021301; 2007, *Symmetries, Horizons, and Black Hole Entropy*, Gen. Rel. Grav. **39**, 1519

[31] Kaul, R. and Majumdar, P. 1998, *Quantum Black Hole Entropy*, Phys. Lett. B **439**, 267; 2000, *Logarithmic correction to the Bekenstein-Hawking entropy*, Phys. Rev. Lett. **84** 5255

[32] Bojowald, M., Kastrup, H. A. 2000, *Quantum symmetry reduction for diffeomorphism invariant theories of connections*, Class. Quantum Grav. **17**, 3009

[33] Di Francesco, P., Mathieu, P. and Senechal, D. 1997, *Conformal Field Theory*, Springer, New York.

[34] Brottcher, A and Grudsky, S.M. 2005, *Spectral Properties of Banded Toeplitz Matrices.*, SIAM

[35] Bekenstein, J. D. 1974, Lett. Nuovo Cim. **11**, 467; V.F. Mukhanov, Pis'ma Zh. Eksp. Teor. Fiz. **44** 1986, 50 [JETP Lett. 44 (1989) 63].

[36] Dreyer, O. 2003, *Quasinormal modes, the area spectrum, and black hole entropy.*, Phys. Rev. Lett. **90** 081301

[37] Hod, S. 1998, *Bohr's correspondence principle and the area spectrum of quantum black holes*, Phys. Rev. Lett. **81** 4293

[38] Corichi A, Díaz-Polo J and Fernández-Borja E. 2007, Quantum geometry and microscopic black hole entropy, *Class. Quantum Grav.* **24** 243

[39] Díaz-Polo, Jacobo 2009, *Black hole entropy discretization in loop quantum gravity*, Universidad de Valencia. Ph.D. Thesis

[40] Newman D. J., Furr F. and Williams L. K. 1959, *The American Mathematical Monthly*, **66** 321

[41] Burton D. M., 2002, *Elementary Number Theory*, McGraw-Hill, New York

[42] De Raedt H., Michielsen K., De Raedt K. and Miyashita S. 2001, *Number partitioning on a quantum computer*, Phys. Lett. **A290** 227

[43] Corichi A, Díaz-Polo J and Fernández-Borja E. 2007, *Black hole entropy quantization*, Phys. Rev. Lett. **98**, 181301

[44] Agulló I, Borja E. F, Díaz-Polo J, 2008, *Black hole state degeneracy in Loop Quantum Gravity*, Phys. Rev. **D77**, 104024

[45] Agulló I, Borja E. F, Díaz-Polo J, 2009, *Computing Black Hole entropy in Loop Quantum Gravity from a Conformal Field Theory perspective*, JCAP07(2009)016 *Preprint* ArXiv: :0903.1667 [hep-th]

[46] Agulló I, Barbero J. F., Díaz-Polo J, Fernández-Borja E, Villaseñor E. J. S, 2008 Black hole state counting in LQG: A Number theoretical approach *Phys. Rev. Lett.* **100**, 211301